

# **Design and Development of a Direct Methanol Fuel Cell for Telecommunications**

**Hardus Joubert  
9612696**

**A dissertation submitted in fulfilment of the requirements  
for the  
Magister Technologiae: Engineering: Electrical**

**Department: Applied Electronics and Electronic  
Communication  
Faculty of Engineering  
Vaal University of Technology  
Vanderbijlpark**

**Supervisor: Dr. H.C. vZ. Pienaar**

**Date: June 2005**

VAAL UNIVERSITY OF TECHNOLOGY	
Bib. No.	11005452
Item No.	11172253
Order No.	DONATION
2005 -09- 3 0	
Price:	R600.00
Call No.	621.38232 JOU
LIBRARY STOCK	

## DECLARATION

I Hardus Joubert hereby declare that the following research information is solely my own work. This dissertation is submitted for the requirements for the Magister Technologiae: Engineering: Electrical to the Department of Applied Electronics and Electronic Communication at the Vaal University of Technology, Vanderbijlpark. This dissertation has never before been submitted for evaluation at any educational institute.

A handwritten signature in dark ink, appearing to read 'Joubert', is written over a horizontal line.

Hardus Joubert

23 June 2005

## **ACKNOWLEDGEMENTS**

I hereby wish to express my gratitude to the following individuals who enabled this document to be successfully and timeously completed:

- Dr. H.C. Pienaar
- Telkom Center of Excellence, TFMC, M-Tech and THRIP
- Vaal University of Technology
- Glynne Case as the language editor

## **DEDICATION**

This dissertation is dedicated to my mom and sister.

## ABSTRACT

The demand for higher efficiency and cleaner power sources increases daily. The Direct Methanol Fuel Cells (DMFC) is one of those power sources that produces reliable electrical energy at high efficiencies and very low pollution levels. Remote telecommunication sites need power sources that can deliver reliable power.

This dissertation informs the reader about the working principles of the DMFC and the materials it consists of. A good amount of theoretical background is also given on the DMFC, especially on the Membrane Electrode Assembly (MEA). Different membranes as well as their properties are discussed. Results from other researchers on DMFCs are also captured.

A DMFC stack including a test rig, was built. The DMFC stack consisted of five single DMFC cells. Each cell contained an MEA, Gas Diffusion Layers (GDLs), highly corrosive resistant metal support grids, bipolar flow field plates and end plates. The DMFC stack was operated and tested in a test rig. The test rig held the air blower which supplied the cathode with the required oxidant (air), and the methanol solution tank plus its liquid pump. The liquid pump circulated the methanol solution through the anode side of the stack.

It was observed that the DMFC is very susceptible to corrosion, especially if the methanol solution becomes conductive owing to solubility of  $\text{CO}_2$  in it. Methanol itself is a corrosive substance. However the results obtained from the experiments clearly indicate that the DMFC can be implemented as an electrical power source for telecommunications.

# TABLE OF CONTENTS

	<b>Page</b>
<b>Declaration</b>	<b>ii</b>
<b>Acknowledgements</b>	<b>iii</b>
<b>Dedication</b>	<b>iv</b>
<b>Abstract</b>	<b>v</b>
<b>List of figures</b>	<b>x</b>
<b>List of tables</b>	<b>xiii</b>
<b>Glossary of terms</b>	<b>xiv</b>
<b>1 Introduction</b>	<b>1</b>
1.1 Background	1
1.2 Problem statement	4
1.3 Delimitations	4
1.4 Objective	4
1.5 Methodology	5
1.6 Summary	5
<b>2 The Direct Methanol Fuel Cell – A detailed study</b>	<b>6</b>
2.1 Introduction	6
2.2 The history of the fuel cell	9
2.3 Components of the DMFC	11
2.3.1 The membrane	12
2.3.1.1 Thickness of a membrane	17
2.3.1.2 Water uptake in a membrane	18
2.3.1.3 Equivalent weight of a membrane	19
2.3.1.4 Different membranes	19
2.3.1.5 Modified membranes	20

2.3.2	The anode	22
2.3.3	The cathode	25
2.3.4	The gas diffusion layers	25
2.3.5	Current collecting ribs and plates	28
2.4	The complete single DMFC	28
2.4.1	The membrane electrode assembly (MEA)	29
2.4.2	Structure of a single DMFC	32
2.5	Electrical characteristics of the DMFC	33
2.5.1	Cell voltage versus current density	33
2.5.2	DMFC output voltage characteristics	34
2.5.3	OCV compared to the thermodynamically expected value	35
2.5.4	Performance of a cell	35
2.5.5	Potential of a cell	37
2.5.6	Power density of a cell	41
2.5.7	Internal resistance of a cell	43
2.6	Changing DMFC parameters	44
2.6.1	Methanol concentration in the DMFC	45
2.6.2	Operating temperature of the DMFC	47
2.6.3	Stoichiometry of reactants	49
2.6.3.1	Methanol solution flow rate	50
2.6.3.2	Oxygen air flow rate	51
2.6.4	Pressurization of electrode feeds	54
2.7	Production and effects of the by product CO <sub>2</sub>	55
2.8	Crossover in the DMFC	57
2.8.1	Methanol crossover	57
2.8.1.1	Using CO <sub>2</sub> levels to determine methanol crossover	61
2.8.1.2	Effects of methanol crossover on cathode	63
2.8.1.3	Reducing methanol crossover	64
2.8.2	Water crossover	66
2.8.3	Carbon dioxide crossover	67
2.9	Chemical side of the DMFC	68

2.9.1	Working of a DMFC	68
2.9.2	Reactions on the anode and the cathode	73
2.9.3	Methanol oxidation on the anode catalyst	73
2.9.4	Performance requirements of the cathode catalyst	78
2.10	Methods of feeding the DMFC with fuel	79
2.10.1	Mixed reactant feed	80
2.10.2	Vaporizing the methanol feed	81
2.10.3	Using different flow field structures	82
2.11	Overall advantages	83
2.12	Summary	83
<b>3</b>	<b>Design and development of the DMFC</b>	<b>85</b>
3.1	Introduction	85
3.2	Structure of a DMFC	85
3.2.1	The MEA	86
3.2.2	The GDLs	87
3.2.3	The flow fields	88
3.3	Direct methanol fuel cell stack	95
3.4	Collecting the current from the stack	98
3.5	Function of end plates	98
3.6	Building of test rig	99
3.7	Pre-conditioning of the DMFC	100
3.8	Briefing on experiments	102
3.9	Summary	102
<b>4</b>	<b>Practical experiments done on the DMFC</b>	<b>104</b>
4.1	Introduction	104
4.2	Startup time of the DMFC	104
4.3	Voltage-current density characteristic curves	109
4.4	DMFC performance with different methanol concentrations	112
4.5	DMFC performance with different operating temperature	114



4.6	DMFC performance with different cathode oxidant flow rates	116
4.7	DMFC performance with hydrogen as a fuel	118
4.8	Summary	119
<b>5</b>	<b>Conclusion on the DMFC</b>	<b>120</b>
5.1	Insights on DMFC manufacturing	120
5.2	Materials used in the stack	120
5.3	Corrosion of the stack	120
5.4	Internal stack currents	122
5.5	Contact pressure between flow field plates and the MEA	124
5.6	Redesigning of flow field plates	124
5.7	Results from the aluminium flow field stack	126
5.8	Results from the graphite flow field stack	127
5.9	Final word	128
	<b>Bibliography</b>	<b>129</b>

## LIST OF FIGURES

		page
Figure 1	Assembly of a fuel cell	7
Figure 2	Endurance test of a 24-cell stack	8
Figure 3	(a) Chemical structure of Nafion ionomer (b) chemical structure of Flemion Asahi polymer ionomer	14
Figure 4	Section through enlargement of a hydrophilic gas diffusion electrode	26
Figure 5	Section through enlargement of a hydrophobic gas diffusion electrode	27
Figure 6	Membrane electrode assembly of a DMFC	29
Figure 7	A simple direct methanol fuel cell design	30
Figure 8	A solid polymer electrolyte membrane for a DMFC with catalytic GDLs	31
Figure 9	A single DMFC assembly	31
Figure 10	Block diagram of a DMFC	32
Figure 11	DMFC performance curve	34
Figure 12	Allocation of efficiency losses in a DMFC	35
Figure 13	Performance curve of a DMFC	37
Figure 14	Variation of current density with methanol concentration	39
Figure 15	Influence of temperature on cell power	42
Figure 16	Effect of methanol concentration on a DMFC	47
Figure 17	Effect of temperature on a DMFC	48
Figure 18	Cell voltage versus air stoichiometry	49
Figure 19	Mass flow within a direct methanol fuel cell	49
Figure 20	Mass flow through the anode and the membrane of a DMFC	50
Figure 21	Mass flow from membrane and through the cathode	51
Figure 22	Influence of air ratio and cathode pressure on cell power	54
Figure 23	Methanol crossover rate as a function of the current density	58

Figure 24	Effect on open circuit voltage at different methanol concentrations	60
Figure 25	DMFC assembly with a liquid electrolyte	66
Figure 26	Working of a DMFC	68
Figure 27	Performance difference between thick and thin catalyst electrode layers	69
Figure 28	Construction of an MEA	70
Figure 29	Three-phase reaction concept	71
Figure 30	Increasing active surface area	72
Figure 31	Pathway of methanol oxidation	76
Figure 32	DMFC with a passive fuel delivery system	80
Figure 33	Channel geometry for fuel cells	83
Figure 34	Membrane electrode assembly (MEA)	86
Figure 35	Gas diffusion layer (GDL)	87
Figure 36	Flow field structure	88
Figure 37	Bipolar plate used in the DMFC	89
Figure 38	Serpentine flow field	90
Figure 39	Carbon dioxide generation at $10 \text{ mA.cm}^{-2}$	91
Figure 40	Carbon dioxide generation at $50 \text{ mA.cm}^{-2}$	91
Figure 41	Carbon dioxide generation at $100 \text{ mA.cm}^{-2}$	92
Figure 42	Carbon dioxide generation at $150 \text{ mA.cm}^{-2}$	92
Figure 43	Carbon dioxide generation at $200 \text{ mA.cm}^{-2}$	93
Figure 44	Designed flow field structure for methanol solution (upwards)	93
Figure 45	Designed flow field structure for air (downwards)	94
Figure 46	Single cell assembly components	95
Figure 47	Seal covers instillation on flow field plate	96
Figure 48	Animated direct methanol fuel cell stack	96
Figure 49	Fuel cell stack under construction, membrane visible	97
Figure 50	Fuel cell stack under construction, flow field visible	97
Figure 51	Complete assembled DMFC stack	98
Figure 52	Stack end plates	99

Figure 53	Block diagram of the test rig	99
Figure 54	Direct methanol fuel cell test rig	100
Figure 55	Setup of experiment	108
Figure 56	Open circuit voltage characteristics of the DMFC stack	109
Figure 57	Voltage-current density curve of the DMFC stack	110
Figure 58	Voltage-power density characteristic curve	111
Figure 59	Effects of methanol concentration on the DMFC stack	113
Figure 60	Effects of temperature on the DMFC stack	115
Figure 61	Voltage-current density results of the DMFC stack for different cathode flow rates	117
Figure 62	Voltage-current density with hydrogen as fuel for the DMFC stack	119
Figure 63	Corrosion of the flow field plate	121
Figure 64	Corrosion on nickel-plated copper grid	121
Figure 65	Copper on the membrane	122
Figure 66	Internal stack current	123
Figure 67	No carbon dioxide blockage in the DMFC test cell	125
Figure 68	Carbon dioxide blockage in the DMFC test cell	125
Figure 69	Graphite flow field plate	126
Figure 70	Fuel flow in anode chamber	127
Figure 71	New graphite flow field plate	128

## LIST OF TABLES

	<b>page</b>
Table 1    Fuel cell types and characteristics	3
Table 2    Effects of methanol concentration on reduction of the oxygen electrode	40
Table 3    Composition of air	52

## GLOSSARY OF TERMS

### A

ac – alternating current  
AFC – alkaline fuel cell  
Au – gold

### C

CH<sub>3</sub>OH – methanol  
Co – cobalt  
CO – carbon monoxide  
CO<sub>2</sub> – carbon dioxide  
Cr – chromium

### D

DMFC – direct methanol fuel cell

### E

e<sup>-</sup> – electron

### F

Fe – iron

### G

GDL – gas diffusion layer

### H

H<sup>+</sup> – hydrogen proton  
H<sub>2</sub>O – water  
HOR – hydrogen oxidation reaction

### I

IR – impregnation reduction method  
Ir – iridium

### M

MEA – membrane electrode assembly  
Mo – molybdenum

### N

Ni – nickel

### O

O – oxygen  
OCV – open circuit voltage  
ORR – oxygen reduction reaction  
Os – osmium

### P

PBI – polybenzimidazole  
PEEK – polyether ether ketone  
PEMFC – proton exchange membrane fuel cell  
PFSA – perfluorosulfonic  
POP – polyoxiphenylenes  
ppm – particles per million  
PSSA – polystyrene sulfonic acid  
Pt – platinum  
PTFE – polytetrafluoroethylene  
PVA – polyvinyl alcohol  
PVDF – polyvinylidene fluoride

### R

Ru – ruthenium  
Re – rhenium

### S

SO<sub>3</sub>H – sulfonic acid  
Sn – tin

### W

W – tungsten

### Z

Zr – zirconium

# **Chapter 1 Introduction**

## **1.1 Background**

The current age and environment we live in require that the air we breathe should be pollutant free. Even the water that we drink must be purified. Very few of the current systems that generate electrical energy do it in a pollutant free manner. Their pollutant emission levels are mostly way above stipulated regulations. In contrast with this there are devices that generate electrical energy very efficiently and with very low emission levels. Some of these electrical energy sources are already in use at remote telecommunication sites.

These devices are the widely known battery, photo-voltaic cells, windmill power, hydro-power, bio-energy, generators, using heat to generate electricity even the utilization of storage devices like super capacitors and ultra capacitors. Then there is a new kid on the block, the fuel cell, which although it was discovered over 160 years ago, has in recent years enjoyed renewed interest.

When investigating the input energy required for each of these sources mentioned above it is clear that for the photo-voltaic cells sunlight is the best source. Wind is required for the windmill and for hydro generators the flow of water will do the trick. Each of these sources is found abundantly on the earth. Fuel cells use a hydrogen-based element as a fuel, and oxygen or air.

Reading through the previous paragraphs an interesting observation can be made. Power sources can be divided into two categories. The first being portable power sources versus stationary power sources. Batteries are an example of portable power sources and windmills as stationary power sources. The second category is where the reactants for these power sources are found. For batteries the reactants are stored internally and for solar cells the source of energy is external through the absorption of photons (Archer & Hill 2001:16).

An interesting fact is that for portable power sources the energy source is most likely stored internally and for stationary power sources the energy source is most likely obtained externally. Fuel cells are a bit of both. Their energy sources are obtained externally but yet they can be portable as well as stationary. An example of a portable power source is described by Linden (1984:42-9). This portable hydrogen-air fuel cell stack was developed for military use as a power source for radio sets and other electronic equipment. It was even used as a battery charger. An example of a stationary hydrogen-air fuel cell power source can be found in Kordesch & Simander (2001:186). This is an 11-Mw  $H_2$ - $O_2$  fuel cell power plant, at that time the largest plant in the world.

It is obvious from these descriptions that all fuel cells are very modular and can lend themselves out for many applications. Applications such as supplying power for space missions, undersea expeditions, for cities, for portable laptops and cell phones and even remote telecommunication sites. Power sources such as windmill generators and photo-voltaic cells are not considered in this work as an electrical supply for telecommunications because wind is an unreliable source of energy and the same goes for sunlight which is lacking on a cloudy day. Therefore, the focus of this work is to use a fuel cell as a power source for telecommunications.

Different types of fuel cells are available. The most common are: Alkaline fuel cells (AFC), proton exchange membrane fuel cells (PEMFC), direct methanol fuel cells (DMFC), phosphoric acid fuel cells (PAFC), molten carbonate fuel cells (MCFC) and solid oxide fuel cells (SOFC). Table 1 gives a comparison between all of the abovementioned fuel cells.

The operating temperature of the fuel cell plays a major role in deciding which of the above fuel cells will be suited for telecommunications. The fuel cell must be able to operate as a primary power source and as a backup power source. For the backup power source, energy must be available immediately after startup. Therefore, low temperature fuel cells are more suitable. This leaves the AFC, PEMFC and the



DMFC as viable solutions from Table 1.

**Table 1** Fuel cell types and characteristics (Laughton 2002:39).

	<b>AFC</b>	<b>PEMFC</b>	<b>DMFC</b>	<b>PAFC</b>	<b>MCFC</b>	<b>SOFC</b>
<b>Electrolyte</b>	Aqueous potassium hydroxide (30-40%)	Sulphonated organic polymer (hydrated during operation)	Sulphonated organic polymer (hydrated during operation)	Phosphoric acid	Molten lithium/sodium/ Potassium carbonate	Yttria-stabilized zirconia
<b>Operating temperature, °C</b>	60-90	25-90	25-90	150-220	600-700	650-1000
<b>Charge carrier</b>	OH <sup>-</sup>	H <sup>+</sup>	H <sup>+</sup>	H <sup>+</sup>	CO <sub>3</sub> <sup>2-</sup>	O <sup>2-</sup>
<b>Anode</b>	Nickel (Ni) or precious metal	Platinum (Pt)	Platinum/ ruthenium (Pt/Ru)	Platinum (Pt)	Nickel/ Chromium oxide	Nickel/ Yttria-stabilized zirconia
<b>Cathode</b>	Platinum or lithiated NiO	platinum	platinum	platinum	Nickel oxide (NiO)	Strontium (Sr) doped lanthanum manganite
<b>Co-generation heat</b>	Low quality	Low quality	Low quality	Acceptable for many applications	high	High
<b>Electrical efficiency, %</b>	60	40-45	30-35	40-45	50-60	50-60
<b>Fuel sources</b>	H <sub>2</sub> , removal of CO <sub>2</sub> from both gas streams necessary	H <sub>2</sub> , reformat with less than 10 ppm CO	Methanol-water solution	H <sub>2</sub> reformat	H <sub>2</sub> , CO, natural gas	H <sub>2</sub> , CO, natural gas

According to Fickett (1984:41-3) fuels such as hydrogen, hydrazine, hydrocarbons, coal gas, methanol etc. are used in fuel cells. All of the fuels except for hydrogen and methanol have to be reformed in order to obtain the hydrogen from the element structure of these fuels before it can be used within the fuel cell.

It is also clear from Table 1 that all fuel cells use highly flammable gasses except one, the direct methanol fuel cell. It uses a methanol-water solution that is not at all flammable. Methanol is poisonous but a methanol-water solution poses no threat to humans or the environment if treated correctly. A decisive argument for using the

methanol-water solution as a fuel is because it is in a liquid form and can therefore be transported and stored easily. It is also a more energy dense fuel than hydrogen. Methanol was originally distilled from wood but is now produced primarily from natural gas. Methanol can even be manufactured synthetically from carbon monoxide and hydrogen. The main requirement of the raw material used is that it must contain carbon. Other materials that can also be used are coal, oil, biomass, seaweed, garbage and waste wood. Methanol can even be produced from a basis of fossil or renewable sources (Methanol, chronic toxicity summary 2004:1). Therefore, it can be seen that the fuel for DMFCs is readily obtainable. The disadvantage with hydrogen gas is that it cannot be easily stored, and highly pressurized cylinders are required. The fuel cell that is chosen as a power source for telecommunications is the direct methanol fuel cell.

## **1.2 Problem statement**

Telecommunications need environmental friendly power sources that can deliver electrical power to the equipment for long unattended time durations.

## **1.3 Delimitations**

This project will have no practical exploitation of a complete fuel cell power plant. There will also be no control devices for managing input variables to the direct methanol fuel cell. The output of the DMFC will also not be converted or stepped up to obtain a regulated output.

## **1.4 Objective**

The objective of this work is to design and develop a direct methanol fuel cell to be used in the telecommunication industry.

## **1.5 Methodology**

There will be theoretical side as well as practical side to this project. The first phase of the project is the theoretical part that will consist of research done on the operation of the DMFC and its characteristics.

The second phase, which will be parallel with the first phase, is the design and development of a practical DMFC.

The third phase will be the manufacturing and construction of the DMFC and the fourth and final stage will be the testing of the DMFC.

## **1.6 Summary**

In this chapter, the reader was familiarised with the different electrical power sources. The problem of obtaining power for telecommunications is discussed. It was mentioned that fuel cells will be looked at as a power source and more specifically at the direct methanol fuel cell. This fuel cell uses a liquid as a fuel and its operating temperature is low.

## **Chapter 2    The Direct Methanol Fuel Cell – A detailed study**

### **2.1 Introduction**

According to Hirschenhofer and McClelland (1995:84) the hydrogen-air fuel cell was almost unknown 10 years ago. Yet Ter-Gazarian (1994:138) stated that hydrogen-air fuel cells have even a longer history than batteries. People are saturated with the idea that batteries are the only portable electrical source. This could change in the near future because direct methanol fuel cells can even be used in a portable environment. Even a greater reason to look at direct methanol fuel cells is the fact that these devices are clean energy sources. By itself, the DMFC emits few harmful environmental emissions.

Direct methanol fuel cells can be used to supply most systems that use electricity for power. One of the advantages of the direct methanol fuel cell is its ability to be easily installed on a required site without disturbing the environment around it. Some telecommunication sites are remotely situated. Most of these sites do not have any power grid readily available. Currently some of these sites do use solar power together with a battery bank. During daytime the solar panels supply the telecommunication equipment with power as well as charging the battery bank. During nighttime the battery bank takes over and supply the equipment with power. When day comes again the solar panels supply the equipment again and charge the battery bank. The process repeats itself.

The problem with this solar energy system is that these panels take up a large amount of space and they get stolen. It is expensive to replace these panels each time. This is where the direct methanol fuel cells can fit in. Direct methanol fuel cells are small and modular. In other words the power requirements of the equipment determine the size of the direct methanol fuel cell. The direct methanol fuel cell could be in a closed building or container as long as there is adequate supply of clean air.

The first question to be answered is: What is a direct methanol fuel cell? A DMFC can be explained as an electrochemical device that converts chemical energy of a fuel and an oxidant into electrical energy. Fuel is oxidized at the anode and oxygen is reduced at the cathode. This conversion will continuously take place as long as a fuel and an oxidant is supplied to the DMFC (Kordesch & Simander 2001:9).

Direct methanol fuel cells are often compared to batteries. The elements of DMFCs are the same as that of batteries and they work on a similar principle. DMFCs, as do batteries, have an anode, a cathode as well as an electrolyte. An example of a single direct methanol fuel cell assembly is given in Figure 1.

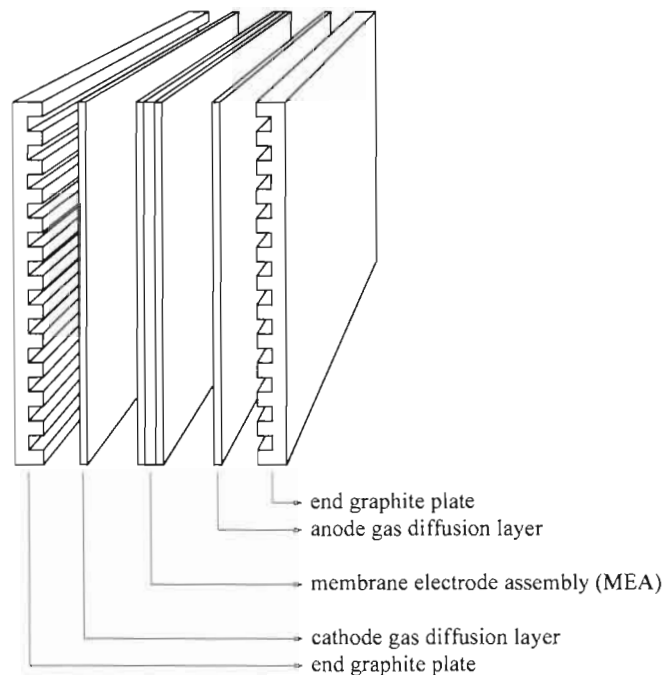


**Figure 1** Assembly of a fuel cell.

The heart of a DMFC is the membrane electrode assembly (MEA). The diffusion layers help with the transfer of the reactant gas and the oxidant to the surface of the catalyst. End plates or flow fields ensure that the reactant fuel and oxidant are contained in the cell. The main difference between fuel cells and batteries is that, in the case of batteries, the reactants are stored internally, whereas, in fuel cells the

reactants are stored externally (Laughton 2002:37). The disadvantage of batteries with this method is that the batteries will need replacement after a time period if primary batteries are used, or recharging if secondary batteries are used. The advantage of fuel cells is that the cell will continue to operate as long as reactants are supplied to it. According to Hyder *et al.* (2000:226) the parameter that best describes a battery is its capacity and the parameter that best describes a direct methanol fuel cell is its power.

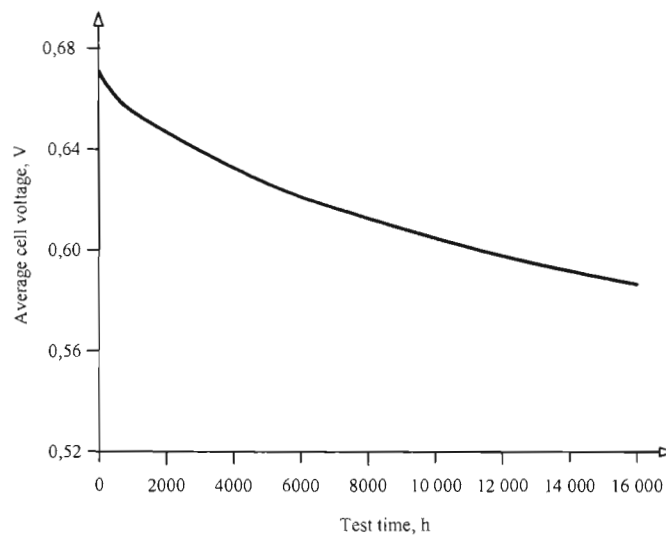


**Figure 2** Endurance test of a 24-cell stack (test conditions:  $130 \text{ mA}\cdot\text{cm}^{-2}$ ,  $190^{\circ}\text{C}$ ,  $10^5 \text{ Pa}$  pressure) (Fickett 1984: 43-12).

The output voltage of a DMFC is in the order of 0,3 – 0,5 volts. A number of these cells need to be combined to form a **fuel cell stack**. Therefore, individual cells are connected in series to form this stack. This is done to obtain a required output voltage. An electrical conductive separator plate located between the anode and the cathode of the adjacent cells connects the cells to each other (Fickett 1984:41-7). The advantage of using such a connection method is that no external wiring is required. This is called a bipolar configuration. The active surface area determines the amount of available current or a number of stacks can be connected in parallel to increase the power capability of the complete direct methanol fuel cell system. It is also important that the materials used in manufacturing the direct methanol fuel cell

must be compatible with each other to ensure reliable operation for long periods of time.

But it is not all bloom and glory with all types of fuel cells. They need to be serviced from time to time or replaced (Kordesch & Simander 2001:12). Fuel cells gradually experience a loss of efficiency. The good news about fuel cells is that their operating hours are being constantly improved, increasing the efficiency of these devices. Figure 2 shows the voltage decay of the average voltage of a 24 cell stack over a time period of 16 000 hours. The fuel cell stack used for this experiment was a hydrogen-air fuel cell (Fickett 1984:43-12).

## **2.2 The history of the fuel cell**

The fuel cell has undergone a few name changes from its birth to the present day. It also evolved over a few years to become a usable chemical device. Direct methanol fuel cells have only been developed in the 1990s and have recently enjoyed renewed interest.

The first fuel cell was developed in England in 1839 by Sir William Grove. At that time he was experimenting with the electrolysis of water. He used electricity to split water into hydrogen and oxygen. Grove thought that the reverse of this process must also be possible, i.e. combining hydrogen and oxygen must be able to produce water and electricity. To test his theory, he used two platinum electrodes that were enclosed in two separately sealed bottles. One bottle contained the fuel, hydrogen, and the other the oxidant, oxygen. These two bottles were then immersed in diluted sulphuric acid. A current began to flow from the one electrode to the other. Water was formed in the oxygen bottle. Grove connected fifty of these devices in series to increase the produced voltage. He called this invention of his the gas battery. The gas battery was first used in 1842 to power an electric arc (Hurley 2002:2).

In 1889, Ludwig Mond and Charles Langer also began experimenting with Grove's gas battery. They called it a **fuel cell**. Mond and Langer's fuel cell consisted of platinum electrodes with a clay barrier soaked in a sulphuric acid electrolyte. During this time Frederick Ostwald also did research on the fuel cell. In the first half of the 20<sup>th</sup> century, Emil Baur did experiments on using different electrolytes such as molten silver and clay mixed with metal oxides for use within a fuel cell (Hurley 2002:3).

In 1932, Dr. Francis Thomas Bacon, at Cambridge University in England, implemented a few modifications to the fuel cell developed by Mond and Langer. Less expensive nickel gauze replaced the platinum electrodes. The sulphuric acid electrolyte was substituted with an alkali, potassium hydroxide. This hydroxide was less corrosive to the nickel electrodes. He called his modified version of the fuel cell the Bacon Cell. It was in actual fact the first alkaline fuel cell (AFC). In 1959, Bacon demonstrated that this device could produce 5 kW of usable power, enough to power a welding machine. Later in 1959 Harry Karl Ihrig, of Allis-Chalmers, used the fuel cells to power a vehicle. The fuel cell stack that he built could generate 15 kW and it was capable of powering a 20 horsepower tractor (Hurley 2002:3).

There was renewed interest in the fuel cell during the late 1950s and early 1960s. NASA was looking for a way to power their manned space flights. They looked at batteries but these devices were too heavy at the time. Solar energy was too expensive and nuclear power was considered too dangerous. The fuel cell was thought to be a possible solution. Here the first interest started in developing a proton exchange membrane fuel cell (PEMFC) (FcTec 2004).

In 1955, a scientist working for General Electric (GE), Willard Thomas Grubb, modified the original fuel cell design by using a sulphonated polystyrene ion exchange membrane as the electrolyte. Three years later another GE chemist, Leonard Niedrach, developed a method to deposit platinum onto this membrane. This device was known as the Grubb-Niedrach fuel cell. Here the first membrane electrode assembly (MEA) was developed. GE and NASA further developed this



fuel cell. The end result was the first commercial fuel cell that was used on the Gemini space project (FcTec 2004).

In the early 1960s, the aircraft manufacturer, Pratt & Whitney, set out on the task of reducing the weight and designing a longer lasting alkaline fuel cell. They wanted to improve on the GE proton exchange membrane fuel cell. Pratt & Whitney licensed the Bacon patents for the AFC and improved the original Bacon design. A result of this was that they won the contract from NASA to supply their alkali fuel cell for the Apollo spacecraft. Since then AFCs have been used on most U.S. space missions (FcTec 2004).

During the 1970s, developments followed to use fuel cell technology for systems on earth. This was one way to become less dependant on petroleum imports. Throughout the period of 1970 to 1980, research was dedicated to developing the needed materials, finding optimum fuel sources and drastically reducing the cost of fuel cell technology. In the years to come it is predicted that fuel cell systems will be installed in hospitals, schools, and office buildings and even used in powering cars (FcTec 2004).

## **2.3 Components of the DMFC**

To be able to design and construct a DMFC it is necessary to understand the structure and operation of a DMFC. Various methods are used in manufacturing DMFCs. Therefore, careful attention must also be given to this process. The electrical characteristics of the DMFC will also be discussed as well as the chemical processes taking place in the cell.

A direct methanol fuel cell consists of various components: the membrane that acts as an electrolyte, an anode with a catalyst, a cathode with a catalyst, gas diffusion layers and current collecting ribs or plates. The current collecting ribs or plates are

also known as flow field plates. All of these components are sandwiched together to form a single cell.

### **2.3.1 The membrane**

Most of the earlier fuel cells had liquid-based electrolytes. This is undesirable because the liquid electrolyte could leak out. Therefore, more attractive solid-state proton conducting membranes are used. They serve the same functions as the liquid electrolyte in the DMFC. These functions are: to minimize corrosion, to reject CO<sub>2</sub> to some degree and to separate the anode fuel reactant from the cathode oxidant. But the most important function of them all is to block electrons and allow high proton conductivity. A membrane must have a high temperature stability, good mechanical strength, low reactant diffusion and minimal dimensional variation with changing conditions. Protons can permeate through a membrane in a hydrated form. The better the hydration the better the permeation (Müller *et al.* 2003:851).

The DMFC uses a thin proton conducting polymer sheet as the electrolyte and this sheet is referred to as a proton exchange membrane (PEM) or a solid polymer electrolyte (SPE). Solid polymer electrolyte membranes were introduced to DMFC for the first time in the late 1980s. Problems were experienced with this introduction, and the electrodes were of major concern. Exposed catalyst areas had to be optimized in order to allow good ionic and electron conductivity. Different designs containing the membrane are still being experimented with (Hamnett 2003:306).

Cation conductive membranes are not only used in polymer electrolyte fuel cells but also for chlor-alkali electrolysis, especially if these membranes are highly conductive in protons. They are even being used in the normal electrolysis of water into hydrogen and oxygen.

The requirements for membranes used in DMFC are chemical and electrochemical stability and low methanol permeability, being less than  $10^{-6} \text{ mol.cm}^{-2}.\text{min}^{-1}$ . Several types of membranes have met this criteria, they are (Hamnett 2003:318):

- Perfluorinated polymer (Nafion)
- Polybenzimidazole (PBI)
- Polyvinylidene fluoride
- Styrene grafted and sulfonated membranes
- Sulfonated poly(ether ether ketone) and poly(ether sulfone)(PEEK)
- Zeolites gel film (tin mordenite)
- Membranes doped with heteropdyanions

Polymer electrolyte membranes are often classified under three categories, they are:

- Perfluorinated
- Partially fluorinated
- Non-fluorinated polymers

Nafion is one such material that is used to conduct protons and block electrons. Nafion is prepared by cleansing it and then converting it into an acid form by boiling it first in  $\text{H}_2\text{O}_2$ , then in  $\text{H}_2\text{SO}_4$ , and finally in ultra pure water.

Nafion is a perfluorinated polymer. It contains small amounts of sulphonic acid or carboxylic ionic functional groups. In short, Nafion is fluorocarbon polymer with side chains containing sulphonic acid groups. There are models that explain Nafion's main characteristics but its exact structure is complex. One explanation of Nafion is that it consists of discrete hydrophobic and hydrophilic regions. The hydrophobic regions consist of a fluorocarbon backbone that gives it chemical and mechanical stability. The hydrophilic regions consist of ionic groups and their counter ions. These regions are thought to be where water and proton movement occurs and also methanol crossover in DMFCs (Reeve 2002:34).

The resistance of the electrolyte in a DMFC should be  $R \leq 250 \text{ m}\Omega\cdot\text{cm}^2$ , this corresponds to approximately  $\sigma = 8 \cdot 10^{-2} \text{ S}\cdot\text{cm}^{-1}$  for a membrane thickness of about  $100 \text{ }\mu\text{m}$ . The most important requirement of a membrane is that it must not be electronically conductive (Neergat *et al.* 2003:858).

Perfluorosulfonic acid membranes have high proton conductivity, in the range of  $0,2 \text{ S}\cdot\text{cm}^{-1}$  at  $80^\circ\text{C}$  and have good chemical and mechanical stability. The stability of Nafion is obtained by a polytetrafluoroethylene (PTFE)-based structure that is chemically slow in reducing and oxidizing environments. A PTFE backbone does have regularly spaced perfluorovinyl ether pendent side chains terminated by a sulfonic acid group.

The two membrane structures given in Figure 3 have been compared by Neergat *et al.* (2003:862) to each other and it has been found that the water content and ionic conductivity of  $-\text{SO}_3\text{H}$  based membrane is higher than the  $-\text{COOH}$ -based membrane. Therefore, Flemion Asahi membranes have not often been used in fuel cells.

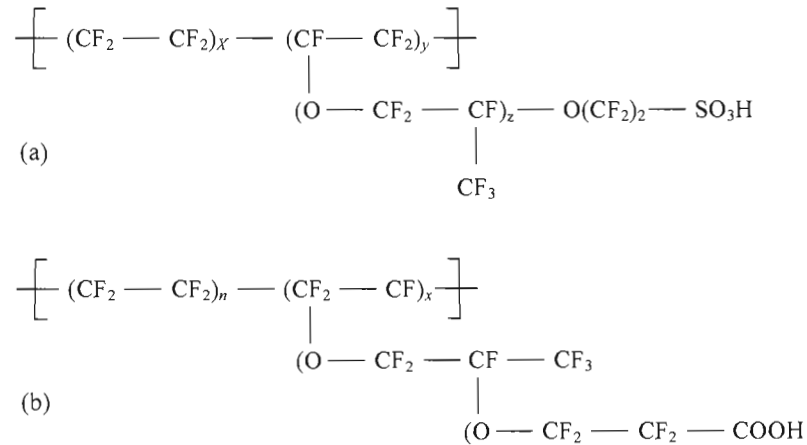


**Figure 3** (a) Chemical structure of Nafion ionomer (b) chemical structure of Flemion Asahi polymer ionomer (Neergat *et al.* 2003:862).

Nafion membrane has a high proton conductivity owing to the acid sites in the membrane. But this conductivity decreases rapidly when the operating temperature goes above 120°C owing to the loss of its water content (Chu *et al.* 2003:336). In contrast, Neergat *et al.* (2003:862) explain that at operating temperatures above 100°C, expansion of the polymer backbone is caused owing to softening of the fluorinated chain in the membrane structure. This leads to the increased permeation of methanol as well as water. This will be of importance in a DMFC because the anode side is completely submersed in a methanol-water solution.

The heteropoly acids possess a high inherent proton conductivity that increases the overall ionic conductivity of the membrane. Nafion membranes that contain silica particles as well as other inorganic materials showed an increase in ionic conductivity that is probably due to an increase of water uptake. A function of these hydrophilic additives is to improve water retention in the membrane (Jörissen *et al.* 2002:268).

Reeve (2002:32) reported a Nafion membrane that was modified with zirconium phosphate. The addition of zirconium phosphate ensured higher operating temperatures and reduced water loss from the membrane. Peak power densities of 380 and 260 mW.cm<sup>-2</sup> were obtained on air and oxygen feed respectively.

Another type of Nafion-based membrane can be prepared by recasting Nafion solution and by adding inorganic additives like heteropoly acids or other inorganic compounds and often silica particles.

Reeve (2002:iii) also mentioned that IonPower Inc. reported a new membrane with significant reduced methanol permeation for the use in DMFCs. The membrane is based on Nafion 117 with a modified barrier layer inside. DuPont have done similar work to a membrane. They have developed a proton exchange membrane with a thin layer of polymer that has a high ratio of backbone carbon atoms to cation exchange groups and act as a methanol barrier membrane. An acid-doped polybenzimidazole (PBI) membrane has also been demonstrated; it gives lower rates of methanol

crossover. This membrane can be used in high temperature DMFCs, with temperatures up to 220°C. This allows for better anode kinetics.

But the disadvantage of these PBI membranes is that their conductivity is lower than that of Nafion when operated at low temperatures. They only start to show good performance when the operating temperature is higher than 130°C. The power density obtained from DMFCs using a PBI membrane with a Pt-Ru alloy catalyst was 210 mW.cm<sup>-2</sup> at 200°C (Reeve 2002:32).

PBI membranes do have several advantages over Nafion, as follows:

- They have good proton conductivity.
- They have good mechanical flexibility at elevated temperatures.
- They have excellent oxidative and thermal stability.
- They have almost zero electro-osmotic drag.
- And they have low methanol permeability.

The conductivity, water content and methanol vapor permeability of the phosphoric acid-doped (PBI) type I membrane was measured. This was reported by Reeve (2002:45). The conductivity of the membrane increased in relative humidity at a constant temperature. It also increased in temperature at a constant humidity. A conductivity range of 0,01 to 0,04 S.cm<sup>-1</sup> was achieved between temperatures of 130 to 200°C at humidities of 0,04 to 0,4 %.

Studies done by Reeve (2002:45) showed that the electro-osmotic drag in the PBI membrane is almost zero and that it has low methanol crossover. They also studied the effects of current density on methanol crossover for the PBI membranes in DMFCs. Methanol crossover did increase with the increase of current density due to methanol drag.

The PBI type II membranes already had acid present in their structure and their conductivity was much greater than the type I membranes. The conductivity of the type II membranes increased from 0,03 to 0,08 S.cm<sup>-1</sup> in the temperature range of 130 to 200°C. The electro-osmotic drag of the type II membrane was similar to that of the type I membrane. The advantage of the type II PBI membrane is its superior ionic conductivity. Therefore, higher cell voltages were obtained at fixed current densities. Reports by Reeve (2002:45) on DMFCs showed that PBI type I and type II membranes operating at 200°C and at atmospheric pressure with a water to methanol ratio of 2:1, gave power densities of 160 mW.cm<sup>-2</sup> and 210 mW.cm<sup>-2</sup> respectively.

The performance of a DMFC that used acid blend membranes was also reported by Reeve (2002:32). These blended membranes were made from sulphonated PEEK with PSU(NH<sub>2</sub>)<sub>2</sub>; it gave power densities of 50 mW.cm<sup>-2</sup> with a cell voltage of 0,5 V at 80°C using 1,5 bar air pressure. Nafion only had a 2 percent better performance with the same experimental setup.

Membranes that are cross-linked co-polymers with styrene sulphonic acid have also been tested in DMFCs using carbon supported Pt/Ru catalysts. It was reported that there is an enhancement in the performance of these membranes at higher current densities. This is due to the superior electrical conductivity of the membrane.

#### **2.3.1.1 Thickness of a membrane**

An important factor that influences the performance of a membrane is its thickness. The ionic resistance in a fuel cell becomes less with a decrease in thickness of the membrane but this also results in a deterioration of membrane mechanical stability. A minimum thickness of 50 µm is necessary for the mechanical stability of Nafion. In a DMFC, the membrane cannot be too thin because if the membrane is thinner, methanol crossover increases. Thinner membranes have lower ionic resistance. It is a win/lose situation where a thicker membrane such as Nafion 120 allows less methanol crossover but it has a higher ionic resistance (Dimitrova *et al.* 2002:76).

### 2.3.1.2 Water uptake in a membrane

An important function of a perfluorinated membrane in a fuel cell is the interaction of that membrane with water and the uptake of water in the membrane. A membrane can swell between 20 – 50 percent with the uptake of water. Spontaneous phase separation in the membrane takes place because of the hydrophobic backbone and the hydrophilic head groups. When the membrane is in the hydrated condition, hydrophilic ionic clusters that are connected through water channels are formed. This forms the water network. The hydrophilic clusters contain the solvated  $\text{SO}_3^-$  groups, water and cations. The  $\text{SO}_3\text{H}$  groups can be seen in Figure 3(a). This water filled network is contained in a hydrophobic backbone and it has a high proton conductivity that resembles an aqueous electrolyte (Neergat *et al.* 2003:862).

The transport of protons in a membrane is a function of the water content of the membrane. The proton transfer through a membrane is similar to that of an aqueous electrolyte. Electro-osmotic drag through the cell and back diffusion of water from the cathode into the membrane influences the water content in the membrane. For every proton, a molecule of water ( $\text{H}_2\text{O}$ ), is also transported through the membrane.

When the membrane takes up water, swelling occurs and plays a role in the membrane properties. Proton conductivity greatly depends on the amount of water absorbed. Methanol permeation across the membrane is also dependant on the amount of water present in the membrane. Water also influences the ionomer microstructure, clusters and channel sizes. This modifies the mechanical properties of the membrane (Dimitrova *et al.* 2002:77).

Apparently the thickness of the membrane does not play a role in the diffusion barrier of water (Dimitrova *et al.* 2002:81).



### **2.3.1.3 Equivalent weight of a membrane**

The acid concentration of a specific membrane is characterized by the equivalent weight, EW, of the membrane. The equivalent weight is the grams of dry polymer.mol<sup>-1</sup> of ion exchange sites (Scott *et al.* 2000:119).

### **2.3.1.4 Different membranes**

Hydrocarbon membranes can be used at low temperatures, but they do have poor chemical stability. These membranes are easily synthesized at a low price unlike commercialized perfluorinated polymers like Nafion, Flemion and Aciplex (Fujiwara *et al.* 2002:4084).

Ma *et al.* (2003:328) reported on good results that were obtained with new membranes. They developed a novel low cost nano-porous proton conducting membrane that consisted of a high surface area inorganic powder such as silica and polymer binders like polyvinylidene fluoride (PVDF). Their experiments showed that the new membrane had much lower methanol crossover and that its conductivity was four times higher than Nafion.

Test run on membranes prepared by Ma *et al.* (2003:334) shows that their membrane had a high open circuit voltage (OCV) and had good performance. They claim that the good performance is due to lower methanol permeation. Their membrane was made from Nafion/Pt/Pd-Ag/Pt/Nafion.

Pervaporation membranes were also examined for use in a DMFC. A study on the ionic conductivity and methanol permeation properties of these membranes showed that better results were obtained than with Nafion membranes.

Hamdan and Kosek (1999:3) developed a low cost, high methanol exclusion proton exchange membrane that was based on a membrane that contained pre-cross linked fluorinated base polymer films and subsequently grafted the base film with selected

materials. The technique used for grafting involved the use of beta and/or gamma radiation. The films were then sulfonated to provide proton conductivity.

According to Shao *et al.* (2002:147), polybenzimidazole (PBI)/H<sub>3</sub>PO<sub>4</sub> blend membranes can block methanol permeation and operate at higher temperatures, in the order of 130 - 150°C. But a disadvantage with this type of membrane is that the phosphoric acid is not covalently bound to the polymer matrix and can therefore leach out of the membrane. This results in a decrease in proton conductivity.

Wu *et al.* (2002:251) prepared polyvinyl alcohol (PVA) blend polystyrene sulfonic acid (PSSA) membranes. The results that they obtained from these membranes showed that better methanol crossover resistance was obtained but also lower ionic conductivity.

#### **2.3.1.5 Modified membranes**

Almost all membranes obtain their conductivity from the water content taken up into the membrane structure. Other additions can be made to a membrane in order to improve its properties. One such improvement is the introduction of inorganic fillers to a perfluorosulfonic acid (PFSA) electrolyte solution. Inorganic fillers that were tested were molybdophosphoric acid, tungstenphosphoric acid and different types of silica powders. The properties of the membranes that were changed by adding these fillers were the proton conductivity, the methanol permeation as well as the water permeation (Dimitrova *et al.* 2002:76).

Kim *et al.* (2002:130) reported on a modified Nafion membrane that exchanges H<sup>+</sup> with cesium ions. They also mentioned the doping of Cs<sup>+</sup> could reduce methanol permeation.

Kim *et al.* (2002:130) also reported a membrane made from sulfonated polystyrene. This membrane is rigid in nature and shows a methanol permeability of about 70 percent less than that of Nafion. This sulfonated polystyrene membrane has better

water uptake and therefore higher proton conductivity but it does have poor chemical and thermal stability.

The researchers, Ma *et al.* (2003:328), mentioned the following membranes for reducing methanol crossover: acid-doped polybenzimidazole (PBI) membranes, cross-linked sulphonated-substituted polyoxiphenylenes (POP) membranes and Nafion/Pt/Pd/Pt/Nafion composite membranes where the Pt/Pd/Pt film is 25  $\mu\text{m}$  thick.

Metallic blocking layers can be introduced in a membrane in order to minimize the permeation of methanol through the membrane. Jörissen *et al.* (2002:268) investigated organic-inorganic composite membranes containing Zr-phosphonates, tin-doped mordenites, Zeolites or silica. They observed a reduction in methanol crossover in these membranes. These researchers also doped Nafion with  $\text{Cs}^+$  and also observed a reduction in methanol crossover.

Ma *et al.* (2003:328) report on both a Nafion-silica composite electrolyte membrane and a Nafion-zirconium phosphate composite membrane that had lower methanol permeation than Nafion and could be operated at temperatures of 140-150°C.

They also mentioned a modified Nafion 117 membrane where methanol permeation was suppressed by dispersing Pt nano-crystal particles in the membrane.

They also gave reports on impregnating a Nafion 117 membrane with poly(1-methylpyrrole) by in situ polymerization. This method had the result of less methanol crossover but also less proton conductivity.

Doping an inexpensive, non-conducting material that serves as the mechanical structure, with a small amount of an ion-transporting polymer that allows the membrane to receive its chemical function, can produce a cheaper membrane. The materials used for membranes are not limited to polymers. Inorganic type materials can also be used (Scott *et al.* 2000:120).

### 2.3.2 The anode

The function of the anode is to make the flow of electrons available to the external circuit. The anode is coated with a catalyst to ensure that the oxidation of methanol does occur. The catalyst used on the anode is a platinum/ruthenium alloy. The catalyst is also sometimes deposited onto the membrane by using the impregnation reduction (IR) method. The impregnation reduction (IR) method consists of a cation exchange membrane with a pre-exchangeable metal specie which it is immersed in a reduction solution that reduces and displaces the metal towards the outer surface of the membrane. This whole procedure can be conducted below 80°C in a wet state. Fujiwara *et al.* (2002:4079) reported that the IR method was developed for the direct contact of the PEM and the metal electrodes. Another method used is by hot pressing the membrane and electrodes to form a membrane electrode assembly (MEA). An efficient catalyst for methanol oxidation should be able to dissociatively absorb water at low potentials and it should also be able to remove poisoning elements from its surface.

Insufficient performance of the electro-catalyst in a DMFC is also a limiting factor in the development of these cells. This is applicable on the anode catalyst where few electrode materials are capable of oxidizing methanol with an acid electrolyte. Only platinum based metals give high enough stability and activity to be used as catalyst. Alloying Pt with other metals is the most commonly used method for increasing the performance of the catalyst in ensuring the best electro-oxidation of methanol (Neergat *et al.* 2003:867).

An efficient catalyst for methanol oxidation should be able to dissociatively absorb water at low potentials and it should also be able to remove poisoning elements from its surface.

In the FY Progress Report (2003:2) it is stated that noble metals such as nickel and cobalt are excellent for the catalysis of hydrogenation and dehydrogenation of

organics but they are not stable in an acidic media. Therefore, creating a catalyst consisting of an alloy containing some mixtures of Ni, Co, Zr, Pt or Ru can provide a suitable catalyst for use in DMFCs. But Pt/Ru alloy is still the most widely used catalyst owing to its activity to the polarization characteristics of methanol electro-oxidation.

Other Pt alloy catalysts are also available. They are Pt/Ru/Os and Pt/Ru/Os/Ir. These catalysts have better performance than that of Pt/Ru alone, but the interest remains in improving the Pt/Ru alloy catalyst. Reeve (2002:28) stated that experiments were done on catalysts containing the five elements Pt, Ru, Os, Ir and Rh. This study showed that the catalyst Pt/Ru/Os/Ir was the most active – 40 percent higher current densities were obtained than for the Pt/Ru catalyst at 400 mV. A DMFC with this Pt/Ru/Os/Ir catalyst operated at 60°C with 1 mole of methanol solution. It gave superior performance compared to that of a commercial Pt/Ru catalyst. Reeve (2002:28) reported that at relatively low temperatures, power densities of 120 mW.cm<sup>-2</sup> were obtained compared to the power density of 60 mW.cm<sup>-2</sup> for Pt/Ru.

The fact that the DMFC uses a noble metal alloy for the anode catalyst makes it even more expensive to manufacture membrane electrode assemblies for this cell.

Studies have indicated that catalysts consisting of Pt/Ni, Pt/Co and Pt/Fe with rotating disc electrode measurements in the presence of methanol have indicated that they are more tolerant to methanol than platinum alone (Neergat *et al.* 2003:872).

The catalysts loading for hydrogen PEM fuel cells have been reduced in recent years. Power densities in excess of 500 mW.cm<sup>-2</sup> have been obtained with catalyst loadings of less than 0,2 mg.cm<sup>-2</sup>. A target of less than 1 mg.cm<sup>-2</sup> is set out for DMFCs.

It is stated by Neergat *et al.* (2003:857) that higher catalytic loadings are required in DMFC to enhance cell performance. The high catalytic loadings are used to counter the effect of the low anode electro catalytic activity. The low activity is due to the

low electro catalytic oxidation rate of methanol on the anode catalyst. Another reason for higher catalytic loadings is the fact that the reaction of methanol on platinum is not a first order reaction. A number of reactions need to take place before methanol is completely oxidized.

Catalysts like Pt/Ru are expensive, therefore, these catalysts are coated onto an electrode. Another reason for depositing the catalyst on the electrode is that the thickness of the layer can be controlled. If the layer is too thick, reduction of electro-catalyst utilization occurs and this causes an increase in ohmic and mass transport polarization (Aricò *et al.* 2002:3724).

Jeng and Chen (2002:374) observed that the thickness of the anode catalyst layer affects the anodic over-potential. Therefore, increasing the thickness of the anodic catalyst may enhance the performance of a DMFC. This stands in contrast with the fact that catalyst loadings are being minimized.

Ma *et al.* (2003:335) make the assumption that it is more important to reduce methanol crossover than it is to increase the catalytic loading at the electrodes in order to improve the performance of a direct methanol fuel cell. They accomplished this by using their fabricated Nafion/Pt/Pd-Ag/Pt/Nafion composite membrane.

The most common use of heterogeneous catalysts in fuel cells is the supporting of precious metal alloys on carbon nano-composites of high surface area. Vulcan VC 72, Ketjen black and Acetylene black are the most commonly used catalyst supports.

Unsupported catalysts have higher current densities for the oxidation of methanol but supported catalysts have higher mass specific catalytic activities. Supported catalysts do have a smaller crystallite size and higher surface area compared to unsupported catalysts. This argument is supported by the conclusion of Neergat *et al.* (2003:873). They said that carbon supported catalysts do have superior performance at elevated temperatures compared to that of unsupported catalysts in DMFCs. The thickness of

an electrode in supporting the catalyst plays an important role in the mass transport of the fuel cell.

Another interesting result obtained by Shimizu *et al.* (2004:5) is that the performance of the DMFC is better with unsupported catalysts than with supported catalysts.

### **2.3.3 The cathode**

The function of the cathode is to enable the flow of electrons from the external circuit to the catalyst. The catalyst at the cathode ensures that reduction of oxygen does occur where the returning electrons are just one of the elements required in the oxygen reduction reaction (ORR). The other elements that must be present at the cathode are hydrogen protons and free electrons. The structure of the cathode is similar to that of the anode. It can also be supported or unsupported. Microporous plastics can be used as a supporting layer for the cathode catalyst instead of carbon paper. It was found by Reeve *et al.* (2004:1) that the oxygen reduction reaction for a platinum electrode with a catalyst loading of  $0,88 \text{ mg.cm}^{-2}$  on a spun-bonded polyethylene substrate had a current density of  $280 \text{ mA.cm}^{-2}$  at  $0,64 \text{ V}$ , with the operating temperature of  $70^{\circ}\text{C}$ . Platinum is the most commonly employed cathode catalyst in low temperature fuel cells. No other promising catalyst that can replace the cathode catalyst has been found thus far.

Catalyst loading is quite high for the cathode compared to that of the anode. Platinum loadings in the order of  $4,6 \text{ mg.cm}^{-2}$  are used whereas loadings of  $1\text{-}3 \text{ mg.cm}^{-2}$  are used for the anode.

### **2.3.4 The gas diffusion layers**

The energy conversion reactions of a fuel cell take place on the electrodes. A porous gas diffusion electrode must be able to provide a large reaction area with a minimum of mass transport resistance for the access of reactants and the removal of products.

Electrode potential changes with the amount of current drawn per unit area, therefore, a change in the electrode area has an effect on total cell performance. This is the reason why smooth platinum electrodes can only give a small amount of current per square centimetre but porous electrodes can deliver more current per  $\text{cm}^2$ .

The anode diffusion layer has the role of facilitating the flow of methanol to the anode catalyst layer. In order for this to happen the anode diffusion layer is made hydrophilic. The porosity of the anode diffusion layer is made big enough to ensure the escape of  $\text{CO}_2$  bubbles from the anode.

These hydrophilic electrodes are made of sintered metal powders, see Figure 4. The gas diffusion layers of these electrodes have larger pores than the reaction layer. The electrolyte is contained in the small pores by capillary forces when the pressure of the reactant gasses are higher than that of the electrolyte. Porous metal electrodes are heavy but they do have high conductivity. This is a great advantage for monopolar plate electrodes where the current is collected from tabs at the edges of the electrodes unlike the hydrophobic carbon powder electrodes that are only acceptable for bipolar-flat plate cell configuration (Kordesch & Simander 2001:38).

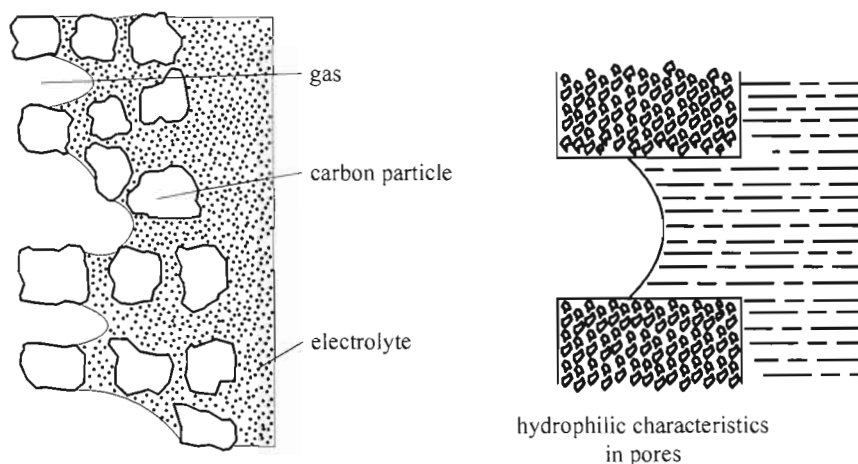


**Figure 4** Section through enlargement of a hydrophilic gas diffusion electrode (Kordesch & Simander 2001:39).



The gas diffusion layers must be highly conductive to the flow of electrons. The internal resistance of a fuel cell greatly depends on the conductivity of these diffusion layers. The reason for using a carbon porous type material instead of a metal is because of the stability of carbon in fuel cells.

In some electrode structures a carbon cloth diffusion layer is used. It is believed by Scott *et al.* (1999:205) that the carbon cloth offers resistance to the methanol diffusion to the catalyst layer. Therefore, the current densities observed were less than in the experimental cell that did not make use of a carbon cloth diffusion layer. It has been shown by them that the current densities are directly associated with the diffusion of methanol at the catalyst.

The cathode diffusion layer has the role of bringing oxygen to the active catalytic area and expels the reaction-formed water from that same site. The diffusion layer is made hydrophobic in order to accomplish this.

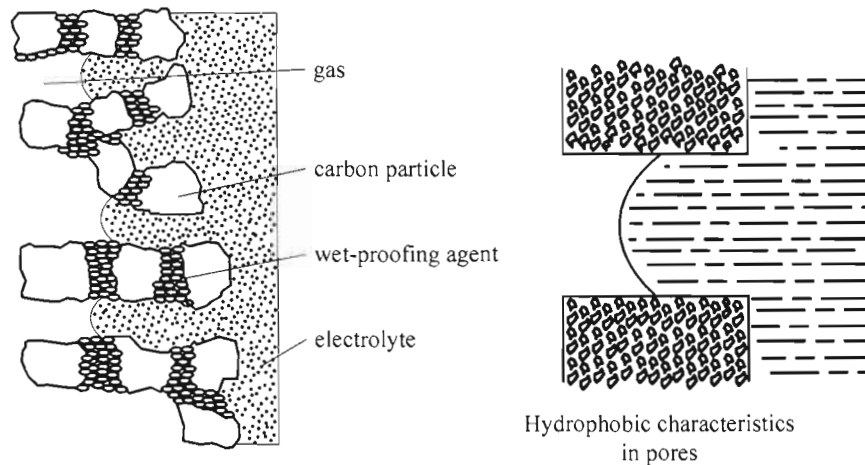


**Figure 5** Section through enlargement of a hydrophobic gas diffusion electrode (Kordesch & Simander 2001:39).

The hydrophobic electrodes are made from fine carbon powder bonded with a plastic material such as polytetrafluoroethylene (PTFE), see Figure 5. The carbon powders are light and they have large surface areas. They are also suitable for the deposition

of active catalyst onto them. A wire screen can be added to serve as a current collector to improve the conductivity of the carbon. A highly hydrophobic porous gas diffusion layer and an electrolyte wettable thin layer are two layers that can be distinguished in such a PTFE bonded carbon electrode. The electrochemical reaction takes place where these two layers meet, and the catalytic active material must also be present. The electrolyte is prevented from penetrating deeper into the electrode structure by the hydrophobicity of the diffusion layer. This keeps the pores free and helps facilitating gas access to the reaction site.

### **2.3.5 Current collecting ribs and plates**

Graphite and stainless steel are the most commonly used bipolar plate materials in DMFC stacks. These plates have flow fields in them to distribute electrode reactants and products. The required characteristics for bipolar plates are low cost, lightweight, small volume and long-term mechanical and chemical stability. Stainless steel does have the advantage of relatively low cost and its high density has the result of using thinner sheets for the bipolar plates. Stainless steel is still rather heavy weight whereas graphite plates will ensure a stack with lower weight. The disadvantage of using stainless steel is the corrosion factor present when used in fuel cells. This corrosion leads to catalyst poisoning and increase in membrane resistance. Passivating layers are also formed on the surface of the stainless steel sheet, and this results in high contact resistance (Neergat *et al.* 2003:875).

## **2.4 The complete single DMFC**

The following few sections will discuss the elements required in order to make up a single cell and how these parts are put together in order to have an operational DMFC.

### 2.4.1 The membrane electrode assembly (MEA)

The MEA of a DMFC can be divided into two regions, the first being the membrane region and secondly the catalyst region that provides a catalytic site for the oxidation of methanol. The diffusion layer that is composed of a highly porous and conducting material is added to either side of the membrane.

There is normally a process followed in putting together the first two regions discussed above. Each electrode is placed on either side of the membrane. The membrane, Nafion 117, normally undergoes pretreatment. The pretreatment involves boiling the membrane for one hour in various concentrations of  $\text{H}_2\text{O}_2$  and  $\text{H}_2\text{SO}_4$  separately and then washing it in boiling Millipore water. The assembly is then hot pressed at a temperature of typically  $135^\circ\text{C}$ .

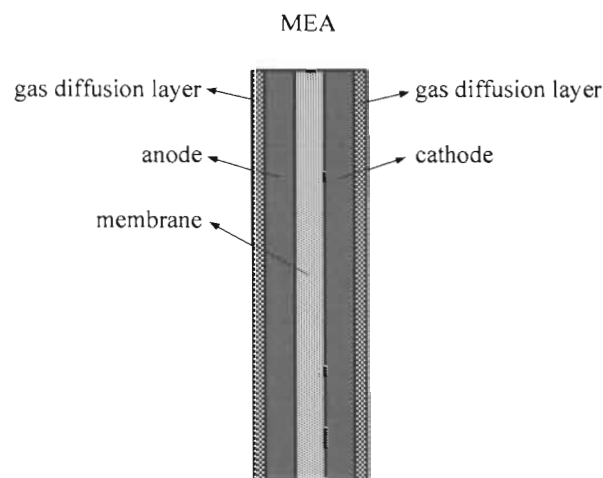
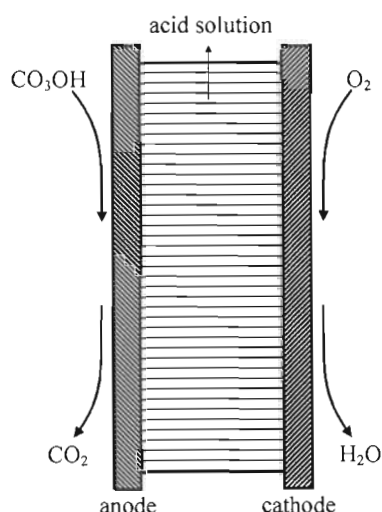


**Figure 6** Membrane electrode assembly of a DMFC (Wei *et al.* 2002:365).

Advanced MEAs have two extra layers attached to the above mention assembly, see Figure 6. These layers are called gas diffusion layers or GDLs. The GDLs are added to the outside of each electrode. It is important that the GDLs provide good electrical contact to the electrode. The GDL used at the anode should be highly porous in order for the methanol solution to reach the catalyst and also to make it

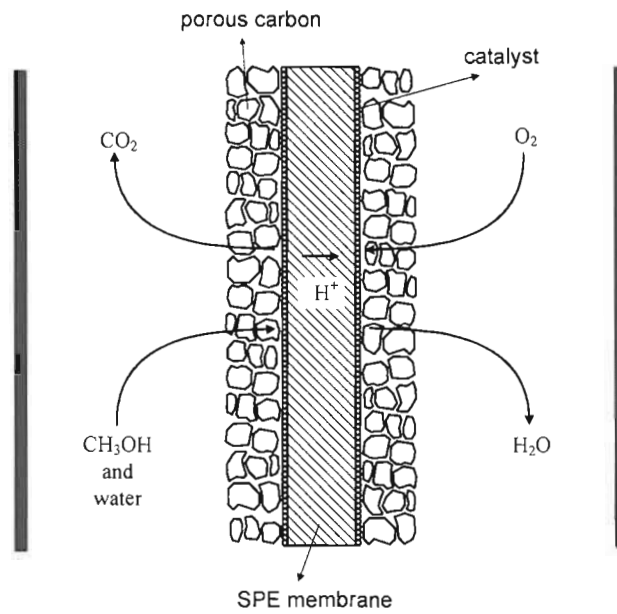
easy for the  $\text{CO}_2$  to leave the catalyst area. The gas diffusion layers normally consist of a carbon mixture with polytetrafluoroethylene (PTFE). The GDL at the anode side must be hydrophilic while the GDL at the cathode must be hydrophobic.

Figure 7 shows the most basic cell design. Shell, Exxon and Hitachi initially designed it. In this design the electrolyte is still in a liquid form. It is difficult to have a porous electrode structure in such a design (Hamnett 2003:306).



**Figure 7** A simple direct methanol fuel cell design (Hamnett 2003:306).

Figure 8 illustrates a cell MEA structure where a catalyst impregnated carbon polytetrafluoroethylene (PTFE) composite is being used the form the gas diffusion electrodes. It can be seen from this figure that the membrane is not electrochemically in contact with all of the catalyzed carbon. Even the PTFE used for structural support of the porous layer, tends to block access. This problem can be overcome by directly mixing the electro-catalyst and ionomer with the PTFE but still some of the ionomer does not penetrate into the smaller pores of the catalyst. Increasing the pore diameter of the catalyst layer and decreasing the size of the ionomer colloidal particles can ensure a more optimal use of the catalyst (Hamnett 2003:306).



**Figure 8** A solid polymer electrolyte membrane for a DMFC with catalytic GDLs (Hamnett 2003:306).

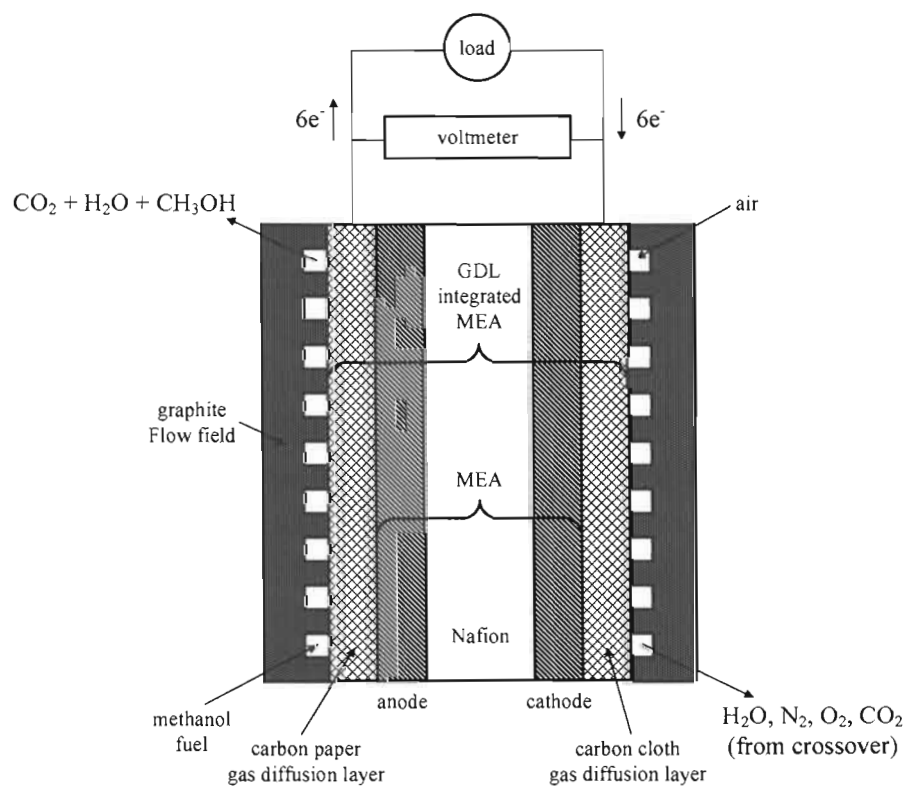


**Figure 9** A single DMFC assembly (Liu & Smotkin 2002:50).

### 2.4.2 Structure of a single DMFC

The direct methanol fuel cell (DMFC) consists of a current collecting plate, gas diffusion layer, anode, membrane, cathode, another gas diffusion layer and the next current collecting plate sandwiched together as illustrated in Figure 9. The current collecting plates serve the function of distributing the fuel or oxidant to the active areas via flow fields. These flow fields can be in the form of straight ribs or serpentine. If the fuel cell requires additional heating, heaters can be mounted inside or behind each graphite block in order to heat the cell up to its required operating temperature or heat can be applied to the methanol solution that circulates through the stack.

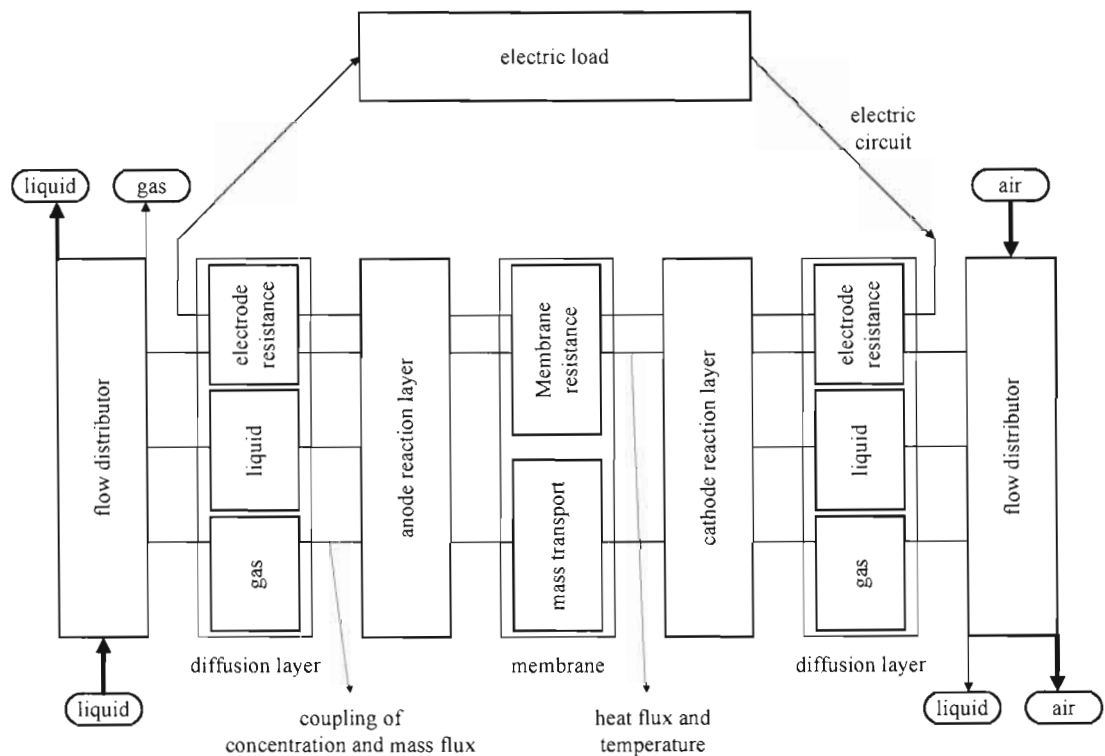


**Figure 10** Block diagram of a DMFC (Siebke 2004:5).

Figure 10 shows all the elements required to make up a DMFC. It comprises flow fields, the diffusion and reaction layers of both the anode and the cathode and the polymer electrode membrane.

## **2.5 Electrical characteristics of the DMFC**

A DMFC is a dynamic electrical power source. It cannot supply a constant voltage or nearly constant voltage such as other power sources for varying load currents. But there is a region that can be utilized in order to supply power. This region is called the ohmic polarization region. Within this ohmic polarization region of the fuel cell voltage drops of 200 to 500 mV per cell under varying load currents can occur. If the DMFC design follows that the average voltage per cell in the stack will not be taken below 200 mV then to obtain a total stack output voltage of 12 volts, a total of 60 cells will be needed. Now if less power is required from the stack the voltage per cell will increase. If the average voltage per cell reaches 500 mV per cell then the total stack voltage will reach a value of 30 volts. It is clear that the stack voltage varies by 18 volts for operation between full power and partial power range. Full power and partial power range will be discussed in section 2.5.6.

### **2.5.1 Cell voltage versus current density**

The thermodynamic reversible potential at 25°C for the overall cell reaction in the DMFC is 1,214 V. The hydrogen fuel cell has a reversible potential of 1,23 V.

Figure 11 shows the characteristic performance curve of a DMFC that was operated by Scott *et al.* (2000:127) with a 2 mole methanol solution. It can clearly be seen in the figure that the limiting current density region is almost constant without any rapid decrease in value. This is the region where the cell voltage is low.

### 2.5.2 DMFC output voltage characteristics

The voltage output of a DMFC can decrease under two conditions. The first is given by Qi and Kaufman (2002:178) where they did an experiment by loading a cell with a current density of  $280 \text{ mA.cm}^{-2}$  to a no load condition and another experiment with a current density of  $312 \text{ mA.cm}^{-2}$  to a no load condition. The temperature of each experiment was  $40^{\circ}\text{C}$  and  $60^{\circ}\text{C}$  respectively. In each experiment the load was removed in order to monitor the open circuit voltage. It was observed that the peak OCV was only reached after ten seconds. Each cell did not stabilize at the peak OCV but both of them had a decline in voltage whereafter stability was reached after three minutes. There was a difference of more than 0,1 volt between the peak OCV and the stabilized OCV. It was also clearly stated by these researchers that the peak voltage obtained when no load is connected to the fuel cell should not be taken as the real OCV but the stabilized OCV.

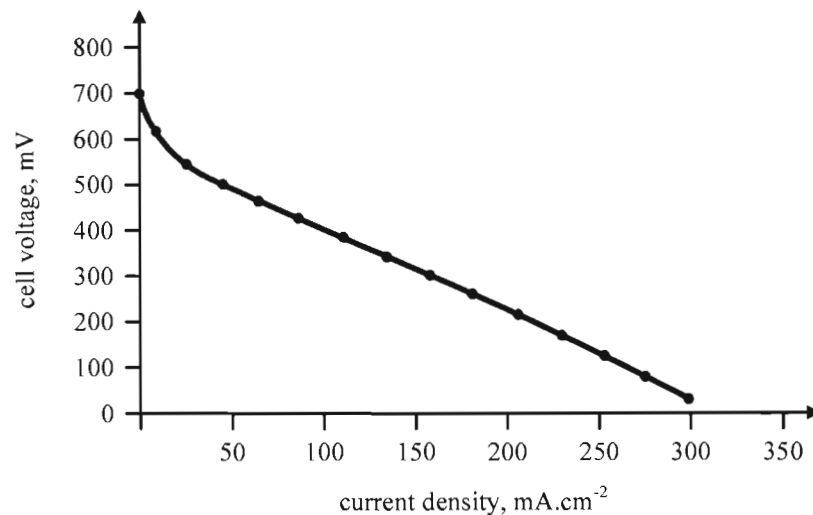


**Figure 11** DMFC performance curve (Scott *et al.* 2000:127).

The second condition where the output voltage of a fuel cell decreases is where the cell is loaded. The reduction in the cell potential is a result of polarization of electrodes or internal cell resistance. Maximum power can be obtained from a fuel cell at lower output voltages.



### 2.5.3 OCV compared to the thermodynamically expected value

The open circuit voltage of a direct methanol fuel cell is in the range of 0,6 – 0,7 volt. It is much lower than the thermodynamically expected value that is in the order of 1,2 volt. This is due to the formation of mixed potentials at the electrodes because of undesired side reactions at both of the electrodes. At the anode, COH groups that are absorbed at the platinum surface are formed. This limits further conversion of methanol and results in an increase of the anodic potential. At the cathode, crossover methanol is also oxidized (Sundmacher *et al.* 2001:338).

### 2.5.4 Performance of a cell

Neergat *et al.* (2003:860) stated that recent literature claims that by applying proper operating conditions and cell design, cell performance could be increased.

Figure 12 represents the allocation of the efficiency losses in the DMFC. Müller *et al.* (2003:854) stated that each loss was measured by using a combination of tools like an AC impedance spectroscopy and gas chromatography.

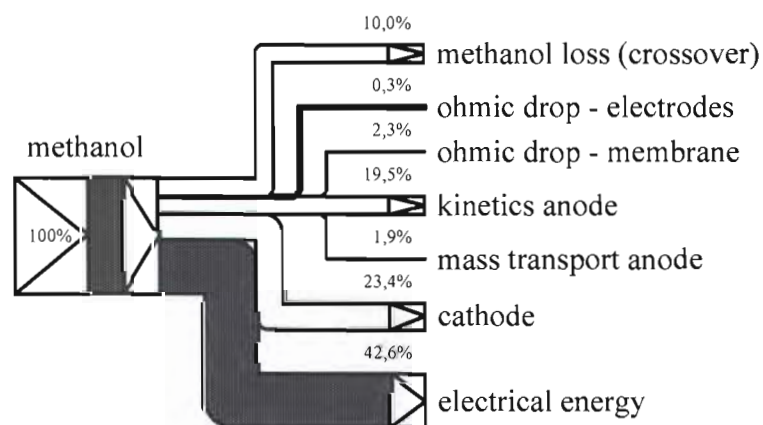


**Figure 12** Allocation of efficiency losses in a DMFC (Müller *et al.* 2003:854).

The performance of a DMFC is dependant on the following most important factors (Thomas *et al.* 2002:3741):

- Electro catalyst activity of the anode,
- Ionic conductivity and resistance to methanol crossover of the proton conducting membrane,
- Water management on the cathode side of the cell.

It is known that for the anode catalyst in a DMFC, Pt and Ru is used as the active material in an alloy state. Different amounts of each of the metals in the alloy do have an effect on the cell performance. Therefore, an optimum cell performance can be reached by using the correct alloy mixture. It is thought that the activity of Ru towards the dissociative adsorption of methanol is increased at higher temperatures (Fujiwara *et al.* 2002:4083).

The most important components in the DMFC are the anode and the membrane. Voltage losses that occur at the anode are in the order of 0,3 V. Anode performance also deteriorates with methanol oxidation. This is a contribution to the reduction in practical energy density. The theoretical cell voltage of a DMFC is 1,2 V and the theoretical energy density of methanol is 6094 Wh.kg<sup>-1</sup>. But the practical energy density is only 1500-3100 Wh.kg<sup>-1</sup> with an operating cell voltage of 0,4 V (Chu & Jiang 2002:591).

According to Valdez and Narayanan (2004:1) the performance of a DMFC at that time was 470 mV at a current density of 150 mA.cm<sup>-2</sup> operating at 60°C with a 5 l.min<sup>-1</sup> ambient airflow.

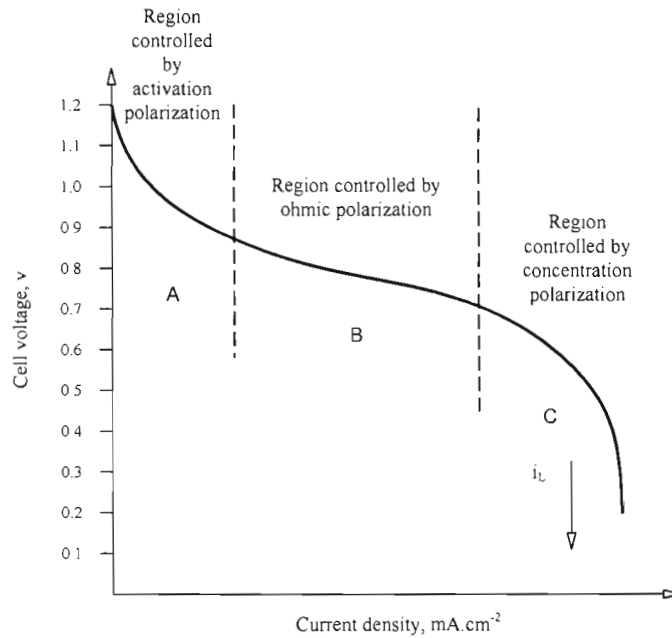


**Figure 13** Performance curve of a DMFC (Shen *et al.* 2003:204).

### 2.5.5 Potential of a cell

Referring to Figure 13: It is already known that there are three regions in the performance of any fuel cell. The cell voltage in region A is dominated by the electrochemical kinetics. It is called the activation controlled current density region. If the load current is increased further, the cell voltage decreases owing to the internal resistance of the cell in region B. This region is called the ohmic controlled current density region. The system then approaches limiting current density in region C. The cell voltage breaks down in this region. Limiting current density depends mainly on reactant mass transport.

Any power source has two important characteristics. They are the internal resistance and output voltage of that specific power supply – the output voltage changes with the operating current required. This voltage/current relationship gives a power source the ability to support the electrical power needed (Shen *et al.* 2003:205).

The DMFC voltage is affected during operation by the following:

- Ohmic losses
- Over voltages at the electrodes
- And by the formation of mixed potentials at the cathode

The total potential of a cell is obtained by the sum of all the over potentials subtracted from the ideal cell potential. Reaction over potentials and ohmic losses due to the conduction of protons in the membrane and electrons in the diffusion layers will have an influence on the available cell potential (Siebke *et al.* 2004:2). Cell voltage is represented by the following equation:

$$V = E - \eta_a - \eta_c - IR - \eta_{crossover} \quad (1)$$

where  $V$  = observed cell voltage

$E$  = ideal standard potential

$\eta_a$  = anode over potential

$\eta_c$  = cathode over potential

$I$  = value of current

$R$  = resistance of cell

$\eta_{crossover}$  = cell voltage drop by methanol crossover

The DMFC open circuit cell voltage can in theory be determined by the Nernst equation. This is possible if the polymer electrolyte membrane prevents any mixing of anode and cathode reactants.

$$U_{cell,o} = U_{cell,o}^{\theta} + \frac{RT}{6F} \ln \left\{ \left( \frac{a_{CH_3OH} a_{H_2O,a}}{a_{H_2O,a}^2} \right) \left( \frac{P_{CO_2,a}}{1,0} \right)^{-1} \left( \frac{P_{O_2,c}}{P^{\theta}} \right)^{\frac{3}{2}} \right\} \quad (2)$$

where  $a_i$  refers to activity of the species

and  $i = \text{CO}_2, \text{CH}_3\text{OH}, \text{H}_2\text{O}$  and  $\text{O}_2$

The equation predicts increasing cell voltage for increasing liquid phase methanol activity at the anode.

Figure 14 shows the different current densities obtained with changing methanol concentrations at fixed values of cell voltages. It is taken that the main cause of voltage reduction with increase in current density is due to anodic polarization (Scott *et al.* 1999:212).

There is an over potential barrier of 0,25 – 0,3 V to overcome before significant oxidation currents can be obtained at the anode. Thereafter, the current density rises exponentially with an over potential that is given by a Tafel slope of 100 – 140 mV<sup>-1</sup>.

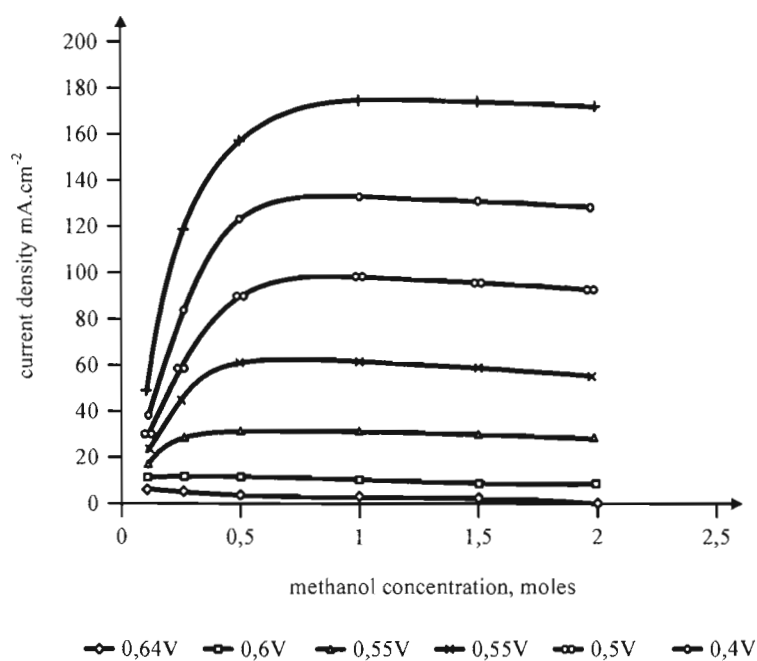


**Figure 14** Variation of current density with methanol concentration (Scott *et al.* 1999:212).

Table 2 shows the effects that different methanol concentrations have on the cell potential with the reduction of oxygen at carbon supported Pt gas diffusion electrodes at a temperature of 80°C.

**Table 2** Effects of methanol concentration on reduction taking place at the oxygen electrode (Reeve 2002:16).

Methanol concentration, M	Potential at 100mA.cm <sup>-2</sup>	Potential at 300mA.cm <sup>-2</sup>
0	770 mV	650 mV
0,03	700 mV	600 mV
0,1	620 mV	530 mV
0,3	540 mV	480 mV
1	510 mV	430 mV
2	500 mV	390mV

Reeve (2002:37) mentioned that pressurizing the oxygen side of a DMFC can even increase the cell voltage, the crossover of methanol is also reduced by this action.

Cell efficiency is defined as the product of the voltage efficiency, cell performance and the faradaic efficiency as well as the current efficiency. Processes at both electrodes affect the voltage efficiency, whereas, faradaic efficiency is a direct measure of methanol crossover and it is affected by the membrane (Müller *et al.* 2003:805).

Faradaic efficiency is defined by the following equation:

$$\eta_{far} = \frac{I_{cell}}{(I_{crossover} + I_{cell})} \quad (3)$$

The methanol to electrical efficiency of the operating cell can be defined as a product of the voltage efficiency and the efficiency of methanol utilization in the current generation process. This efficiency is given by the following equation:

$$\eta_{stack} = \left( \frac{V_{load}}{V_{in}} \right) \left( \frac{I_{load}}{I_{load} + I_{cr,l}} \right) \quad (4)$$

where  $\eta_{stack}$  = the efficiency of the operating stack

$V_{in}$  = the thermo neutral potential

$V_{load}$  = the cell voltage under load

$I_{load}$  = the operating current density

$I_{cr,l}$  = the crossover current density measured at the operating current density

### 2.5.6 Power density of a cell

Improvement in DMFC performance has shown significant growth during the past decade. Peak power densities of 450 and 300 mW.cm<sup>-2</sup> were obtained under oxygen and air feed operation respectively. Stack power densities of 1 kW.dm<sup>-3</sup> and overall efficiency of 37 percent at 0,5 V per cell have been obtained (Scott *et al.* 2004:67).

Reports were made by Reeve (2002:28) on the operation of a DMFC at 145°C. The DMFC that was tested used a Nafion-silica composite electrolyte which was 80 µm thick. The anode was carbon supported with a Pt/Ru catalyst loading of 2 mg.cm<sup>-2</sup>. A peak power density of 240 mW.cm<sup>-2</sup> was obtained at 600 mA.cm<sup>-2</sup> at 0,4 V. They suggested that even higher power densities could be achieved by reducing the internal resistance of the cell. At the lower operating temperature of 75°C, the cell delivered 200 mA.cm<sup>-2</sup> at 350 mV.

Dohle *et al.* (2002:322) have found that at elevated temperatures (77°C) the power density is four times higher than under ambient conditions (22°C). But the operating temperature is limited due to the evaporation of water at the cathode. This is also dependant on the cathode pressure.

A DMFC can operate at full power range. This is the range where the cell supplies its greatest power. The voltage of a single cell operating at full power is about 300 mV. The DMFC can also operate at partial power range. The cell voltage in this range is in the order of 500 mV. The partial power range is about 50 percent of the full power range.

It can clearly be seen from the voltage values given above that when a cell stack is operated at full power range, more cells will be needed in the stack to obtain a required output voltage level. Whereas, if a cell stack is operated at partial power, less cells will be needed in the stack to obtain the same voltage level but fewer power is available (Dohle *et al.* 2002:275).

Figure 15 shows the influence that temperature has on the performance of the cell at partial and full power operation. The nominal cell power that is in the order of a 100 to 200 mW.cm<sup>-2</sup> is set to the reference point of 1 at 110°C and a partial load at 500 mV.

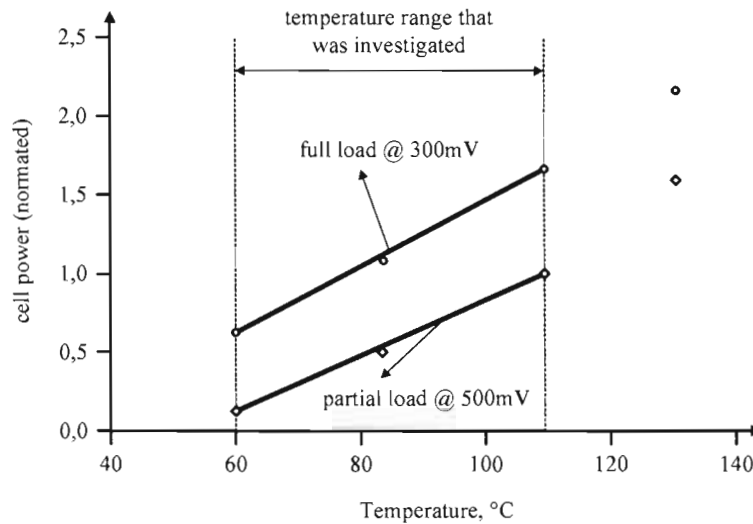


**Figure 15** Influence of temperature on cell power (Dohle *et al.* 2002:277).



Power densities of 450 and 300 mW.cm<sup>-2</sup> under oxygen and air feed have been obtained by Shulka *et al.* (2002:43) from their experimental direct methanol fuel cells. But these results have been obtained at high temperatures far above 100°C and higher cathode feed pressures. Another result reported by these researchers was 200 mW.cm<sup>-2</sup> at an operating cell potential of 0.5 V. The operating temperature for this cell was in the order of 100°C under pressurized cathode feed.

### **2.5.7 Internal resistance of a cell**

The complete cell assembly and materials used do have an influence on the total resistance of a cell. The contact resistance between the current collector and the diffusion layer influence the current density distribution as well as the overall internal cell resistance. The contact resistance is mainly a function of the local contact pressure and the local surface condition, for example the grade of passivation, surface roughness, coating, etc. But probably the most important element in the fuel cell that requires a low internal resistance is the membrane.

The internal resistance of the membrane can be measured by making use of *in situ* alternating current (ac) impedance spectroscopy. This technique is also commonly used in hydrogen/air fuel cells and it measures cell impedances while considering it as cathode impedances. The cathode impedance spectra of a DMFC is obtained by first recording the impedance spectrum of a complete DMFC; the cathode is operated in the normal air environment. The anode spectrum is then recorded. The anode impedance spectrum is then subtracted from the overall cell impedance spectrum. The cathode impedance spectrum is then obtained. The anode and cathode impedances are now known and further calculations can be done on the impedance contribution of kinetic effects at each electrode as well as the mass transport effects. Then finally the membrane resistance can be determined (Müller *et al.* 2003:848).

The researchers, Ma *et al.* (2003:334), attempted to measure the internal resistance of methanol fuel cells and they found that their measurements were much higher than those observed by other researchers. Internal membrane resistance values of 0,12

$\Omega \cdot \text{cm}^2$  at  $130^\circ\text{C}$ ,  $0,26 - 0,10 \Omega \cdot \text{cm}^2$  for the temperature range of  $20-80^\circ\text{C}$  and  $0,76 \Omega \cdot \text{cm}^2$  were obtained in previous experiments. They obtained an internal resistance measurement of  $1,8 \Omega \cdot \text{cm}^2$ . They claim that this was due to the inclusion of other resistances as well and not only the membrane resistance. The other resistances involved are the activation resistance and contact resistance that play a major role at low current densities.

The resistance of the gas diffusion layers also contributes to the total internal resistance of a DMFC. Every milli-ohm GDL resistance does result in a drop of amperes of cell current. The following example easily explains this. If a DMFC is operated at full power range and the resistance of the GDL increases from  $100 \text{ m}\Omega$  to  $200 \text{ m}\Omega$ , the available current from the cell drops by half. This is due to the current limiting effect produced by the higher resistance value. For example if the stack supplied 10 amps there will now only be 5 amps available.

## **2.6 Changing DMFC parameters**

It is stated by Energy Visions Inc. (2004) that the DMFC operates more efficiently under an intermittent duty cycle and it performs well under start and stop conditions. The DMFC can also be made more efficient by making changes to the fuel concentration according to the changes in power demand (Hamnatt 2003:306).

Research done by Scott *et al.* (1999:207) indicated that cell temperature, methanol concentration, cathode oxygen supply and pressure all do have an influence on the performance of a complete fuel cell system.

According to Lamm and Müller (2003:892) the performance of a fuel cell can be increased if fluctuations are brought forth in the operating conditions of a fuel cell. These fluctuations can range from changing the load cycles of the cell, current interruption, and methanol concentration fluctuation to the change in airflow instead of constant steady-state operation.

- Electrochemical sensors measure the current of a diffusion-limited methanol anode at a fixed potential where the current value is a function of methanol concentration.
- Capacitive sensors give an indication of the difference in the dielectric constant,  $\varepsilon$ , between methanol and other liquids.
- Ultrasonic sensors measure the speed of ultrasound in aqueous solutions that depends on the concentration of the dissolved substance.
- Optical sensors that operate with ultraviolet or near infra red light.

DMFC system efficiency can be maximized by carefully controlling the flow rates of both reactants. If the flow rates are too slow, mass transfer of the reactants can be a limiting factor in the performance of the cell and if the flow rates are too fast, energy is wasted. Therefore, it is important to know the correct fuel and air stoichiometry in order to obtain maximum performance of the cell.

When the methanol solution is circulated through the anode chamber, the liquid leaving the chamber is depleted and therefore methanol should be added continuously to the methanol-water solution in order to achieve a uniform methanol solution across the whole DMFC stack (Lamm & Müller 2003:892).

The methanol can also be dynamically fed to the cell stack. The dynamic feeding consists of periodic changes in the methanol concentration. This has the result of cell voltage increase (Sundmacher *et al.* 2001:340).

Figure 16 shows the cell polarization at 90°C (363K) for a methanol concentration in the range from 0,125 mol.dm<sup>-3</sup> to 2,0 mol.dm<sup>-3</sup>. Limiting current characteristics are obviously present at the lower methanol concentrations. At these lower methanol concentrations the open circuit cell voltage is higher. This is due to the methanol mass transport to the anode, anode polarization characteristics and methanol crossover to the cathode (Scott *et al.* 1999:207).

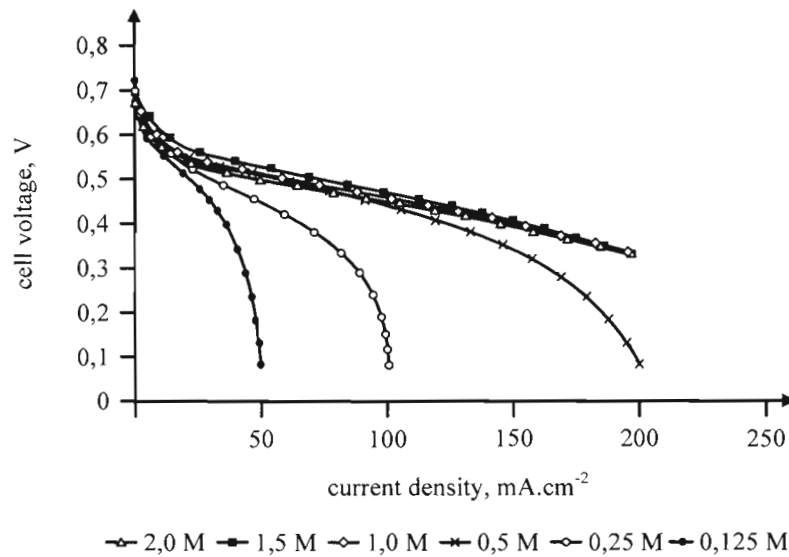


**Figure 16** Effect of methanol concentration on a DMFC (Scott *et al.* 1999:207).

The characteristics of the cell voltage versus current density are derived from polarization at both electrodes, mass transport and the internal resistance of the cell.

### 2.6.2 Operating temperature of the DMFC

Most of the experiments done on the DMFC by all of the different researchers were at higher operating temperatures than normal ambient temperature. The temperature range that they worked in was between 60°C to 90°C. Cao and Bergerns (2003:13) stated that when they changed the operating temperature of their fuel cell under test from 60°C to 90°C, the performance was also higher.

Scott *et al.* (1999:210) observed that cell voltage and limiting current densities were higher at higher operating temperatures.

Sundmacher *et al.* (2001:334) did their experiments by heating the mechanical structure of the fuel cell as well as the anode reactant fuel to the desired operating temperature.

The temperature at which the fuel cell operates influences the electrode kinetics; the higher the temperature the higher the electrode kinetics. But high temperatures lead to water vaporization at the cathode. This reduces the partial pressure of the oxygen at the cathode. In turn the higher temperature causes the membrane of the cell to swell, this again causes water permeation by electro-osmosis to increase, and flooding of the cathode occurs (Dohle *et al.* 2002:276).

Figure 17 indicates the cell voltage versus current density at different temperatures. The performance of the cell improves at higher temperatures owing to the increase in reaction kinetics on the electrode catalysts.

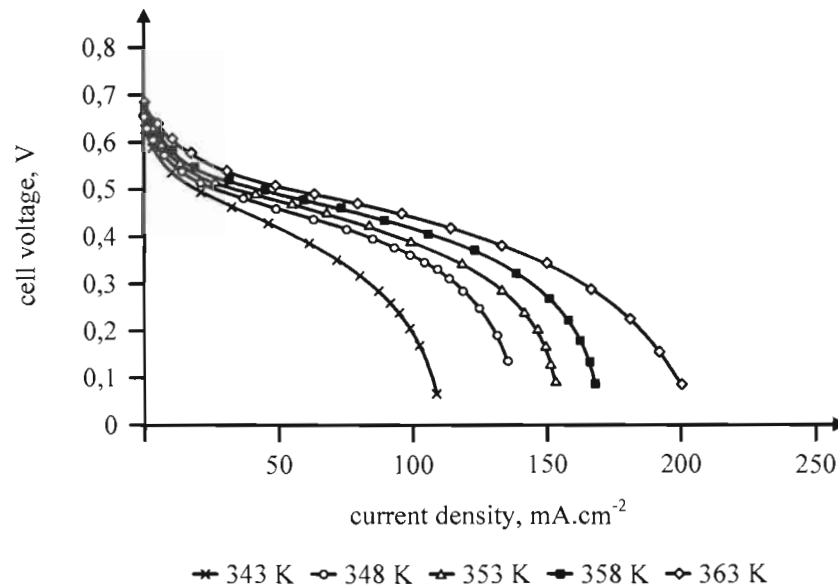


**Figure 17** Effect of temperature on a DMFC (Scott *et al.* 1999:210).

Operating a fuel cell at high temperatures causes permanent material breakdown, especially if the stack is operated at temperatures above 90°C. This shortens the operating lifespan of the fuel cell.

### 2.6.3 Stoichiometry of reactants

The stoichiometry ratio for any gas or liquid fed to a fuel cell is defined as the ratio of the flow rate feed stream to the consumption rate to support the applied current. Figure 18 illustrates the cell voltage versus air stoichiometry for a DMFC operating at a current density of  $200 \text{ mA}\cdot\text{cm}^{-2}$  for concentrations of 1 mole, 2 mole and 4 mole methanol. Figure 19 indicates the total mass flows present in a DMFC.

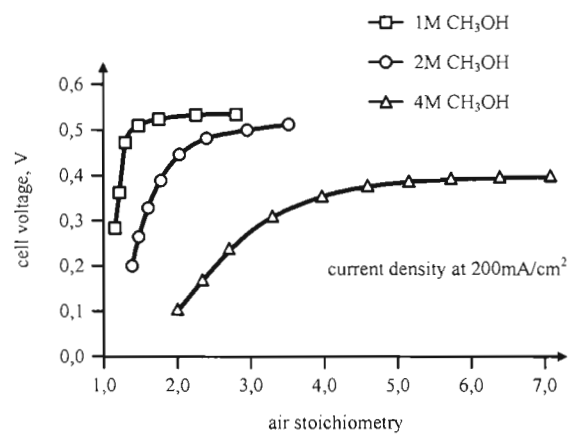


**Figure 18** Cell voltage versus air stoichiometry (Müller *et al.* 2003:849).

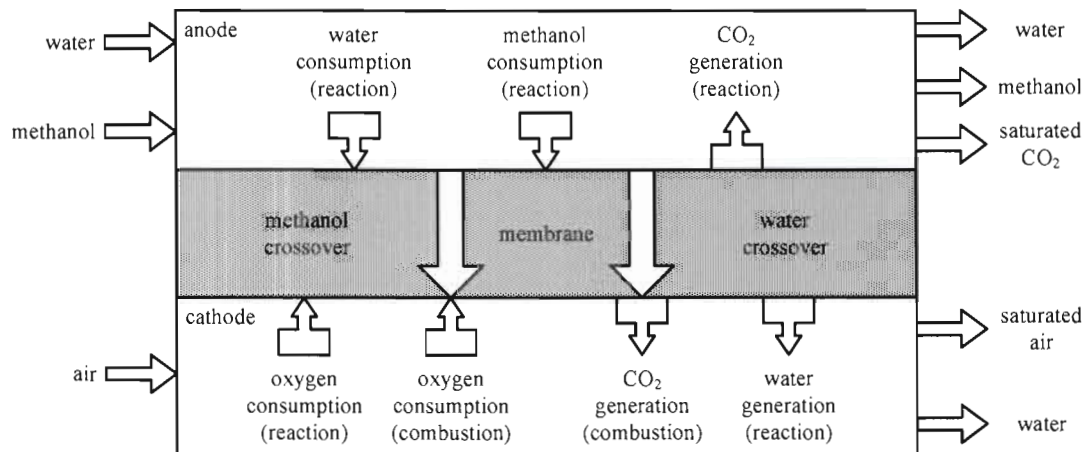


**Figure 19** Mass flows within a direct methanol fuel cell (Lamm & Müller 2003:891).

### 2.6.3.1 Methanol solution flow rate

Liquid feed in a fuel cell does present problems that are not found in a gas feed fuel cell. The liquid fuel must always be fed from the bottom of the stack to the top in order to make sure that all the active catalytic areas do come in contact with the fuel. Another concept that must be kept in mind is the fact that any gases present in the liquid must be driven out of the system even  $\text{CO}_2$  blocking the pores of the anode gas diffusion layer. Luckily most of the time bubbles do escape upwards in a fluid and with the upward flow force of the liquid, getting rid of any gas in the liquid chambers of a cell is easy if the correct flow channel geometry was adopted.

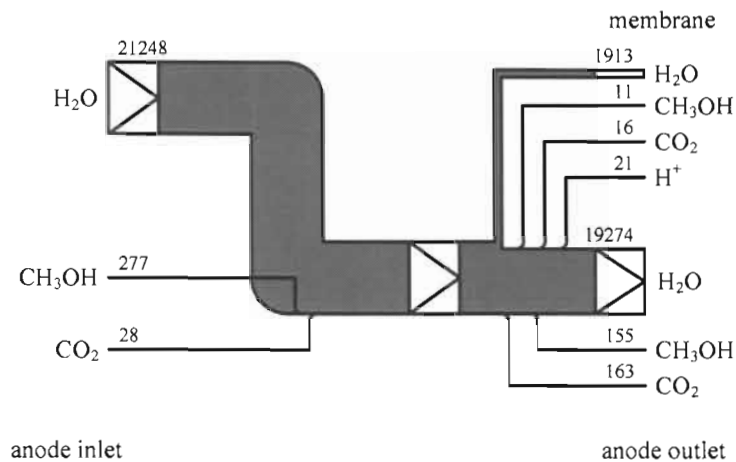


**Figure 20** Mass flow through the anode and the membrane of a DMFC (Müller *et al.* 2003:853).

Methanol solution flow rate in the anode chamber does not have a big influence on the cell performance except if the flow rate becomes lower than the minimum required rate for keeping the methanol solution from depleting (Scott *et al.* 1999:207). But increasing the flow rate above the needed fuel stoichiometry is unnecessary. In fact there will be a small area where the change in current density will require a change in flow rate due to the change in mass transport through the membrane. In other words if less current is required from the stack, the flow rate can

be decreased. If more current is required from the stack, the flow rate must be increased.

Figure 20 shows the mass flows through the anode and the membrane of a DMFC. The values given are in  $\text{mg.s}^{-1}$  for 1 kW of electrical power. The operating temperature was  $110^\circ\text{C}$ , current density was  $250 \text{ mA.cm}^{-2}$  and the methanol concentration was 0,4 mole.

### 2.6.3.2 Oxygen air flow rate

The cathode oxidant stoichiometry is also important. Experiments done by Scott *et al.* (1999:207) indicated that oxidant flow rates must be the same or higher than the stoichiometric requirements. If it is lower than that, flooding of the cathode structure occurs. This has severe mass transport limitations because the oxygen does not reach the cathode catalyst. In DMFC the oxidant stoichiometry is dependant on three factors – they are the replenishment of oxygen at the cathode, the flushing out of the nitrogen gas in the cathode chamber and getting rid of the water on the cathode structure.

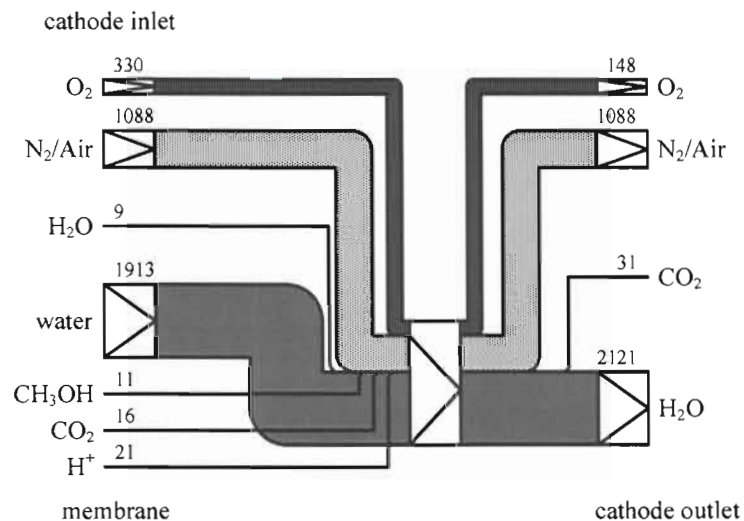


**Figure 21** Mass flow from membrane and through the cathode (Müller *et al.* 2003:853).



Figure 21 shows the mass flow from the membrane and through the cathode of a DMFC. The same operating conditions as for Figure 20 apply for Figure 21.

According to Narayanan *et al.* (2003:897) when the cathode of the DMFC is supplied with inadequate oxidant feed, the performance sharply decreases with methanol concentrations higher than 1 mole. This is due to the methanol crossover. Methanol that reacts at the cathode produces heat. The result of this is a higher temperature at the cathode and it has a higher water vapour pressure as a result. Mass transfer of oxygen is made difficult by this increase in pressure.

The researchers, Reeve *et al.* (2004:7), found that when air is used instead of pure oxygen on the cathode side, optimum currents were only achieved at high oxidant flow rates. They said that it was due to the blanketing effect of nitrogen. Nitrogen accumulates over the catalyst after the oxygen component has been consumed. This argument is supported by Hamnett (2003:306). They say that the oxygen in the air, fed to the cathode, reacts to form water but the nitrogen remains trapped in the pores of the cathode electrode. This acts as a diffusion barrier to the next oxygen molecule.

**Table 3** Composition of air.

Component	Symbol	Volume	
Nitrogen	N <sub>2</sub>	78.084%	99.998%
Oxygen	O <sub>2</sub>	20.947%	
Argon	Ar	0.934%	
Carbon dioxide	CO <sub>2</sub>	0.033%	
Neon	Ne	18.2 ppm	
Helium	He	5.2 ppm	
Krypton	Kr	1.1 ppm	
Sulfur dioxide	SO <sub>2</sub>	1.0 ppm	
Methane	CH <sub>4</sub>	2.0 ppm	

Hydrogen	H <sub>2</sub>	0.5 ppm
Nitrous oxide	N <sub>2</sub> O	0.5 ppm
Xenon	Xe	0.09 ppm
Ozone	O <sub>3</sub>	0.07 ppm
Nitrogen dioxide	NO <sub>2</sub>	0.02 ppm
Iodine	I <sub>2</sub>	0.01 ppm
Carbon monoxide	CO	trace
Ammonia	NH <sub>3</sub>	trace

This argument can be realized when looking at Table 3 which gives the composition of air. It can be seen from the table that air consists of 20.947 percent oxygen and 78.084 percent nitrogen. An interesting remark found is that the air that leaves a person's lungs during exhalation contains 14 percent oxygen and 4,4 percent carbon dioxide. It is also stated that atmospheres with oxygen concentrations below 19,5 percent can have adverse physiological effects on humans and atmospheres with less than 16 percent oxygen can become life-threatening. It makes one think how fragile we are if it is realized that there is only about 21 percent oxygen in our atmosphere (Mistupid.com, the online knowledge magazine 2004).

Using thinner electrodes can partially solve this problem of nitrogen accumulating on the cathode but due to the higher catalyst loadings to thin electrodes they cannot be used. Therefore, controlling the inflow and outflow of the gases correctly is important to obtain maximum cell performance.

A fourth method to use in solving this problem is to add PTFE in the electrode structure. This is done by mixing the electro catalyst ionomer mixture ultrasonically with the PTFE composite. This is then spread onto a carbon cloth or carbon paper current collector. A series of pores are provided to allow the nitrogen to escape without affecting the use of the electro catalyst.

The structure of the Nafion bonded electrode can also be cured at a higher temperature, i.e. higher than 150°C. This degrades the Nafion membrane, increasing the hydrophobicity of the electrode structure.

A fifth method can be used by means of pore formers such as  $(\text{NH}_4)\text{CO}_3$ . The decomposition of this material gives solely gaseous products. It can be used to produce micro-structures (Hamnett 2003:306).

#### 2.6.4 Pressurization of electrode feeds

The cathode pressure ( $p$ ) also influences the performance of a cell. This can be seen in Figure 22. The cell was again operated at partial and full load. It is common practice to pressurize the cathode feed and, to some extent, the anode feed of a hydrogen/air feed fuel cell. But in direct methanol fuel cells the anode feed cannot be pressurized because the anode fuel reactant is in an aqueous form and pressurizing a liquid is not considered. The cathode air feed on the other hand can be pressurized. This greatly increases the performance of a DMFC (Dohle *et al.* 2002:277).

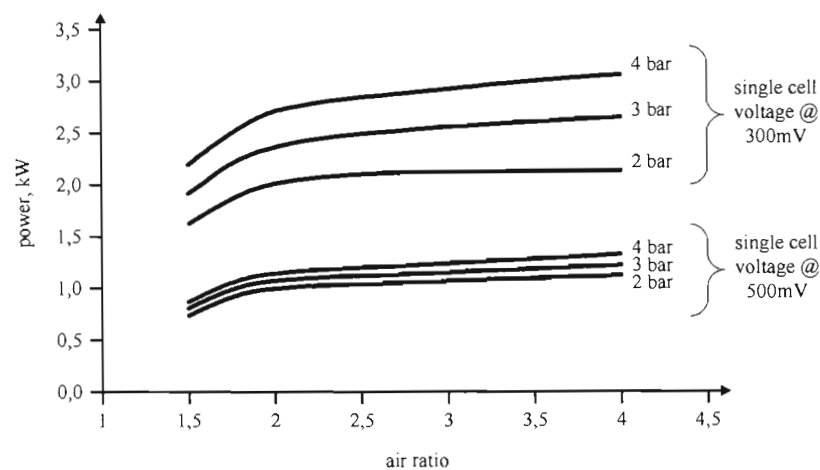


**Figure 22** Influence of air ratio and cathode pressure on cell power (Dohle *et al.* 2002:277).

It was also found that a reduction of oxygen pressure at the cathode would have a reduced cell performance as a result. This is due to the reduction in cathode potential. One reason given for this effect is the crossover of methanol from the anode to the cathode. A higher cathode pressure can impede the methanol diffusion.

## **2.7 Production and effects of the by product CO<sub>2</sub>**

One factor that a large number of researchers are looking at is the methanol conversion in the cell and then also the CO<sub>2</sub> produced. When the methanol solution reacts at the anode catalyst, carbon dioxide is formed. It is estimated that a DMFC system operating at 20 W has the same amount of CO<sub>2</sub> emission as a human being. Some of this CO<sub>2</sub> dissolves in the methanol solution. This increases the conductivity of the fuel reactant. Tests done by Lamm and Müller (2003:883) showed that ultra pure methanol added to ultra pure water had no significant increase in conductivity but when CO<sub>2</sub> was added to the methanol mixture, there was an increase in conductivity. Therefore, not only gaseous CO<sub>2</sub> removal from the fuel reactant but also removing dissolved CO<sub>2</sub> can increase the performance of a DMFC.

The oxidation of methanol is a multi-step reaction. This means that at some stage in the reaction sequence carbon monoxide molecules are released. This CO causes the cell performance to decay because it is absorbed on the active surface of the platinum electro catalyst. The CO limits the number of active catalyst sites and therefore inhibits the hydrogen oxidation reaction (HOR). In the DMFC, the hydrogen atom is still the energy carrier. It is only contained in methanol, CH<sub>3</sub>OH. The methanol needs to be dissociated in order to get to the hydrogen atom. This is all done by the anode catalyst. When the CO poisons the fuel cell, its total impedance increases (Wagner & Schulze 2003:3899).

Platinum is the most effective catalyst for the dehydrogenation of methanol. But as mentioned above CO poisons it. In order to stop this poisoning effect, platinum is alloyed with ruthenium. Ru is a noble metal that can dissociate water at low

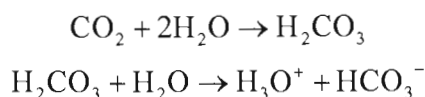
potentials to create oxygen containing surface groups that are needed to convert CO to the end by-product CO<sub>2</sub> (Qi & Kaufman 2002:180).

Residues of aldehydes, carboxylic acids or other intermediates that are produced during the electro-oxidation of methanol also poison the catalysts in the direct methanol fuel cell (Energy Visions Inc. 2004).

As already mentioned CO<sub>2</sub> is formed when the methanol solution is oxidized at the anode catalyst. The production of CO<sub>2</sub> increases as the current generation of the fuel cell increases. Two things happen to this gaseous CO<sub>2</sub>. Firstly, bubbles are formed and need to escape from the anode catalytic area going upward. Secondly, some of the gaseous CO<sub>2</sub> is dissolved in the methanol solution.

The disadvantage of gas bubbles that form in the anode fuel chamber is the counter-current flow created in the anode diffusion layer. The gas bubbles want to get away from the catalytic site while the aqueous methanol solution wants to get to the catalytic site via the same pores. This has the result of fuel reactant mass transport limitations (Siebke *et al.* 2004:1). It has also been observed through various custom experiments that CO<sub>2</sub> gas bubbles tend to stay on the diffusion layer or active catalytic site. Increased flow velocity in the fuel reactant can clear these blockages (Bewer *et al.* 2004:2).

The dissolved carbon dioxide in the liquid solution permeates through the membrane. A low percentage of the dissolved CO<sub>2</sub> is converted into carbonic acid. Carbonic acid is unstable in this fuel reactant mixture and therefore decomposes to H<sub>3</sub>O<sup>+</sup> and HCO<sub>3</sub><sup>-</sup> ions. The following chemical reaction occurs:



The result of this is an increase in ion conductivity in the anode circuit (Lamm & Müller 2003:883).

## **2.8 Crossover in the DMFC**

The membranes used in DMFC and PEMFC are the same. Therefore, Dimitrova *et al.* (2002:82) stated that the voltage losses due to ionic resistance in the membrane are the same for both types of fuel cells. They say it is important to decrease the permeation of methanol through the membrane because it is the mixed potentials produced at the cathode that bring the performance of the DMFC down. It is suggested that the membrane must be made thicker in order to limit the methanol permeation but a thicker membrane has lower ion conductivity. There will be a point reached where the thickness of the membrane and less methanol permeation will deliver the best DMFC performance.

### **2.8.1 Methanol crossover**

The biggest unwanted reaction in the DMFC is the methanol permeation from anode to cathode. There are two causes for this phenomenon, the first is the diffusion of methanol from the anode to the cathode and secondly, the methanol transported by electro-osmosis. The cause for methanol diffusion is the concentration difference between the anode and the cathode. There will not be a state where the methanol concentration at the cathode will reach the same level as that of the anode side. This is because the diffused methanol is constantly oxidized at the cathode catalyst. The amount of methanol molecules transported by electro-osmosis is dependant on the current density. If no current is drawn from the cell then there will be no methanol crossover due to electro-osmosis but there will still be crossover due to anode/cathode concentration differences.

Methanol is able to permeate through the membrane owing to the fact that it can be diluted in water and the membrane structure consists of a water percentage uptake.

The faradaic efficiency of a DMFC is reduced due to methanol crossover. The following researchers, Nunes *et al.* (2002:215), stated that due to methanol crossover, DMFC efficiency is reduced to 35 percent. Figure 23 shows the methanol crossover rate as a function of operating current density for different concentrations of methanol.

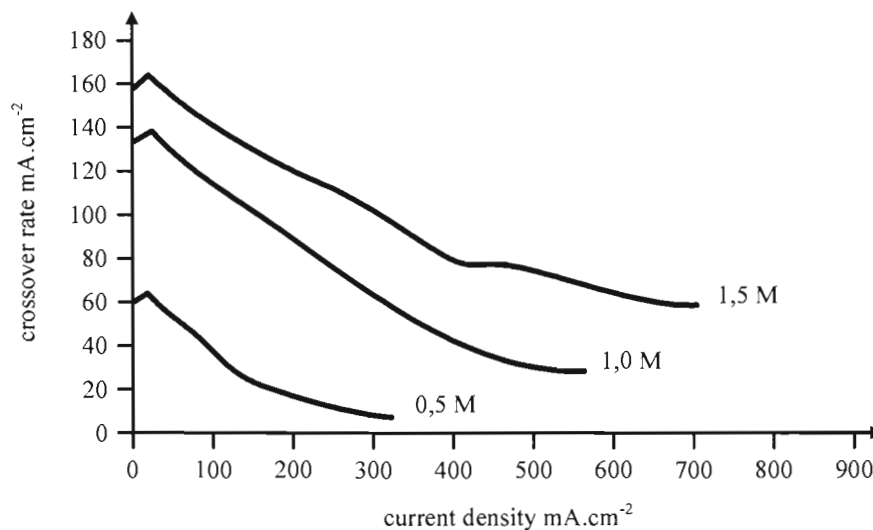


**Figure 23** Methanol crossover rate as a function of the current density (Lamm & Müller 2003:897).

Müller *et al.* (2003:849) state that all of the methanol that crosses over from the anode to the cathode is oxidized to CO<sub>2</sub>.

Mixed potentials are created when crossed over methanol reacts at the cathode. Therefore, it would be an advantage to develop a cathode catalyst that doesn't react with methanol. This will definitely eliminate losses due to the mixed potentials (Dohle *et al.* 2002:273).

Another disadvantage of methanol that ends up at the cathode due to the crossover effect is that this methanol is fuel wasted, therefore, lower fuel conversion efficiency in the DMFC occurs (Sandhu *et al.* 2003:2295).

Methanol concentrations that are too high also have a disadvantage. Higher methanol concentrations at the anode will have a higher methanol diffusion rates as a result. This will have the effect of a greater quantity of methanol at the cathode, therefore, a higher mixed potential is generated and the cell voltage will drop (Scott *et al.* 1999:204).

Diluting the methanol in pure water can minimize the methanol crossover. The concentration of the methanol solution is dependant on the amount of power required from the fuel cell. In other words the cell is operated at its maximum fuel efficiency for delivering needed power to the load (NASA's Jet Propulsion Laboratory 2002:1).

But when the methanol concentration is too low, methanol depletion will occur faster. This means that there is not enough methanol present in the solution to supply the fuel cell. The lack of fuel reactants slows down the electrochemical reaction that leads to a decrease in cell potential. Concentration over potential occurs under these conditions. Losses during this over potential are mainly due to mass transport limitations (Yu *et al.* 2003:43).

Voltage losses in the order of a few hundred millivolts are present in a DMFC due to methanol crossover and its side reactions. It has already been discussed that the DMFC has polarization losses at the cathode, as does the PEMFC but the DMFC has polarization losses at its anode as well. This brings down the performance of this type of fuel cell even further.

Reeve (2002:15) mentioned that the oxygen reduction current is affected by the presence of methanol at the cathode. He also found that the fall in cell voltage could be as high as 300 mV when the methanol concentration is increased. This fall in cell voltage is due to an increase in the polarization at the cathode during practical operation and potentially a modification of the proton conductivity in the membrane.



Figure 24 illustrates the direct methanol cell voltage at different methanol concentrations. These measurements were reported by Reeve (2002:37) under open circuit voltage conditions.

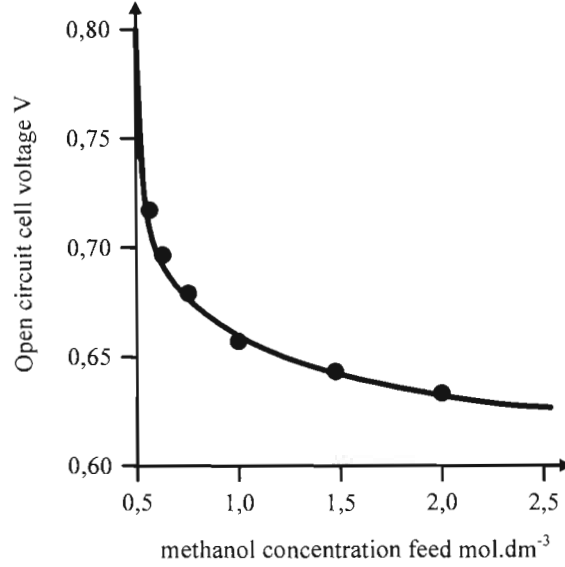


**Figure 24** Effect on open circuit voltage at different methanol concentrations (Reeve 2002:36).

Another big disadvantage of methanol that diffuses or permeates through the membrane is the fact that methanol dissolves Nafion over a long period of operation time. Nafion membranes are commonly used in direct methanol fuel cells (Neergat *et al.* 2003:871).

The rate ( $\text{ml.cm}^{-2}.\text{s}^{-1}$ ) of methanol crossover is given by Munichandraiah *et al.* (2003:99):

$$-dn/dt = \left( \frac{v}{1000p} \right) \left( \frac{dC_b}{dt} \right) \quad (5)$$

where  $n$  = number of mol of methanol crossing an area of  $p$  ( $\text{cm}^2$ ) at time  $t$   
(s)

$v$  (ml) = volume of electrolyte in cell B

$C$  is expressed in mol.liter<sup>-1</sup>

A major problem with perfluorinated ionomer membranes such as Nafion from DuPont, Flemion from Asahi Class Co. and Aciplex from Asahi Chem Co. Ltd, is that they have a high permeability to methanol. This goes hand in hand with the high electro-osmotic drag.

Electro-osmotic transfer of methanol through the membrane becomes the dominant factor in methanol crossover at high current densities, and crossover due to concentration differences percentage wise is less (Reeve 2002:40). It is suggested by Neergat *et al.* (2003:871) that the effects of methanol crossover at high current densities is small.

It is turning out to be a difficult task to manufacture a membrane that is immune to methanol crossover. Methanol does find its way into the cathode chamber due to methanol crossover. Not all of the methanol present at the cathode reacts with the catalyst and some of it is present in the exhaust stream. Therefore, it is suggested that the exhaust stream must be passed through a cleanup stage using catalyst oxidation devices in order to completely convert any traces of methanol to carbon dioxide before it is released into the environment (Narayanan *et al.* 2003:903). This is in contrast to the remark made by Lamm and Müller (2003:891) that it is assumed 100 percent of the methanol is oxidized at the surface of the cathode.

#### **2.8.1.1 Using CO<sub>2</sub> levels to determine methanol crossover**

It is stated in a number of papers and books that the methanol crossed over from anode to cathode is catalytically converted at the cathode. Some researchers use the carbon dioxide formed at the cathode to determine the amount and rate of methanol crossover. But as mentioned by Narayanan *et al.* (2003:903) some methanol escapes the cathode reaction and finds its way into the exhaust water. This leads to a mis-

calculation in the amount of methanol crossover, and a toxic waste product if it is not reused in the anode fuel feed.

Methanol permeation measurements are mostly based on the analysis of the CO<sub>2</sub> content of the cathode exhaust gas stream. According to Thomas *et al.* (2002:3742), measuring the CO<sub>2</sub> as an indication of methanol crossover appears to be less reliable at high current densities. They claim that some of the detected CO<sub>2</sub> may have originated at the anode and diffused through to the cathode. Neergat *et al.* (2003:860) had the same argument. This will lead to the wrong calculation of methanol crossover. For measuring methanol crossover at high current densities a methanol balance experiment is used to find a more accurate value. But it must be taken into consideration that methanol crossover is least important at high cell current densities due to the large fuel utilization at the anode.

Munichandraiah *et al.* (2003:98) stated that it is unlikely that all of the methanol crossed over to the cathode has been completely oxidized to CO<sub>2</sub>. Therefore, they have developed a new potentiometric method to determine methanol crossover. This is done by monitoring the potential of a Pt/Ru/C electrode. From this they can calculate the rate of methanol crossover.

A question that rises from this suggested new method is the effectiveness or accuracy of this method. As stated by these researchers, the conventional way of determining methanol crossover is measuring the CO<sub>2</sub> content in the cathode chamber by using an optical infra red sensor. Methanol that doesn't oxidize at the cathode doesn't create CO<sub>2</sub> as a by-product. This is potential CO<sub>2</sub> not measured by the optical infra red CO<sub>2</sub> sensor. But the same principle holds truth for their own method where they measure the cathode potential. Any methanol that oxidizes at the cathode creates mixed potentials. This causes a change in cathode potential. Methanol that escapes in the exhaust of the cathode did not oxidize at the cathode catalyst. Therefore, no mixed potential was generated. The potential change can then not be observed. Methanol crossover cannot be determined accurately by either of these two methods if some of the crossed over methanol escapes through the cathode exhaust.

Tests were done by Müller *et al.* (2003:849) on a Nafion 117 membrane, where it was operated at a constant methanol concentration of 0,4 mole at temperatures of 100-110°C. It was found that CO<sub>2</sub> measurement was as much as 25 percent at low current densities (50 mA.cm<sup>-2</sup>) and more than 95 percent at higher current densities (300 mA.cm<sup>-2</sup>). These measurements accounted for CO<sub>2</sub> crossing over the membrane from anode to cathode.

### 2.8.1.2 Effects of methanol crossover on cathode

Methanol that oxidizes at the cathode reacts chemically with the cathode just as it does at the anode and it consumes oxygen. But the anode catalyst is made of a Pt/Ru alloy. The Ru ensures that the catalyst is not poisoned by any intermediate formation of CO. The cathode catalyst is only made of Pt. Therefore, CO formed at the cathode catalyst will poison the catalyst (Qi & Kaufman 2002:180).

The cathode is depolarized when methanol oxidation occurs at the catalyst. Results obtained from experiments done by Thomas *et al.* (2002:3747) showed clearly that methanol crossover in a cell had an influence on the cathode in the order of 20 mV at a current density of 100 mA/cm<sup>2</sup>. The influence on the cell was small. The cell in this experiment had sufficient loading on the Pt cathode and the operating conditions were optimized. The potential of the cathode is given by:

$$\begin{aligned}\Delta E_{cat} &= b \log[(J_{cell} + J_{x-over}) / J_{cell}] \\ &= b \log(1 + J_{x-over} / J_{cell})\end{aligned}\tag{6}$$

where  $b$  = Tafel slope for the oxygen reduction reaction (ORR)

$J_{cell}$  = cell current density at the relevant cathode potential  $E$

$J_{x-over}$  = methanol crossover current density

The sum of  $J_{cell}$  and  $J_{x-over}$  is equal to the overall rate of ORR in the cell,  $J_{ORR}$

Energy Vision Inc. (2004) has identified a method of recovering methanol that has crossed over the membrane from anode to cathode for re-use. It is most probably the methanol that is left in the exhaust stream.

### **2.8.1.3 Reducing methanol crossover**

The membrane used in a DMFC is the main reason for methanol crossover. Methods of reducing methanol crossover range from improving solid polymer electrolytes, cathode catalysts and the most promising way is the application of methanol impermeable but hydrogen proton permeable layers of metallic palladium to the membrane. This metallic palladium layer can be coated onto the Nafion membrane by electroless metallization (Hejze *et al.* 2002:15-2).

A company called BetaCure Technologies Inc. (BCT) is developing advanced membranes. Sulfonated fluorocarbon films are produced by them in order to provide proton conductivity. These films were then irradiated to produce free radicals for subsequent grafting to promote pre-cross linking of the base film to increase tortuosity that reduces methanol permeation. They claim that by using this technique methanol permeation is reduced to 66 percent compared to that of Nafion. They did make use of the method whereby the CO<sub>2</sub> levels are measured in the exhaust gas to determine the amount of methanol crossover (Hamdan & Kosek 1999:1).

Casting a thin film on a perfluorosulfonic membrane like Nafion can also reduce methanol crossover. The mixture is made up of polyvinyl alcohol (PVA) and Nafion. The proton conductivity of the membrane can be improved by sulfonating it. Sulfonation is where the SO<sub>3</sub>H group is introduced into the membrane. Films like recast polybenzimidazole film, laminated Pd film and impregnated composite film consisting of polymeric composites have been cast onto Nafion. A disadvantage was a decline in mechanical membrane strength and an increase in membrane resistance (Shao *et al.* 2002:147).

Methanol crossover can also be minimized by plasma etching of Nafion and palladium sputtering. The function of the palladium sputtering was to plug the pores of the membrane because of its excellent hydrogen storage capability. No decrease in proton transfer was observed by Reeves (2002:39). Methanol permeation was decreased by 40 percent by using both of these membrane modification methods.

A method that can be applied in order to limit methanol crossover is to operate the fuel cell at lean anode feeds. In other words if the direct methanol fuel cell is loaded with only a small load compared to its full load capability, the methanol concentration can be made less in order to sustain the same cell performance as with maximum fuel concentration. If the methanol concentration is lower then the methanol crossover will also be less. At high operating current densities the fuel utilization can reach values in excess of 90 percent (Thomas *et al.* 2002:3743). A disadvantage of controlling the methanol concentration in the fuel cell according to the load requirements is that it takes time to consume the higher methanol concentration to reach a lower concentration if there is a sudden drop in the needed power.

Methanol crossover is a function of the membrane. Membrane materials other than Nafion have been used to reduce methanol crossover. They are, for example, polybenzimidazole and perfluorinated sulphonimides (Scott *et al.* 1999:205).

One reason for using thicker membranes like Nafion 117 in DMFCs is that they act as a barrier for the diffusion of methanol from the anode to the cathode.

Periodic pulsing of the methanol concentration can also reduce methanol crossover (Sundmacher *et al.* 2001:333).

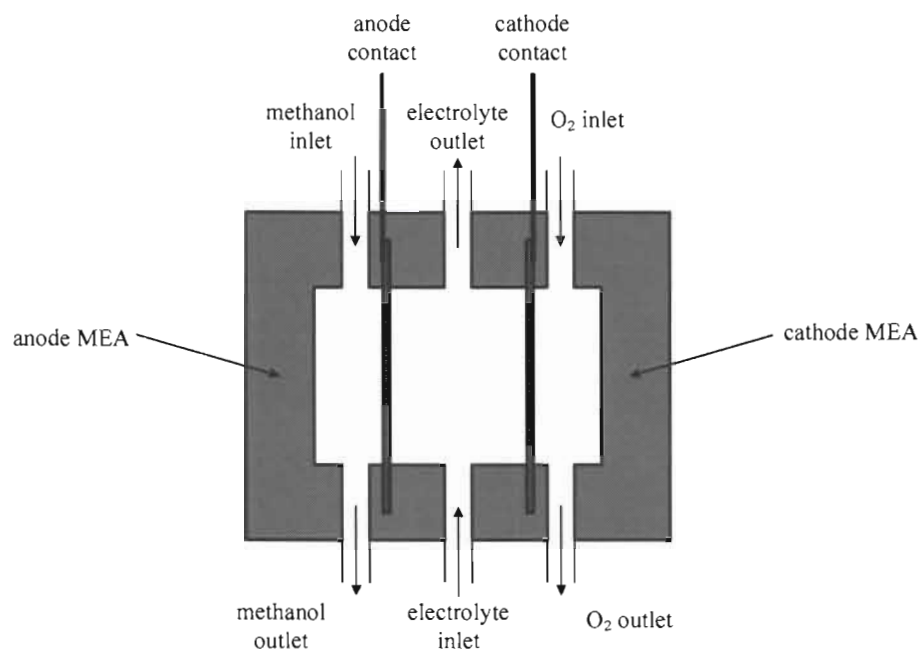


**Figure 25** DMFC assembly with a liquid electrolyte (Reeve *et al.* 2004:4).

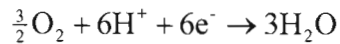
A liquid electrolyte system, such as the sulphuric acid electrolyte direct methanol fuel cell shown in Figure 25, should have the ability to circulate the electrolyte. The advantages of this are that simple thermal control of the cell and better water management can be applied. It is even possible to remove methanol that crosses over as well as impurities continuously during operation. In other words, methanol cannot end up at the cathode because it is flushed away (Energy Visions Inc. 2004).

As a summary, crossover of methanol can be reduced by increasing membrane thickness and equivalent weight, by increasing the cathode reactant pressure, by decreasing cell temperature and by decreasing methanol concentration (Qi & Kaufman 2002:177).

### **2.8.2 Water crossover**

The occurrence of water at the cathode is due to two reasons. The first is the normal production of water at the cathode due to the chemical reaction that takes place. The

chemical reaction is given by:



The second reason is the permeating of water through the membrane from anode to cathode. The permeation occurs because of the electro-osmosis of methanol through the membrane. It is estimated that only 10 percent of the water present at the cathode is due to the oxygen reduction reaction. The other 90 percent is due to electro-osmotic drag. There is in actual fact only 2 mole of methanol in the reactant fuel solution, therefore, more water permeates through the membrane than methanol (Müller *et al.* 2003:853). Neergat *et al.* (2003:862) stated that for every proton that crosses through the membrane one water molecule is also transported. This is in contrast with what Narayanan *et al.* (2003:897) has stated. They said that 2.5 to 3 molecules of water are being transported for every proton that flows as an ionic current.

Water permeation through the membrane is only present in the direct methanol fuel cell since a liquid fuel is used. A negative effect of water permeation is the flooding of the cathode. In PEMFC extra humidifiers are required to keep the stack humidified but in a DMFC there is more than enough water present in the cell to keep it humidified (Neergat *et al.* 2003:861).

### **2.8.3 Carbon dioxide crossover**

With the oxidation of methanol at the anode, carbon dioxide is formed. Some of this carbon dioxide permeates through the membrane owing to electro-osmotic drag especially the carbon dioxide that dissolves in the fuel reactant solution. This permeated carbon dioxide together with the CO<sub>2</sub> produced at the cathode during methanol oxidation can decrease the active surface area for the reduction of oxygen. The performance of the fuel cell then decreases.



## 2.9 Chemical side of the DMFC

Although methanol has a high-energy capacity, the practical energy and power density of a DMFC are low due to the slow kinetics of methanol oxidation in an acidic media even with highly active precious metal catalysts such as platinum (Reeve 2002:55).

Poor kinetics of the anode for methanol oxidation reaction makes the DMFC a lower performer than the hydrogen PEMFC. The anode and cathode make use of higher noble metal catalyst loadings than any other type of fuel cell. CO and CO<sub>2</sub> easily poison the platinum catalyst. This leads to cell performance decay (Wagner & Schulze 2003:3899).

### 2.9.1 Working of a DMFC

The DMFC allows direct electrochemical oxidation of methanol to carbon dioxide under generation of electricity. The reaction occurring at the anode and cathode catalyst takes place at the catalysts layer where they are directly attached to the membrane (Sundmacher *et al.* 2003:333).

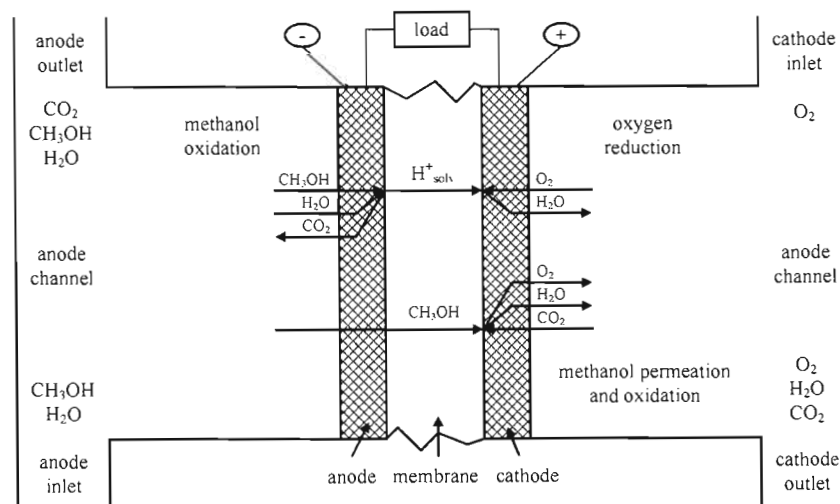


**Figure 26** Working of a DMFC (Dohle *et al.* 2002:270).

Figure 26 illustrates the working of the DMFC. As can be seen from this figure a methanol solution is pumped into the anodic chamber. The methanol solution reacts with the catalyst where protons and electrons are formed, carbon dioxide is formed as a by-product. The  $\text{CO}_2$  escapes in the anode outlet exhaust with a lower methanol concentration in the solution to that which entered the cell. Protons are conducted to the cathode through the acid ionic polymer membrane and the electrons follow the external circuit. On the other side of the membrane the protons react with the external returning electrons and oxygen to form water. The cathode outlet exhaust consists of depleted oxygen levels, water and  $\text{CO}_2$  (Dohle *et al.* 2002:269).

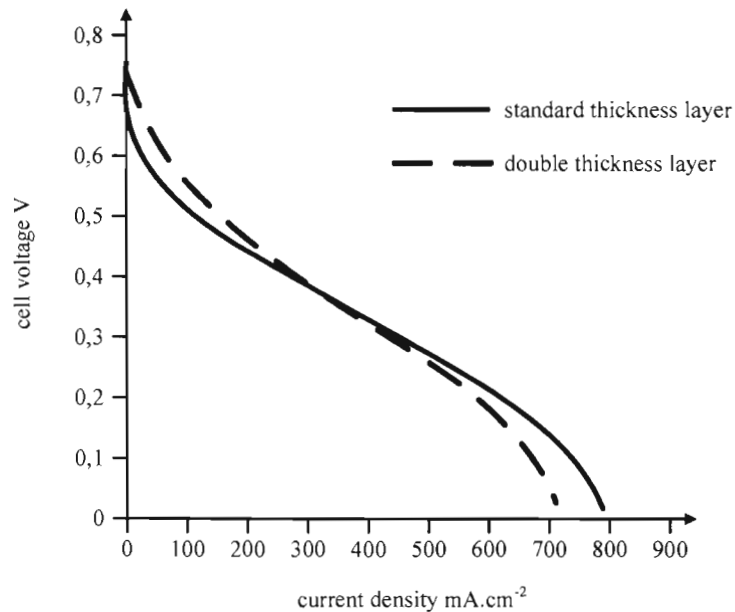


**Figure 27** Performance difference between thick and thin catalyst electrode layers (Siebke *et al.* 2004:6).

Siebke *et al.* (2004:3) have found that at low current densities cell voltages are improved due to higher catalytic loadings. But at high current densities, cell voltages are lower when compared to low thinner catalyst loadings. They made the statement that increasing the catalytic surface area and keeping the catalyst layers thin, additional losses such as fuel supply and proton conductivity will be kept to a

minimum. These researchers did tests in optimizing the electrodes, and cell performances were calculated for different reaction layers. The results are presented in Figure 27.

A membrane electrode assembly is made up of the supported or unsupported catalyst electrodes bonded to the membrane. Figure 28 illustrates the bonding of the MEA. The electrolyte starts off in a liquid form; it is then bonded with a structural material that gives the required solid electrolyte mechanical strength but the structural material must be able to let the flow of protons through itself. The porous catalyst electrodes are then attached to this solid electrolyte structure by means of hot pressing or other methods. The end product is a usable direct methanol fuel cell membrane electrode assembly.

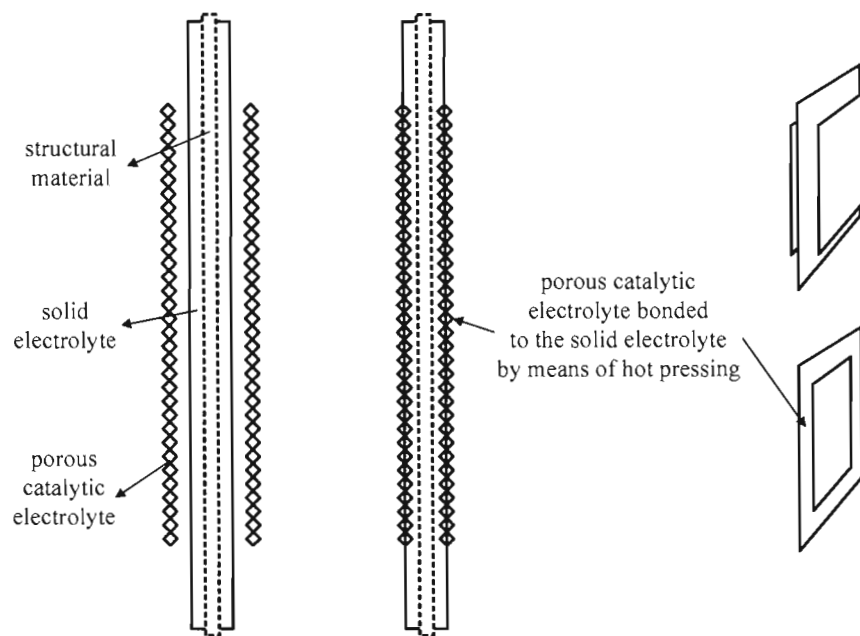


**Figure 28** Construction of an MEA.

These catalyst sites on the anode and cathode must give proton access, gas or reactant access and electronic path continuity to be electrochemically active. This three-phase reaction concept is illustrated by Figure 29. The three elements needed in the fuel cell to work are the fuel, the electrolyte and the catalyst. These three

elements come together when a reaction is formed. The fuel is the methanol that contains hydrogen atoms. The catalyst delivers the ability to oxidize the methanol to produce protons and electrons and also to conduct electrons. The electrolyte enables the conductance of protons.

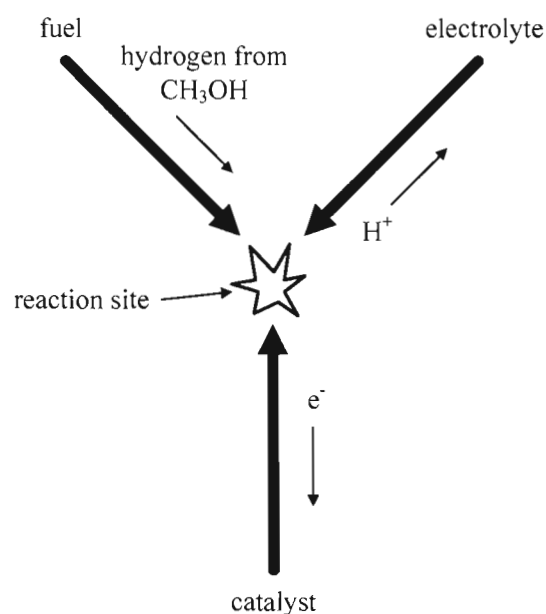


**Figure 29** Three-phase reaction concept.

The active catalytic surface area that is available for reactions to take place is a limiting factor on the available cell current. The current densities in a fuel cell are directly proportional to the reaction rate at the anode and cathode (Yu *et al.* 2003:44).

It is important for an electrode surface area to be as big as possible. This will improve the electrode performance. The disadvantage of a solid polymer electrode membrane is that it doesn't penetrate as deeply into the electrode structure as a liquid electrolyte does. Therefore, the reaction area is limited to the contact surface between the electrode and the membrane. One way to improve the contact surface area is to impregnate ionomer like Nafion into the catalyst layer (Chu *et al.* 2003:334).

Figure 30 illustrates the concept of enlarging the active surface area of the catalyst. A highly proton conductive material is added between the porous catalytic electrode and the membrane before hot pressing the MEA. This added material must also be high in methanol uptake.

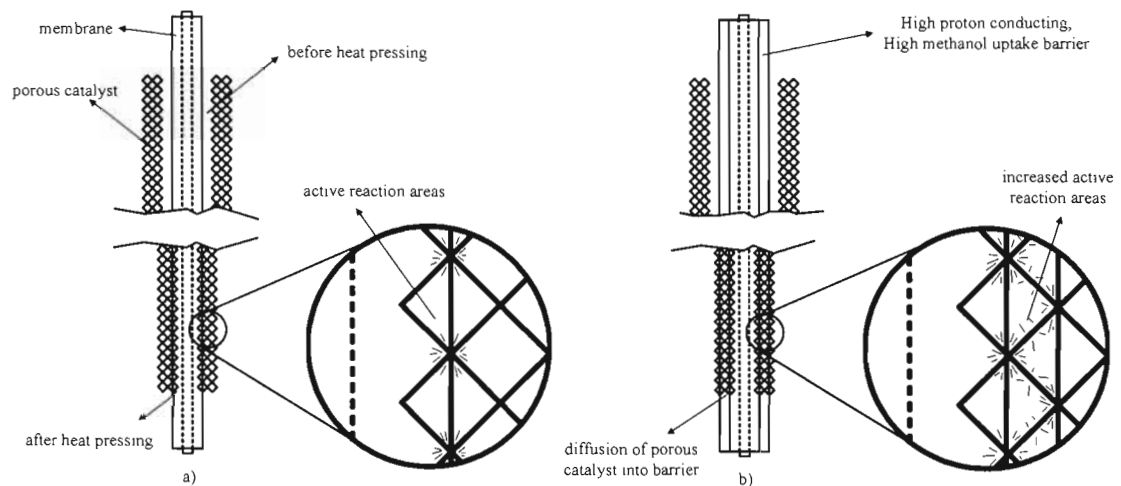


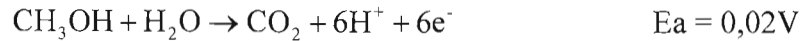
**Figure 30** Increasing active surface area.

The methanol is taken up in the added material where the three-phase reaction sites are created between the material, the electrode catalyst and the methanol in the material. It can be seen that the active surface area is greatly increased. One disadvantage of this idea is getting rid of the by-product  $\text{CO}_2$  from the solid electrolyte structure that is formed due the oxidation of methanol because the  $\text{CO}_2$  gas will probably loosen the highly proton conductive material from the electrode catalyst.

It is also important to understand that the catalyst in conjunction with the ionomer and other components like the GDL forms an electrically conductive network. Electrons are conducted by the catalyst from the reaction site to external current collectors (Neergat *et al.* 2003:872).

### 2.9.2 Reactions on the anode and the cathode

On the anode of a DMFC, methanol is electrochemically oxidized to carbon dioxide according to:



The hydrogen obtained from this reaction is split into hydrogen ions and free electrons (Scott *et al.* 2004:67).

At the cathode, oxygen is reduced to water according to:

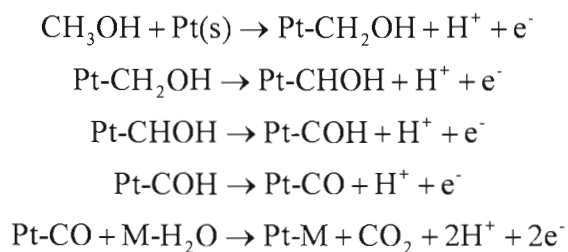


The overall reaction is given by:

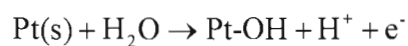


### 2.9.3 Methanol oxidation on the anode catalyst

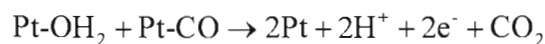
The overall reaction of methanol oxidation on pure Pt is quite slow and it involves the transfer of six electrons to the electrode. The electrochemical oxidation of methanol consists out of several intermediate steps. The first of them is probably the dehydrogenation of the methyl group of methanol. The adsorption and reaction of methanol on platinum takes place in the following steps, it is clear that, in total, six electrons are dissociated from the hydrogen atoms contained in the methanol-water solution (Reeve 2002:2):



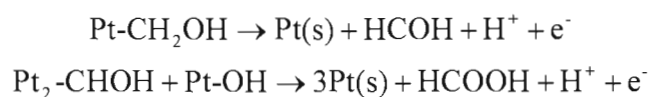
The dissociative adsorption of water on pure Pt is slow at normal operating potentials of a DMFC. Therefore, the dissociative chemisorption of  $\text{H}_2\text{O}$  is the rate-determining factor below 0,7 V. The following steps are:



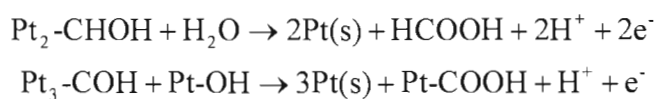
In the final reaction step  $\text{CO}_2$  is formed when the Pt-OH group reacts with a neighboring methanolic residue:



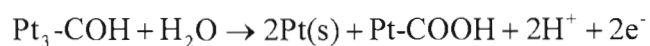
Additional reactions that have also been suggested in the report of Reeve (2002:2) are:



or



or



The rate of the above processes and the dominant species on the surface of the platinum are not known. But the primary processes that occur can be summarized as:

- Methanol adsorption onto the surface on the Pt
- Sequential proton stripping giving a series of multiple bonded intermediates that convert to linearly bonded CO
- Oxidation of CO to CO<sub>2</sub>

The platinum catalyst can be enhanced to ensure a more rapid methanol oxidation by doing the following (Reeve 2002:3):

- Pt-O species can be generated on the Pt surface by using metals as alloys. Examples of these metal alloys are Pt<sub>3</sub>Cr and Pt<sub>3</sub>Fe. These metals dissolve to leave highly active surfaces in the form of fibers.
- The use of ad-atoms. These ad-atoms are deposited onto the surface of the Pt by using under potential depositing. Gold (Au) can be used in this process.
- Alloying Pt with metals that form a surface oxide in the potential range for methanol oxidation. Ruthenium (Ru) is used mostly in this process. Other metals including Ir, Re, Os, W and Sn have similar effects. Another metal alloy, Pt-Mo (Mo – molybdenum), has been shown to be highly active to methanol oxidation at low current densities.
- The combination of Pt with base metal oxides. Using WO<sub>3-x</sub> as a promoter has produced an effective catalyst. Pt can be deposited onto its surface or it can be co-deposited onto a carbon substrate.
- Pt can be incorporated directly into oxide structures.
- Amorphous non-noble metal alloys are active for methanol oxidation. NiZr and NiTi is the most stable in acid. When only a few percent of Pt is added to these metals, its activity as a catalyst is enhanced.

It is difficult to explain the exact pathway of methanol oxidation because it is sensitive to many factors. They are the structural form of the Pt surface, the nature



of co-adsorbed anions, temperature, methanol concentration, the presence of adventitious impurities, pH and the previous electrochemical polarization history. These pathways for methanol oxidation are illustrated in Figure 31. The end product is  $\text{CO}_2$ .

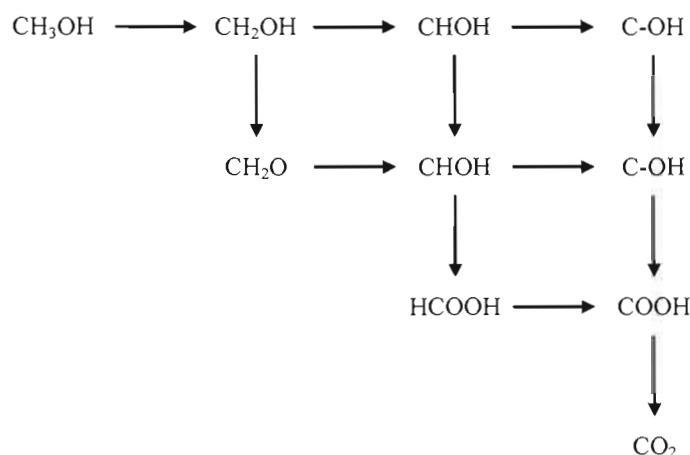


**Figure 31** Pathway of methanol oxidation (Reeve 2002:4).

The performance of a catalyst varies with the nature of the electrolyte. This is because of differences in the ionic conductivity, the degree of adsorption of acid radicals on the catalyst surface and the influence corrosion has on to stability of the catalyst. High acid concentrations reduce the activity of Pt catalysts especially if levels of higher than 5 mole are reached. It has been shown that phosphoric acid levels higher than 5 mole help with better methanol oxidation than sulfuric acid at the same concentration level. But it has been shown that the best electrolyte at low temperatures ( $60^\circ\text{C}$ ) is 3 mole sulfuric acid.

Researchers started to look for a catalyst that can dissociate water at lower potentials than Pt and at the same time has a high reactivity for CO oxidation. Ru is an example of such a catalyst where the adsorption of methanol starts at 0,3 V. It also provides oxygen-containing species to oxidize CO, adsorbed on Pt, to  $\text{CO}_2$ . Methanol dehydrogenation occurs on Pt below 0,2 V.

methanol to form strong adsorbed CO-like species that are difficult to oxidize to CO<sub>2</sub>. The catalyst must be able to provide hydroxyl species to complete the oxidation of the adsorbed methanol oxidation intermediates to CO<sub>2</sub>. It is believed that Pt provides the main catalytic sites for the dehydrogenation of the methanol oxidation reaction and Ru provides the catalytic site for the hydroxide group production and to further oxidize CO-like species to CO<sub>2</sub>. It also serves as a third body to weaken the bond strength of the metal-CO. The Os performs the function of an electron transfer facilitator and a provider of hydroxide groups to the Pt surface. Os also performs the third body function of weakening the interaction of CO species with the Pt surface.

#### **2.9.4 Performance requirements of the cathode catalyst**

The reduction of oxygen in a fuel cell is an important factor in the operation of that cell and it is given by:



Developing a more active and methanol tolerant cathode catalyst is just as important as a better anode. A requirement for good electro catalysis of O<sub>2</sub> reduction is the breaking of the O-O bond. The breaking of this bond leads directly to water if hydrogen is present. The rate of oxygen reduction depends on the interaction rate of molecular oxygen with the adsorption site of the catalyst. Metalloporphyrins or metal phthalocyanines can catalyze the 4-electron reduction of oxygen to water. Therefore, a heat-treated binary prophyrin catalyst composed of two different centre metal sites was designed by Chu and Jiang (2002:592) to increase the catalytic activity for oxygen reduction.

Various other phthalocyanines and phirine metal oxides and ruthenium based chalcogenides have been reported to have an activity towards oxygen reduction for

use as cathode catalysts. But Pt is still the most active. Other cathode catalysts are seldom stable at high temperatures (Neergat *et al.* 2003:870).

In an acidic environment the reduction of oxygen takes place at high anode potentials. A majority of metals dissolve at high potentials, therefore, the cathode catalyst material is platinum and its alloys (Reeve 2002:14).

At high current densities, the mass transport of reactants and products of the electrochemical reaction becomes the main limitation of the fuel cell potential. Take the electrochemical reaction at the cathode as an example, which is the chemical reaction given above. Here the mass transport of the reactant protons depends on the membrane thickness while the removal of water at the cathode depends on the structure of that electrode and the gas flow rate in the cathode chamber (Yu *et al.* 2003:44).

Reeve *et al.* (2000:4242) have found that by using a methanol tolerant cathode catalyst a cell voltage increase of 20 mV was possible at  $100 \text{ mA.cm}^{-2}$  current density.

## **2.10 Methods of feeding the DMFC with fuel**

The liquid fuel allows the proton exchange membrane to be well humidified as well as being cooled down properly, widening the operating condition of the fuel cell stack. Temperature is a strong function for the kinetics of methanol oxidation reaction and therefore the overall power output doubles every  $30^{\circ}\text{C}$  in the range between  $10 - 90^{\circ}\text{C}$ .

While the DMFC stack is in operation no extra water should be needed for the system. This system can operate on an entire closed loop principle where water is recycled from the cathode to the anode (Narayanan *et al.* 2003:900).

The liquid fuel also simplifies the requirements at the front end of the DMFC, bringing down the complexity.

Guo and Cao (2004:1) proposed a passive fuel delivery system for DMFCs. As Figure 32 indicates, pure methanol is present in the one container. This container is connected to the anode feed reservoir via a wick. The wick is a porous material that consists of fiberglass, carbon fiber, polymers and cotton. All of these materials are hydrophobic to water but they can be wetted by methanol. The wick carries the pure liquid methanol to the anode feed reservoir by means of capillary action. Therefore, the methanol solution in the anode feed reservoir is kept at a concentration of 0,5 to 2 moles of methanol.

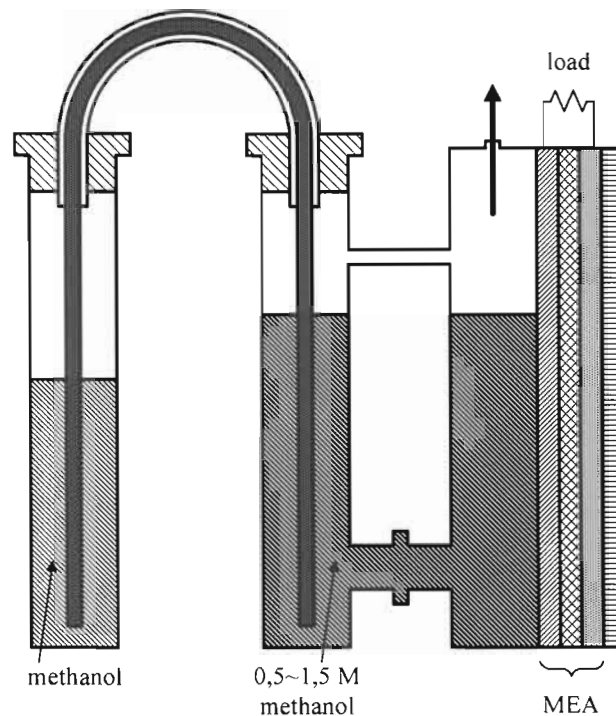


**Figure 32** DMFC with a passive fuel delivery system (Guo & Cao 2004:3).

### 2.10.1 Mixed reactant feed

Mixed reactant feed at the anode can improve the performance of the DMFC. Shulka

*et al.* (2002:48) found that by using mixed reactant feed, improvement in the performance of the anode is visible at load current densities beyond  $400 \text{ mA.cm}^{-2}$ . They did two experiments where the mixed reactants of the first were 1 mole of aqueous methanol plus air and the second was 1 mole of aqueous methanol plus nitrogen. For both experiments the anode polarization data was obtained.

After the first experiment they thought that the oxygen helped in the oxidation of methanol at the anode but after they had done the second experiment, using nitrogen in the mixed reactant feed, it was clear that this was not true. What they did find was that the air stream did not slow down the mass transfer of methanol to the anode, instead the air stream helped in getting rid of the carbon dioxide from the active catalyst. This improved methanol oxidation on the anode.

Evolving carbon dioxide will create a backpressure in the electrode pores effectively pushing the liquid fuel out and away from the membrane. This hinders the escape of the gas from the pores. The end result is a reduction in active surface area. Concentration polarization is observed much later in the DMFC with mixed reactant anode feed than with normal aqueous methanol solution feed.

### **2.10.2 Vaporizing the methanol feed**

Researchers at NASA's Jet Propulsion Laboratory used an aerosol feed to get the reaction at the anode catalyst. The objective of this method was to reduce methanol crossover. Nearly pure methanol droplets were contained in a suitable gas, and this aerosol mixture is fed to the anode catalyst. The gas used to contain the methanol droplets was  $\text{CO}_2$  generated at the anode during normal operation but nitrogen can probably also be used owing to its neutral characteristics. Good control over the methanol aerosol feed must be exercised, whereafter, methanol droplets will come in contact with the anode catalyst and oxidation will take place. Little methanol will be in contact with the membrane ensuring less methanol crossover. The high concentration of the methanol will ensure in high dehydrogenation and, therefore, high cell performance (NASA's Jet Propulsion Laboratory 2002:1).

### 2.10.3 Using different flow field structures

A flow field plate typically has flow channels on its surface ensuring that the reactant fuel gets in contact with the complete catalyst active surface. Another function of the flow fields is to keep methanol fuel reactant from leaking out which then ends up as lost fuel. Reactant flow at the anode is always forced feed. On the other hand oxidant gas at the cathode may be free airflow or also forced feed. With free airflow, concentration polarization may occur earlier than with forced feed. Therefore, better cell performance can be obtained when forced feed is used at the cathode. Different flow field structures can be used at both the anode and the cathode to improve reactant distribution to the active areas (Mennola 2000:19).

The different flow field designs that are currently in use in fuel cells are:

- Serpentine channel geometry
- Parallel channel geometry
- Parallel straight channel geometry
- Parallel serpentine channel geometry
- Discontinuous channel geometry
- Spiral channel geometry

In Figure 33 these different flow field designs are shown. Most of these designs can be used in a DMFC system except for the parallel straight channel geometry and the discontinuous channel geometry for the anode chamber. The reason why the parallel straight channel geometry cannot be used is due to the fact that sealing the open flow field ends on the flow plate will surely be difficult. For the discontinuous channels, the methanol aqueous solution must flow over the catalyst active surface in order to replenish the depleted methanol solution. There is now continuous reactant flow in the discontinuous channel geometry. The other types of flow field designs do enable methanol solution replenishment.

operation was explained, the characteristics of this type of fuel cell was given as well as the problems that were experienced. Anode catalysts, cathode catalysts and membrane qualities were also discussed.

## **Chapter 3 Design and development of the DMFC**

### **3.1 Introduction**

Reading through Chapter Two one can start to understand the requirements and design aspects that must be met in order for a DMFC to operate properly. A variable that must be looked at is there must be a MEA present in the cell. This MEA generates electrical energy from the chemical energy of a fuel but the MEA must also be able to separate the fuel at the anode from the oxidant at the cathode. The fact that the fuel at the anode is in a liquid form and the air at the cathode is in a gas form has the result of some design ideas being successful and others not.

In the following chapter the reader will be familiarized with the ideas and concepts used to make the operation of the DMFC a success. This design might not be the best one but it surely seemed to be the most logical, and the success of this design will be determined by the results obtained.

### **3.2 Structure of a DMFC**

The complete design of the DMFC evolves around the MEA. The shape and size of the MEA was determined by the amount of power required and design of the flow field plates. A MEA with an active area of 5 cm by 5 cm gives a total active area of 25 cm<sup>2</sup>. This was considered to be too small due to the low performance of the DMFC, therefore, a total active surface area of 10 cm by 10 cm was used. This gave an active area of 100cm<sup>2</sup>. The flow field plates had then to be designed around this 100 cm<sup>2</sup> area. The extra space required around MEA must accommodate anode and cathode reactant flow channels as well as sealing between MEA and flow field plates.



### 3.2.1 The MEA

A membrane electrode assembly is shown in Figure 34 and is used in the experiments on the direct methanol fuel cell. This assembly has a total surface area of 170 mm x 170 mm. The active catalytic surface is a 100 cm<sup>2</sup>. The holes are cut or punched according to the flow field design requirements. The MEAs are obtained from suppliers and are not produced by the researcher. The MEAs are the heart of the direct methanol fuel cell and must be handled with care. It is also the most expensive part of the fuel cell.

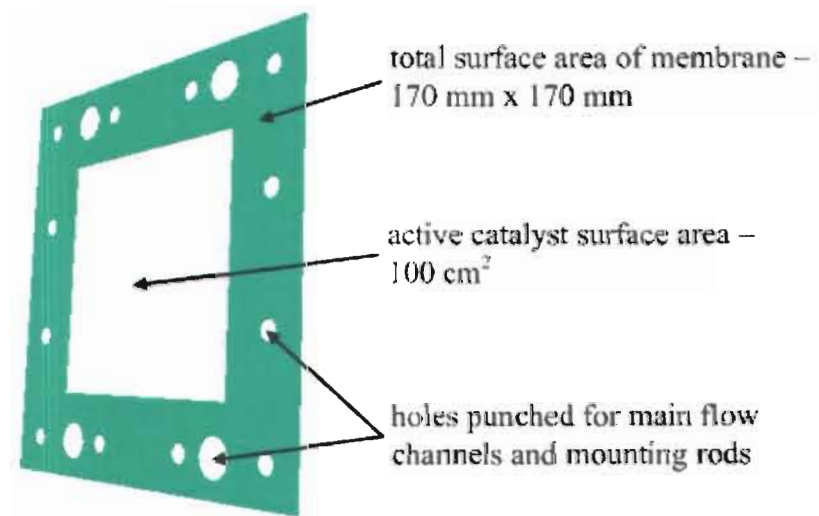


**Figure 34** Membrane electrode assembly (MEA).

Different types of MEAs have been bought and shipped to the Vaal University of Technology. The first type of MEA was obtained from Lynntech, Inc. in the USA and the second type from Golden Energy Fuel Cell Co., Ltd. in Beijing. The MEAs from Lynntech, Inc. had a Nafion 117 membrane and the MEAs from Golden Energy Fuel Cell Co. had a perfluorinated proton exchange membrane.

The physical dimensions of these MEAs were the same for all types and were given

to the companies who manufactured it. The dimensions given for the 100 cm<sup>2</sup> MEAs were:

- Active area of 100 mm x 100 mm
- Total area of 170 mm x 170 mm
- Membrane type that the specific company supplies
- Catalyst on the anode must be Pt/Ru with a 4 mg.cm<sup>-2</sup> loading
- Catalyst on the cathode must be Pt with a 4 mg.cm<sup>-2</sup> loading

The cut or punched holes in the MEA were done after the researcher obtained them.

### 3.2.2 The GDLs

A gas diffusion layer is illustrated in Figure 35. The size of the GDL must be the same as the active area of the MEA, 100 cm<sup>2</sup>. The GDL is a porous material that is highly conductive to electron flow. It also has the characteristics of being hydrophobic or hydrophilic.



**Figure 35** Gas diffusion layer (GDL).

The gas diffusion layer is placed over the active surfaces on either side of the MEA. They are held in this position by the flow field structure. The porosity of the GDL

ensures that maximum reactant flow is possible between the fuel or oxidant in the flow fields and the MEA.

The GDLs were supplied with the MEAs. The GDL used at the anode is carbon cloth and the GDL used at the cathode is ELAT. The GDLs were already cut to size and they only needed to be fitted into the cell.

### 3.2.3 The flow fields

Figure 36 illustrates the flow field structure for this specifically designed direct methanol fuel cell.

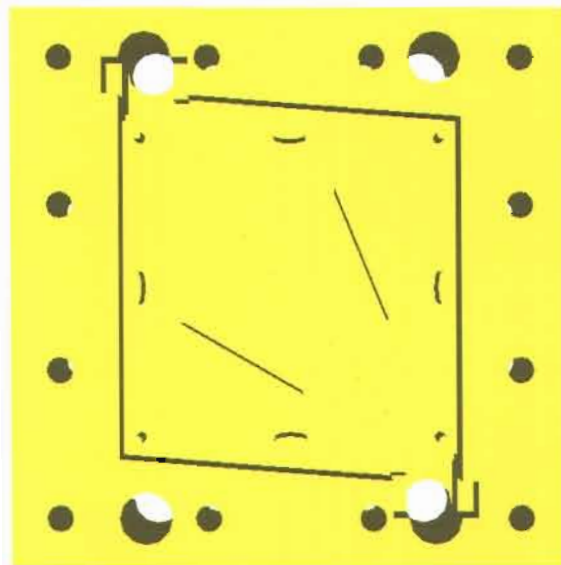


**Figure 36** Flow field structure.

The design was done in AutoCAD. The flow field must ensure that the reactant gases come in contact with the complete active surface of the MEA and it must also ensure that no leaks occur during operation. The flow field must have very high

electron conductivity characteristics. Mechanical strength is also given to a cell by the flow fields. Because this is a direct methanol fuel cell, the material used for the flow field must be resistant to methanol. Methanol tends to weaken the structure of materials that are not resistant to it. This can in turn cause the stack to start a leak or even an increase in internal stack resistance.

Figure 37 is a photograph of the bipolar flow field plate that is used in the direct methanol fuel cell. The technology station at Vaal University of Technology machined this plate.

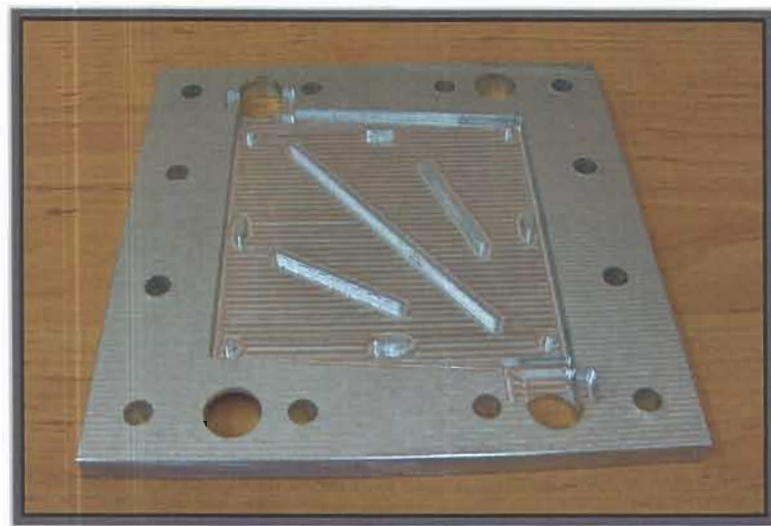


**Figure 37** Bipolar plate used in the DMFC.

Direct methanol fuel cells are connected in series to form what is known as a DMFC stack. Electrical conductivity between each cell is obtained via the flow fields. It is for this reason that the resistivity of the flow fields must be as low as possible. Currently the quickest, cheapest and easiest way of manufacturing flow fields is by using an aluminium plate that is machined to the required design specifications. Another method of manufacturing the flow field structure is to use a resin filled with graphite powder. The resin mixture is pumped into a mold that represents the flow field. A requirement for this method is that the resin must be resistant to methanol. Graphite is highly conductive and it doesn't react with alkalis, acids or methanol.

A popular flow field design that is often used is the serpentine flow field structure. This type of flow field is shown in Figure 38. It has, however, been decided that the serpentine flow field design will not be used in this direct methanol fuel cell design. The reason for this is that the CO<sub>2</sub> bubble removal is not successful with serpentine flow designs especially at high current densities. A report by Yang *et al.* (2004:83) supports this statement and it illustrated the CO<sub>2</sub> bubble generated at different current densities. The removal of CO<sub>2</sub> in this type of flow field structure can only be from the active MEA area by high liquid flow rates. Another disadvantage of the serpentine flow field structure for liquid feed fuel cells is that this flow field must be in a horizontal position. The slightest deviation from being horizontal will have an increase in bubble resistant removal. For example if a bottle is half filled with water and the other half is normal air with the bottle sealed, the air will always seek out the highest available point even if the bottle is rotated. The water will always gather at the bottom. The same happens in the serpentine flow fields. If the flow fields are not horizontal, the CO<sub>2</sub> bubbles will gather at the highest point at any given curve in the serpentine structure and it will be difficult to remove these gas pockets.

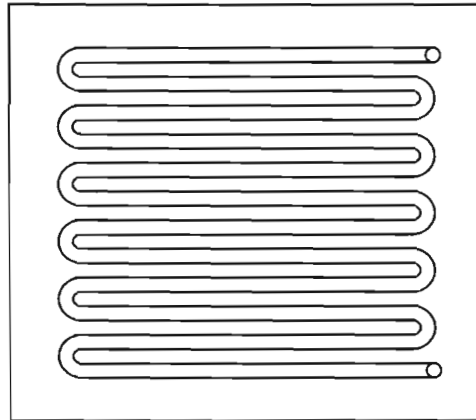


**Figure 38** Serpentine flow field.

Figure 39 through to Figure 43 illustrate the experiments done by Yang *et al.* (2004:83) indicating how the CO<sub>2</sub> bubbles influence the liquid flow rate through a serpentine design and how liquid reactant fuel contact with the MEA is minimized. Little carbon dioxide is generated at low current density. It can clearly be seen from this work how drastically the carbon dioxide generation increases with an increase in

current density of the MEA. The current densities range from  $10 \text{ mA.cm}^{-2}$  to  $200 \text{ mA.cm}^{-2}$ . Clearly the carbon dioxide present in the flow fields is more than the liquid methanol solution at a load current of  $200 \text{ mA.cm}^{-2}$ . This is undesirable because the performance of the cell is severely limited.

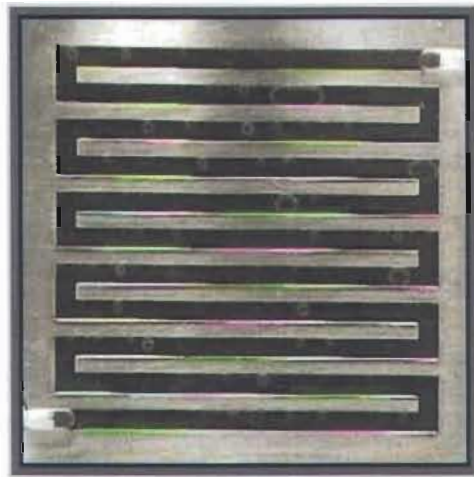


**Figure 39** Carbon dioxide generation at  $10 \text{ mA.cm}^{-2}$ .



**Figure 40** Carbon dioxide generation at  $50 \text{ mA.cm}^{-2}$ .



**Figure 41** Carbon dioxide generation at  $100 \text{ mA.cm}^{-2}$ .

It was already mentioned that the flow field design in Figure 36 would be used for the direct methanol fuel cell. It can clearly be seen from this design that any  $\text{CO}_2$  bubbles that are generated in the anode chamber can go freely to the top and out at the main channel. The work piece has dimensions of 170 mm X 170 mm with a thickness of 10 mm. The MEA active area supported by this flow field is  $100 \text{ cm}^2$ . The anode and cathode chamber thickness is 3 mm.



**Figure 42** Carbon dioxide generation at  $150 \text{ mA.cm}^{-2}$ .





**Figure 43** Carbon dioxide generation at  $200 \text{ mA.cm}^{-2}$ .

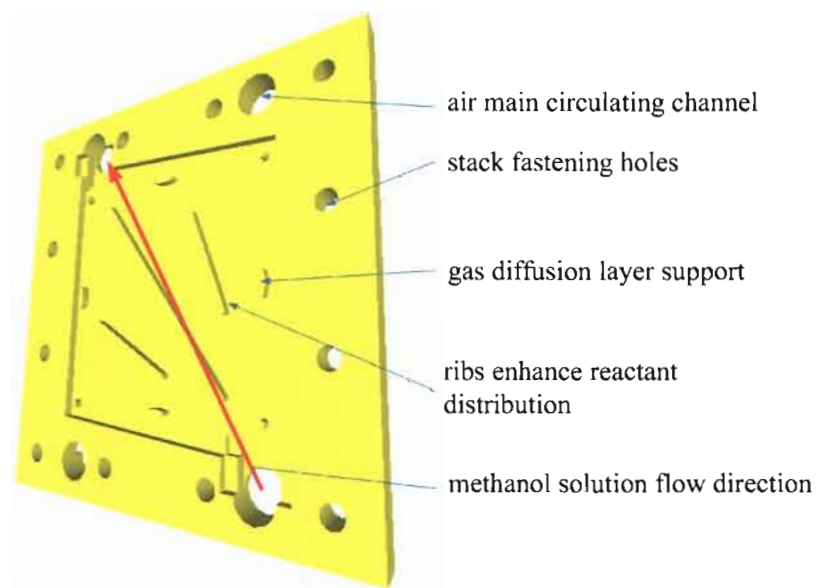
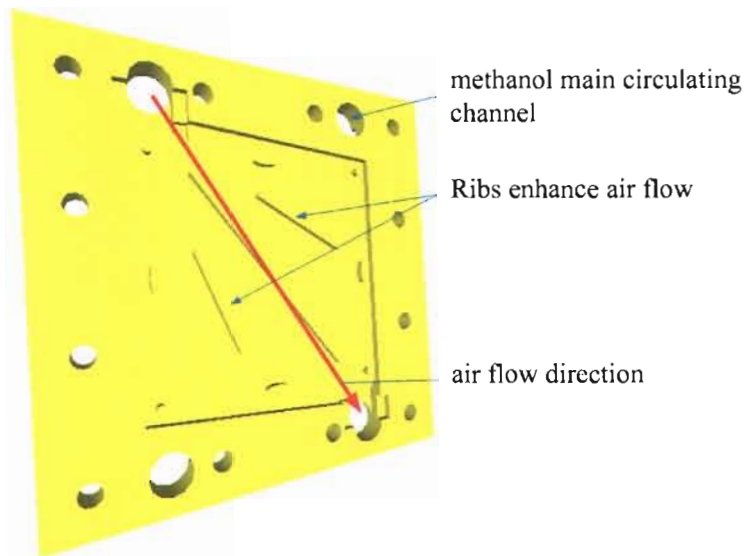


**Figure 44** Designed flow field structure for methanol solution (upwards).

As can be seen from the thick arrow in Figure 44 the flow of the methanol solution is from the bottom of the plate to the top. This will ensure that the methanol solution



will come in contact with the complete active area of the MEA on the anode side due to gravity. The flow ribs ensure that the depleted methanol solution is replenished by the correct new methanol solution all over the active area. All carbon dioxide ( $\text{CO}_2$ ) bubbles will also be helped quickly to the top by the flow of the liquid. The function of the gas diffusion layer support ribs is to support the GDL in the cell as well as to provide good current collecting capability from one cell to the next. Current is only collected through the ribs that enhance reactant distribution and the extruded GDL supports.



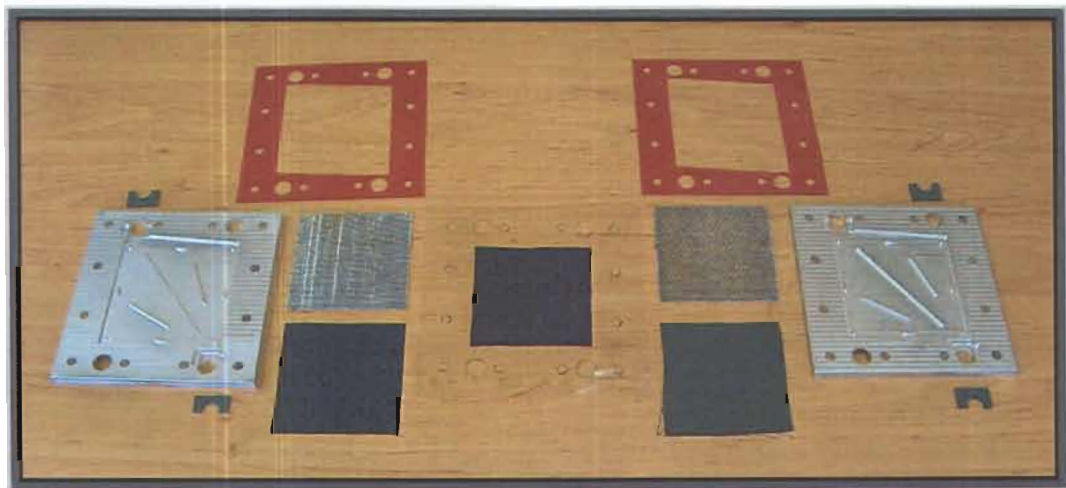
**Figure 45** Designed flow field structure for air (downwards).

Figure 45 illustrates the other side of the flow field where the air is circulated at the cathode. As can be seen the air flows from the top to the bottom as indicated by the thick arrow. This will help in getting rid of the water that is formed at the cathode of the DMFC, again due to gravity. The water exits the cathode chamber at the bottom air main circulating channel. The ribs on the cathode side of the flow field have the

same function as the ribs on the anode side and that is to replenish the cathode with adequate air containing oxygen plus ensuring good electrical contact with the GDL. A support grid will be placed between the flow field ribs and the gas diffusion layer in order to ensure uniform contact pressure over the complete active surface area of the membrane electrode assembly. These support grids will also be placed at either side of the MEA.

### 3.3 Direct methanol fuel cell stack

The direct methanol fuel cell stack will, at least, consist of two or more single DMFCs in series. Figure 46 illustrates the individual components of a single cell. In Figure 46 there are four grey half round PVC seal covers that are used to prevent the methanol or air from leaking into the chamber on either side of the membrane.



**Figure 46** Single cell assembly components.

Figure 47 illustrates where these seal covers have been installed into the flow field plate. It is recommended that these covers are sealed properly in their positions in order to avoid any fuel or oxidant leakage.

For the animated direct methanol fuel cell stack in Figure 48, flow field plates are used to connect cells in series. Gasket seals are used between each membrane and

flow field in order to prevent any fluid as well as gas leaks. It is suggested that threaded rods with a diameter of 6 mm are used to bolt the stack together. It is also of great importance that the rods must be insulated, by covering them with shrink tubing, in order to prevent a flow field plate from being shorted with any other plate.

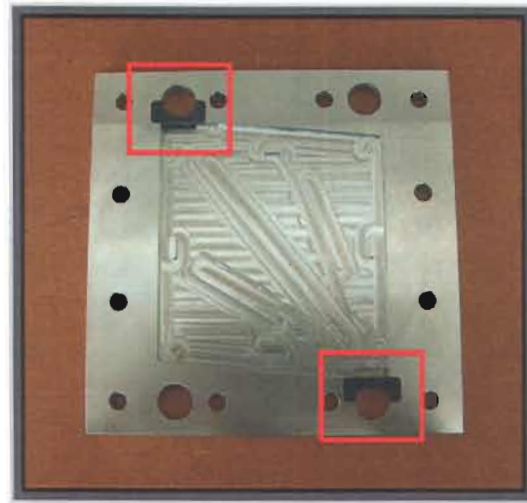


**Figure 47** Seal covers installation on flow field plate.

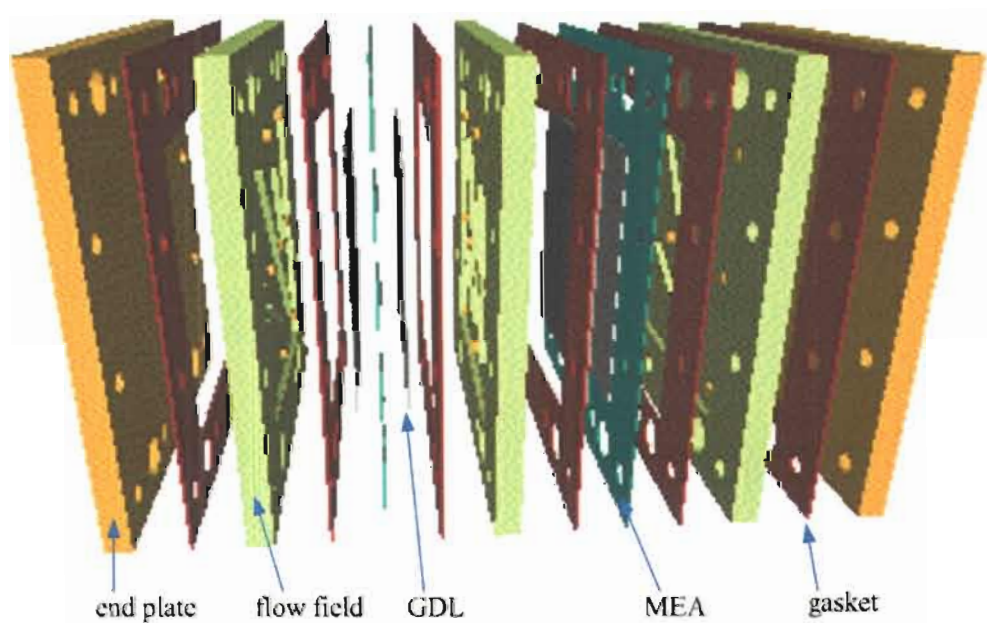


**Figure 48** Animated direct methanol fuel cell stack.

In Figure 49 and Figure 50 a fuel cell stack under construction is shown. Silicone rubber gasket seals seal each cell.



**Figure 49** Fuel cell stack under construction, membrane visible.

The stack is more easily assembled when the insulated threaded rods are all pressed through as each flow field plate is added to the rest. This method keeps all plates aligned with the silicone gasket seals and membranes.



**Figure 50** Fuel cell stack under construction, flow field visible.

In Figure 51 a complete assembled direct methanol fuel cell stack is shown. The methanol solution flow and airflow connectors are clearly visible.

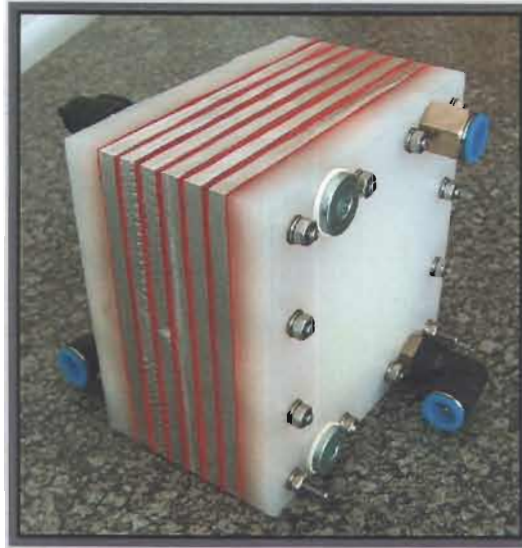


**Figure 51** Complete assembled DMFC stack.

### **3.4 Collecting the current from the stack**

The current generated by the stack can be collected from the inner end flow field plate just before the polypropylene end plate is reached. The total stack voltage will also be available at these inner end flow field plates. A power cable is connected via high current banana plugs to each flow field plate. This simplifies measurement connections.

### **3.5 Function of end plates**

The end plates are made from polypropylene. These plates give the final strength to the stack. They also perform the function of sealing off the stack at the ends like a lid on a jam tin can. The end plates can be 15 mm or thicker. The reason for this is that the main circulating channels goes through the whole stack and it must be connected to piping that will go to the various pumps. These connections in the end plates are tapped with a predetermined size that is the same as that of the connectors. The connectors are screwed into the end plate and the piping attached to the connectors. The end plates used for this stack are shown in Figure 52.





**Figure 52** Stack end plates.

### 3.6 Building of test rig

The mechanical structure of the test rig consists of a frame with a platform onto which all the various pumps, tanks and a blower are mounted. Figure 53 gives a block diagram of the test rig. It is important to make sure that the materials used to store, block, mix or guide methanol or the methanol solution must be resistant towards this liquid and its mixtures.

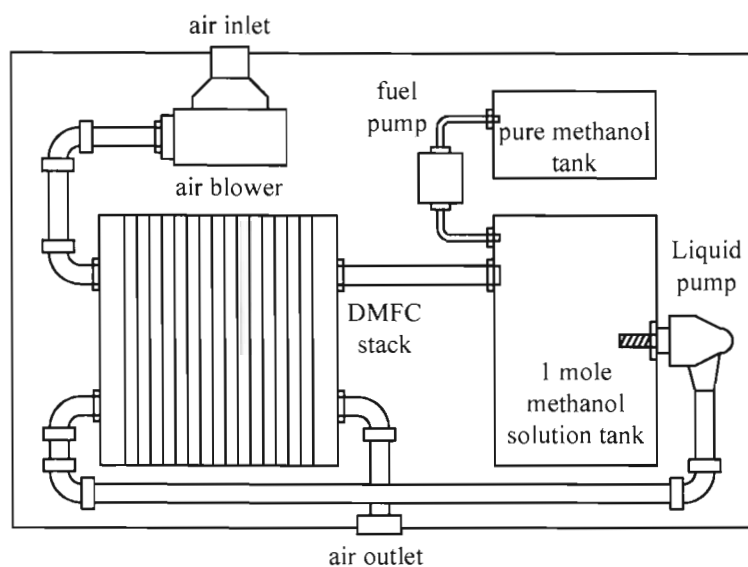


**Figure 53** Block diagram of the test rig.

It is also recommended that the blower and all pumps must be able to operate on 12

volts. Careful attention must be given not to choose a device that is overrated for the function that it must perform. This will only use more power than necessary. The devices must also be able to operate on voltages lower than 12 volt. The reason for this is to control air and fuel flow rates.

Figure 54 shows the complete test rig that will be used to run the direct methanol fuel cell stack in. This test rig simulates a complete production unit installation.

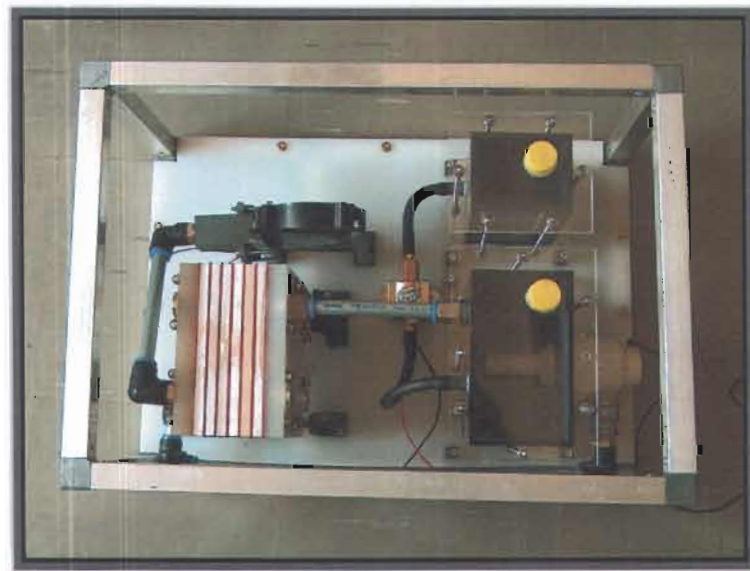


**Figure 54** Direct methanol fuel cell test rig.

The DMFC stack is easily mounted in and removed from the test rig. It is held in place by two extended threaded rods from the stack. Piping to the stack can also be easily attached or removed from the stack.

### **3.7 Pre-conditioning of the DMFC**

According to Scott *et al.* (1999:207), the performance of a fuel cell depends on the correct conditioning of the electrode assembly. Cao and Bergens (2003:13) suggest that the conditioning process should start 3 days prior to the use of the cell. A method followed by most of these researchers was to circulate a methanol solution

through the cell together with the circulation of the oxygen or air through the cathode compartment. It is important that the cell must not be connected to a load during this conditioning process.

The pre-conditioning method followed by Scott *et al.* (1999:207) involved the feeding of the MEA with a 2 mole.dm<sup>-3</sup> methanol solution for 48 hours at 75°C and at atmospheric pressure. The cell was operated at open circuit whereafter a constant load was applied. Operating the cell at a constant low load improved the cell performance.

Liu *et al.* (2002:50) operated their cell at selected cell voltages and currents for 1 to 3 days. It is stated that recent studies indicated that the conditioning process is more likely just ensuring the rewetting of the catalyst surface with the ionomeric electrolyte than the involvement of chemical changes to the catalyst and membrane.

Cao and Bergens (2003:13) did their pre-conditioning for 3 days by heating the DMFC up to 60°C. A one mole methanol solution was then circulated through the cell with an oxidant present. The cell was operated under these conditions in open circuit mode for a predetermined time. Thereafter, the cell was operated under a constant low load of about 20 mA.cm<sup>-2</sup> for four hours. The cell temperature was then raised to 90°C and the load changed to 100 mA.cm<sup>-2</sup> for another four hours. After the conditioning, experiments on the fuel cell commenced.

It was stated by Kho *et al.* (2004:1) that it takes time for the fuel cell to reach a steady state before it can deliver best results. Pre-conditioning can be done with a methanol solution or just pure water. But they did find that pre-conditioning with the methanol solution was more effective than the pure water treatment. It was also observed that storing the cell in a closed container with its fuel reservoir filled with the methanol solution shortened the startup time. The closed container was needed for air breathing fuel cells because it preserved the humidity of the exposed cathode.



### **3.8 Briefing on experiments**

A few experiments will be done on the direct methanol fuel cell stack in the following chapter. These experiments will clearly show the performance characteristics of the DMFC. The results obtained will also have an influence on the design consideration of the researcher to produce a direct methanol fuel cell for telecommunications. The first prototype must be able to provide any electrical load with 100 watts of output power. The experiments to be done on the DMFC stack are to:

- Determine how long the direct methanol fuel cell takes to be ready in supplying a load when it is started up.
- Plot the voltage-current density characteristics of the each individual cell. Also do a power density plot with the gathered information. Divide this first experiment up into a two sections. The first where the cell is operated at full power range and secondly where the cell is operated at partial (half) power range.
- Experiment on different concentrations of methanol in water as a fuel. Plot the performance curves. Determine if there is a difference between 1 mole and 2 mole methanol solution.
- Plot the voltage curves for different operating temperatures for the cell.
- Measure the open circuit voltage as well as the cell voltage under full load and partial load for different cathode oxidant flow rates.
- Change the fuel reactant from methanol to hydrogen in the DMFC stack. Take down the results and compare it to those obtained when the stack was operated on the methanol solution.

### **3.9 Summary**

This chapter explains the assembly of the DMFC together with the building of a stack. The external components needed to operate the stack are also built into a test

rig. The flow characteristics of liquids as well as gases play a major role in the design of the DMFC stack and also in the construction of the test rig.

## **Chapter 4 Practical experiments performed on the DMFC**

### **4.1 Introduction**

This chapter gives an overview of all of the experiments performed on the DMFC. The method followed and results obtained for each experiment are also given. The experiments chosen will clearly show the capabilities of a DMFC and it can help in determining if such a DMFC can be used as a power supply in telecommunications. All experiments are performed on a five-cell stack where each cell has an active area of a 100 cm<sup>2</sup>.

### **4.2 Startup time of the DMFC**

An experiment will be done on the stack in order to determine the startup time. The aim of this experiment is to determine the time taken for the DMFC to be fully operational from startup. The open circuit voltage of each cell in the stack must be monitored the moment methanol solution starts circulating through the stack. The stack must then run for a few minutes to allow the open circuit voltage to settle down. Voltage measurements are taken throughout this settlement process. The voltage at which each cell settles is practically lower than the theoretical value. This will also be proven in this experiment.

The theoretical value of the open circuit voltage can be calculated by making use of Gibbs free energy. Gibbs free energy can be explained as the energy that is available to do external work, ignoring any work done by changes in pressure and/or volume within the fuel cell. The external work done is the movement of electrons in an external circuit.

According to Larminie and Dicks (2003:26) ‘exergy’ is a term that is widely used and it refers to the external work that can be extracted from the fuel cell, including that due to volume and pressure changes.

Enthalpy is the Gibbs free energy plus the energy connected with the entropy.

The chemical energy of a direct methanol fuel cell can be explained and divided in two ways: The first is the point of zero energy. When working with chemical reactions, the zero energy point is where pure elements are in their normal state in the reaction at standard temperature and pressure (STP). At this point the Gibbs free energy,  $G_f$ , for the input is zero.

At the second point it is the change in energy that is important. The change in the Gibbs free energy,  $\Delta G_f$ , gives the energy released in the direct methanol fuel cell. This change is the difference between the Gibbs free energy of the products and the Gibbs free energy of the input reactions.

$$\Delta G_f = G_f \text{ of products} - G_f \text{ of reactants} \quad (7)$$

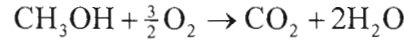
It is convenient to consider these quantities in their per mole form. It is indicated with a “ $\bar{\phantom{x}}$ ” sign over the lower case letter, for example  $(\bar{g}_f)_{CH_3OH}$  is the molar specific Gibbs free energy of formation of methanol.

The molar mass of  $CH_3OH = 32,04$  amu, therefore, one gram mole is 32,04 g and one kilogram mole is 32,04 kg.

A mole of any substance always has the same number of molecules. This number is  $6,022 \times 10^{23}$  and it is called the Avogadro's number. This number is represented by the character  $N$ . The amount of electrons in one mole is  $6,022 \times 10^{23}$ . The charge on one electron is  $1,602 \times 10^{-19}$  C. From this one can calculate the Faraday constant, designed by the letter  $F$ .

$$\begin{aligned}
F &= N \times e \\
F &= 6,022 \times 10^{23} \times 1,602 \times 10^{-19} \\
F &= 96485C
\end{aligned}
\tag{8}$$

The basic reaction of the direct methanol fuel cell is:



The product is one mole of carbon dioxide and 2 moles of water and the reactants are 1 mole of methanol and  $\frac{3}{2}$  moles of oxygen. Therefore, the change in Gibbs free energy is given by:

$$\begin{aligned}
\Delta \bar{g}_f &= \bar{g}_f \text{ of products} - \bar{g}_f \text{ of reactants} \\
\Delta \bar{g}_f &= \left[ (\bar{g}_f)_{\text{CO}_2} + 2(\bar{g}_f)_{\text{H}_2\text{O}} \right] - \left[ (\bar{g}_f)_{\text{CH}_3\text{OH}} + \frac{2}{3}(\bar{g}_f)_{\text{O}_2} \right]
\end{aligned}$$

But the Gibbs free energy of formation is not constant, it changes with temperature and whether the element is in a liquid or gas form. The Gibbs free energy for the methanol reaction at room temperature and 1 atm is  $-698,2 \text{ KJ.mol}^{-1}$ .

It was already mentioned that six electrons pass through the external circuit for each molecule of methanol used. Therefore, for one mole of methanol used,  $6N$  electrons passes through the external circuit.  $N$  is Avogadro's number. If  $-e$  is the charge on one electron, then the charge that flows is:

$$-6N \times e = -6F \text{ Coulombs} \tag{9}$$

$F$  is Faraday's constant or the charge on one mole of electrons.

If  $E$  is the voltage of the direct methanol fuel cell then the electrical work done moving this charge in the external circuit is:

$$\begin{aligned}\text{Electrical work done} &= \text{charge} \times \text{voltage} \\ &= -6FE \text{ joules}\end{aligned}\tag{10}$$

If the system is reversible or has no losses, then the electrical work done will be equal to the Gibbs free energy released,  $\Delta \bar{g}_f$ .

$$\Delta \bar{g}_f = -6F \cdot E \tag{11}$$

$$E = \frac{-\Delta \bar{g}_f}{6F} \tag{12}$$

This equation gives the electromotive force (EMF) or reversible open circuit voltage of the direct methanol fuel cell and the result yields:

$$\begin{aligned}E &= \frac{-(-698.2 \times 10^3)}{6 \times 96485} \\ E &= 1,21 \text{ V}\end{aligned}$$

The setup for this experiment was done with the following equipment:

- Test rig
- 1 mole methanol solution
- Digital multimeters (data logging capability)
- Dual variable power supply or two single variable power supplies

The direct methanol fuel cell stack is to be run in the test rig with a 1 mole methanol solution. No load is connected to the stack. The stack is operated at room temperature.

A digital voltage meter is connected in parallel to the last conductive plates at the ends in the stack. This is easily accomplished owing to the fact that the current collecting plates of each cell is accessible. The measurements taken by the

multimeter is logged. The dual variable power supply or two single variable power supplies are used to control the speed at which the air blower and the liquid methanol solution pump operate separately. Figure 55 shows a photograph of the experiment where all of the necessary equipment has been set up.



**Figure 55** Setup of experiment.

The execution of this experiment started with supplying the stack with its required reactants. Readings are logged at regular predetermined intervals until the open circuit voltage of the cell has settled down. From the logged data, graphs that give a clear indication of the settlement of the stack are derived. Figure 56 illustrates the results of this experiment that was performed on the stack.

The graph in Figure 56 named initial is the response of the stack when it was started up for the very first time. The graph named startup is where the stack has been operated previously. It can clearly be seen that the second time of operation and operation after that ensures that the stack reaches its stabilized OCV much quicker. This is due to the hydration of the membranes.

It is concluded that the DMFC stack will not be able to deliver power immediately after startup. The stack must be given a time for the methanol solution to fully

hydrate the membrane or, put in other words, to soak into the membrane. Whichever way one looks at it, the stack must be given time to become fully operational.

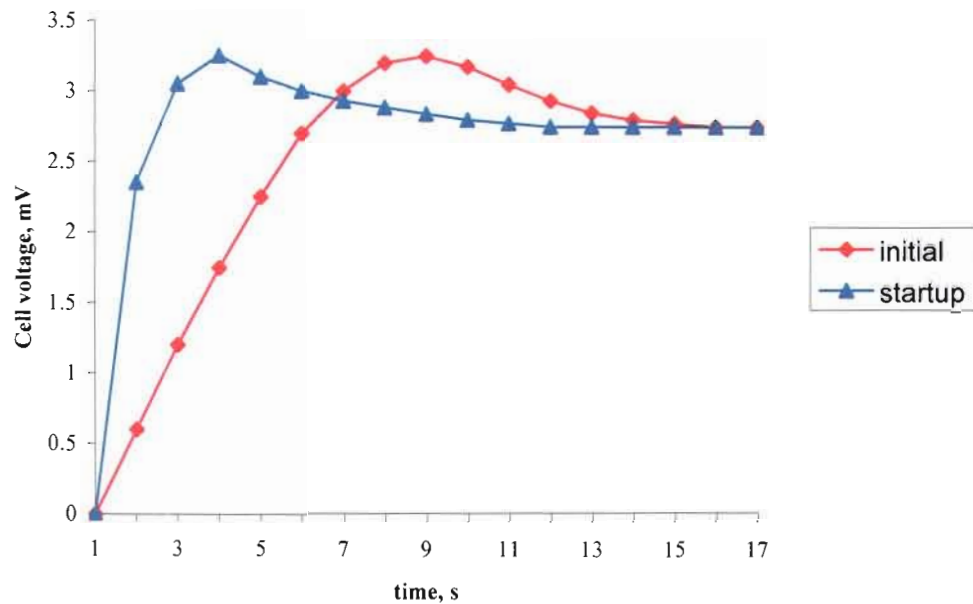


**Figure 56** Open circuit voltage characteristics of the DMFC stack.

The practical open circuit voltage of 0,6 to 0,7 volts is lower than the calculated theoretical value of 1.21 volts. As already explained this is due to electro chemical kinetics of the catalytic electrodes plus mixed potentials that are generated at the cathode because of methanol crossover.

### 4.3 Voltage-current density characteristic curves

The aim of this experiment is to determine the full power and the partial power range of the DMFC stack. The voltage-current density characteristic curve of each cell in the stack is required in order to determine these two ranges.

The setup for this experiment was done with the following equipment:

- Test rig



- 1 mole methanol solution
- Digital multimeters
- Dual variable power supply
- DC electronic load

The direct methanol fuel cell stack is run in the test rig with a 1 mole methanol solution for approximately an hour. No load is connected the stack. The reason for this one hour pre-run is to allow the DMFC stack to settle down after startup. The stack is operated at room temperature.

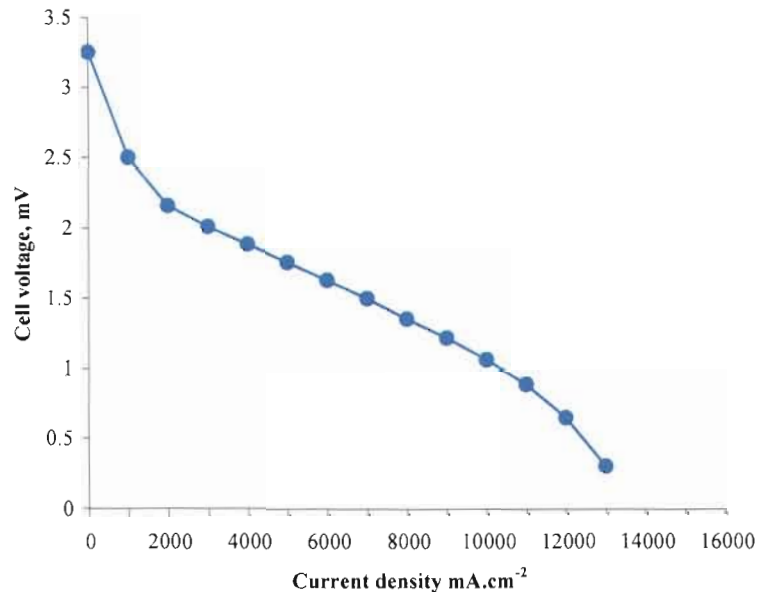


**Figure 57** Voltage-current density curve of the DMFC stack.

A voltmeter is again connected over each cell in the stack. The dual variable power supply is used to drive the air blower and the liquid methanol solution pump. The power generated from the stack is not used to drive all of these pumps. The fuel cell stack is connected to the dc electronic load.

After one hour of operation has been completed, measurements on each cell can commence. The dc electronic load is set to generate a resistive transient load

characteristic, where, the transient changes from a low load to a high load resistance. Measurements are taken while the load resistance is changed. The data are recorded and performance graphs are compiled for each cell in the stack. Figure 57 portrays the recorded data in graphical form.

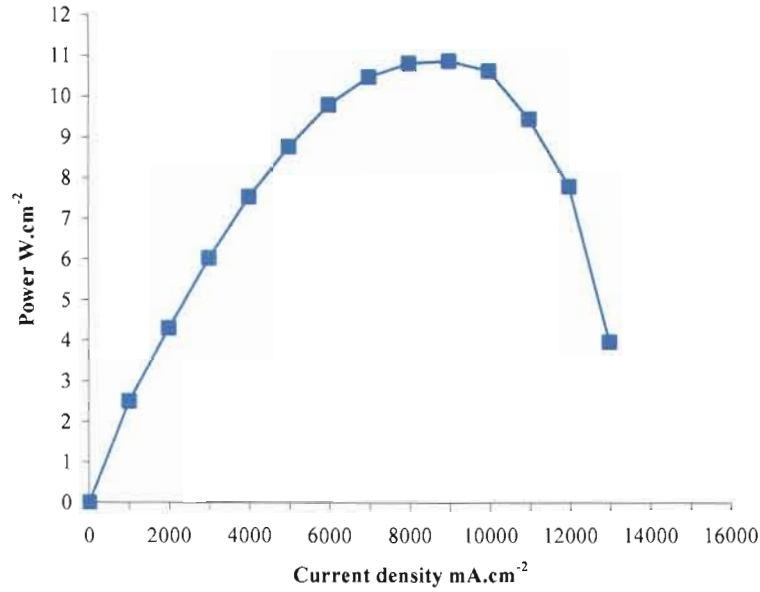


**Figure 58** Voltage-power density characteristic curve.

Figure 58 gives the average value of the data recorded for experiment two. From this figure the voltage-power density of the DMFC stack can be determined. The instantaneous power value for voltage-current value was calculated by using the following simple formula:

$$P = VI \quad (13)$$

Full power operation capability can be released for the stack in Figure 58 where the power curve has a maximum curvature. This maximum power value will take place at the corresponding stack voltage. Partial power operation will take place at approximately halfway between zero and full power operation.

In general this experiment showed the researcher what voltage characteristics a single direct methanol fuel cell has when different load currents are being drawn from the cell. It is also concluded that the performance of each cell in the stack can be duplicated. This means that the addition of direct methanol fuel cells in series will be able to perform together in order to obtain a higher voltage value while the current that can be delivered is equal to that produced by one cell.

#### **4.4 DMFC performance with different methanol concentrations**

The aim of this experiment is to determine at what methanol concentration the direct methanol fuel cell will deliver best performance.

The setup for this experiment was done with the following equipment:

- Test rig
- 0.25, 0.5, 0.75, 1, 1.5 and 2 mole methanol solution
- Digital multimeters
- Dual variable power supply
- DC electronic load

The stack is rinsed with distilled water for an hour in order to completely get rid of any methanol that might still be trapped in the anode chamber or in the gas diffusion layer. When an hour of rinsing is completed, the output of the stack is short circuited for an hour in order to get rid of any methanol that may also be trapped in the membrane. The output voltage of the stack should be zero or very close to zero after this process. If it is not, the process must be repeated.

A digital voltage meter is again connected in parallel with each cell. The dual variable power supply is used to control the speed of the air blower and the methanol liquid pump. The stack is also connected to the dc electronic load. The setup of this experiment is the same as that of experiment two.

The DMFC stack must be operated with a 0.25 mole methanol solution for an hour before measurements can commence for the lowest methanol solution operation. The dc electronic load is again set to generate a resistive transient load characteristic. The voltage-current density data for each cell is recorded and thereafter, the methanol concentration is increased to the next level. The stack must be operated for an hour after the methanol solution has been increased before the next set of measurements can be taken. This process is repeated until a methanol concentration of 2 mole is reached.

Figure 59 gives the results that methanol concentration has on the DMFC stack. The results for the complete range of methanol concentrations on each cell are given in one graph for each cell.

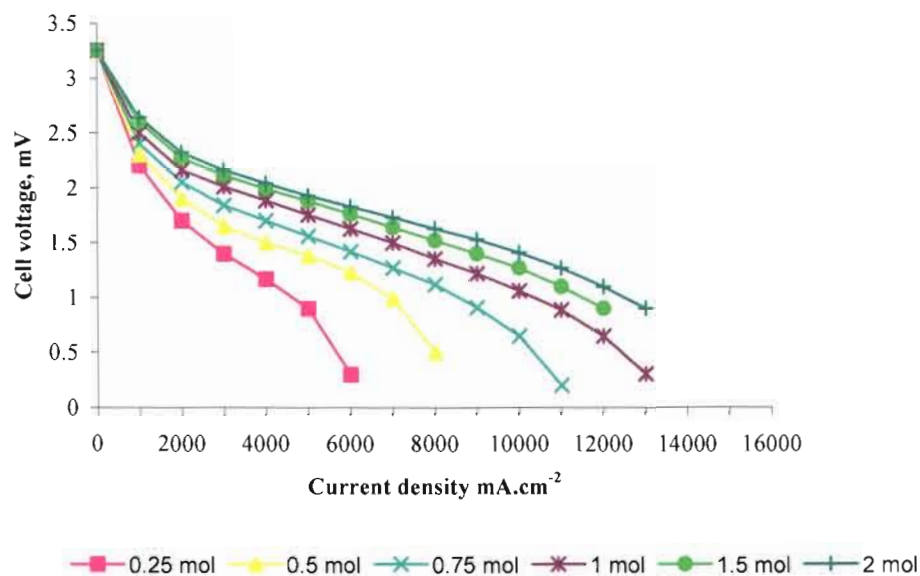


**Figure 59** Effects of methanol concentration on the DMFC stack.

According to the results obtained from the figures above, the methanol concentration that yields the best stack performance is 1 mole. Methanol solutions of less than 1 mole can be used if it is not required that the stack perform at full power. The

disadvantage of this is that if the load requires a sudden increase in power, the direct methanol fuel cell stack will not be able to support that sudden increased demand for power and the load will experience a blackout event. Therefore, it is recommended that the stack be operated with the higher 1 mole methanol solution.

It is clear from Figure 59 that no increase in power delivery by the stack is accomplished by increasing the methanol feed above 2 mole. It will only cause fuel to be wasted due to methanol crossover.

#### **4.5 DMFC performance with different operating temperatures**

The aim of this experiment is to determine the performance of each cell in the stack when the stack is operated at different temperatures. The temperature of the stack must not be increased above 90°C. Temperatures higher than this are too close to the boiling point of water and the membrane will be damaged.

The setup for this experiment was done with the following equipment:

- Test rig
- 1 mole methanol solution
- Digital multimeters
- Dual variable power supply
- DC Electronic load
- Liquid heating element
- Temperature controller

A digital voltmeter is connected to each cell in the stack. The dual variable power supply is used to control the speed of the air blower and the methanol solution pump. The direct methanol fuel cell stack is operated for one hour with a 1 mole methanol solution at room temperature. The liquid heating element is placed in the methanol solution tank. The sensor of the temperature controller is also placed in the methanol

solution tank. The heating element is connected to the controlling output of the temperature controller.

The first operating temperature must be room temperature. In this temperature range the first set of measurements must be recorded. The second temperature range is 60°C then the second set of measurements are recorded. The last measurements must be recorded with the temperature range of 90°C. The experiments can be executed quicker if the operation of the stack is started off with lower temperatures. It is quicker to heat up the methanol solution than to wait for it to cool down. The stack must run for about ten minutes after each temperature increase before measurements commence. This will ensure that the temperature of the stack has stabilized.

Figure 60 shows the results of temperature on the DMFC stack. The results obtained for all three different temperature ranges are given on one graph for the specific stack.

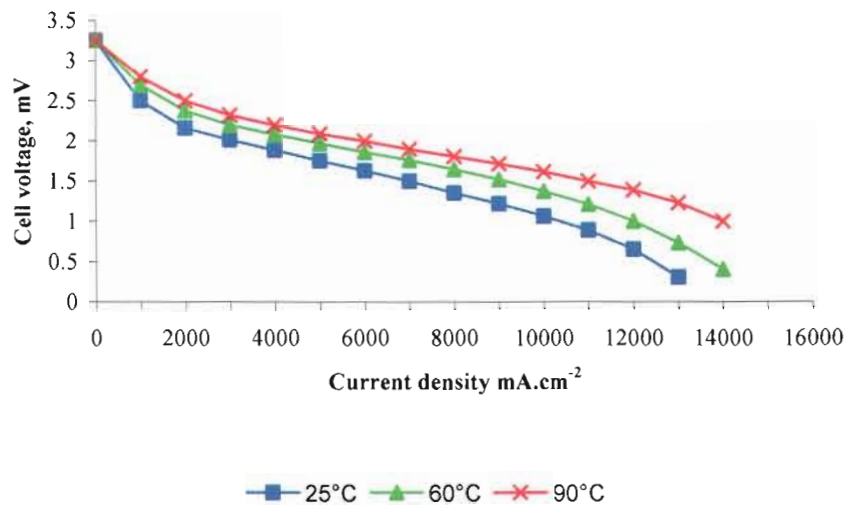


**Figure 60** Effects of temperature on the DMFC stack.

There is a definite increase in cell performance when the operating temperature is increased. Obviously best results are obtained at 90°C but this is not a practical operating parameter. The reason for this is that it takes time for the stack to reach an operating temperature of this magnitude, the stack must be able to deliver full power immediately, and no external heat source will probably be available to heat up the DMFC stack in the environment where it might be in operation.

One has to settle for a lower stack performance at room temperature. This problem can easily be solved by adding a few extra cells. The disadvantage of this is an increase of stack cost and volume.

#### **4.6 DMFC performance with different cathode oxidant flow rates**

The aim of this experiment is to determine the performance of each cell in the stack when the stack is operated at different cathode oxidant flow rates. Careful attention must be given not to operate the stack at too high flow rates, this will not damage the membranes but it is useless to consume so much power with no stack performance increase.

The setup for this experiment was done with the following equipment:

- Test rig
- 1 mole methanol solution
- Digital multi meters
- Dual variable power supply
- DC electronic load
- Gas flow meter

The DMFC stack is again run on 1 mole methanol solution for one hour in order for the stack to normalize. The gas flow meter is connected in the air outlet of the stack.

The digital voltmeters, dual variable power supply and the dc electronic load are connected as normal to the stack.

After one hour of stack operation, measurements on each cell commence. The first set of measurements is taken when the cathode flow rate is well below the required stoichiometry. Thereafter the flow rate is increased by a small amount just so that an increase in the performance is visible. The third set of measurements is taken at a point where no stack performance increase is visible. At this flow rate the stoichiometry of the DMFC stack can be determined. A last set of measurements is taken where the flow rate is increased above the stoichiometry of the stack.

Figure 61 shows the results for the DMFC stack on all of the cathode flow rates.

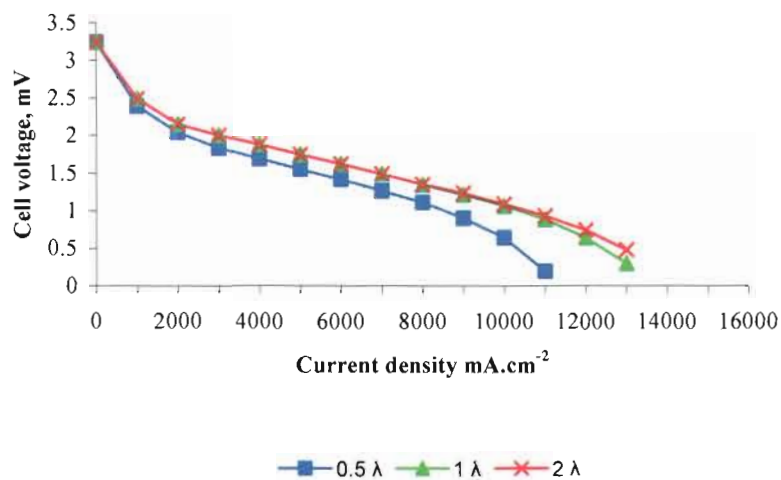


**Figure 61** Voltage-current density results of the DMFC stack for different cathode flow rates.

It is clearly visible from the different cathode flow rate results that cell performance increases as the flow rate increases. One reason for this is the fact that depleted oxygen levels at the cathode are replenished and that the nitrogen is blown out of the



stack. As stated previously nitrogen does have a masking effect at the cathode when all of the oxygen is consumed from the air in the cathode chamber. There will be a point reached where an increase in flow rate will not have an effect on the performance of the stack. The flow rate where this occurs is known as the air stoichiometry of that specific DMFC stack.

#### **4.7 DMFC performance with hydrogen as a fuel**

The aim of this experiment is to determine if a direct methanol fuel cell, that normally operates on a methanol solution and air, will deliver an electrical current when the methanol solution is replaced by hydrogen.

The setup for this experiment was done with the following equipment:

- Test rig
- Hydrogen source
- Digital multimeters
- Dual variable power supply
- DC electronic load

The liquid pump that is used to circulate the methanol solution is intended for liquid only, therefore, it will not be used in this experiment. The anode chamber of the DMFC stack is connected to a hydrogen source. The hydrogen must be fed from the top of the stack to the bottom owing to the fact that hydrogen is much lighter than air. Feeding the stack in this way will ensure that all of the air is expelled from the stack and replaced with hydrogen. Normal measurements are then taken from each cell in the stack.

The hydrogen is circulated through the DMFC stack at a low rate and no pressure at all. The outlet on the stack must just be vented to the outside of the laboratory. Air must be circulated at the cathode side of the stack. Pure oxygen is not considered as

an oxidant in this experiment owing to the fact that hydrogen forms a violent reaction with pure oxygen and if there are any leaks this reaction will take place.

Figure 62 gives the performance characteristics for the DMFC stack when hydrogen is used as a fuel.

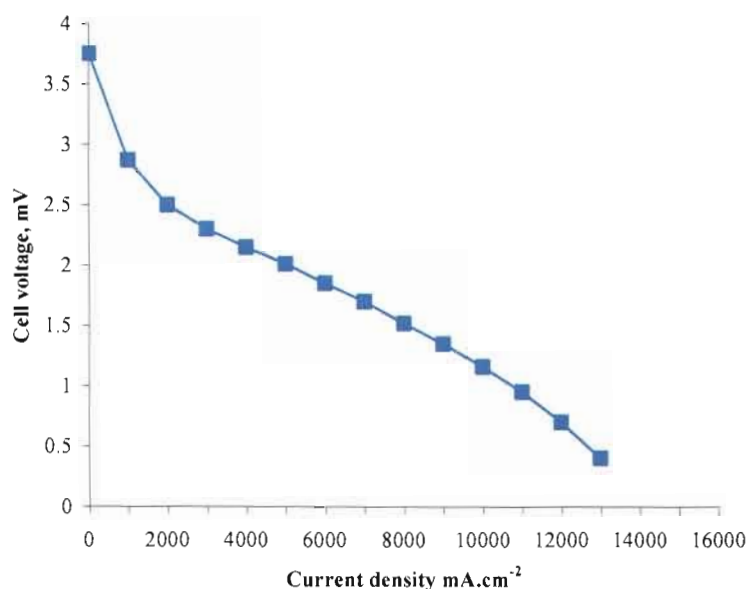


**Figure 62** Voltage-current density with hydrogen as fuel for the DMFC stack.

As can be seen from the results obtained it is also possible to operate the DMFC stack on hydrogen. The performance with hydrogen as a fuel is higher than that of methanol. The reason for this is explained in Chapter two. There are intermediate steps involved in the dehydrogenation of methanol that have lower energy levels as a result for methanol.

## 4.8 Summary

This chapter brings forth the results of all the experiments done on the DMFC stack. It is concluded that the results are satisfactory for delivering adequate power to any electrical system.

## **Chapter 5 Conclusion on the DMFC**

### **5.1 Insights on DMFC manufacturing**

A large amount of theoretical research was done to understand the working of a direct methanol fuel cell. But the ultimate method to truly understand and observe the working of the fuel cell is to build and test a stack. Therefore the researchers set out to design and built a working DMFC stack. All engineers, designers and researchers know that a large number of unforeseen events do occur that would probably not have been known if only a theoretical research study had been done.

### **5.2 Materials used in the stack**

The original stack consisted of a number of different materials. These materials were copper wire mesh that was nickel-plated and aluminium flow field plates. The nickel-plated wire mesh served the function of supporting the membrane between the flow field plates and the flow field plates gives structure to the cell plus it gives electrical continuity from one cell to the next. As mentioned already the end plate was made from polypropylene and as was discovered probably the only material in this particular stack that was resistive to the methanol solution.

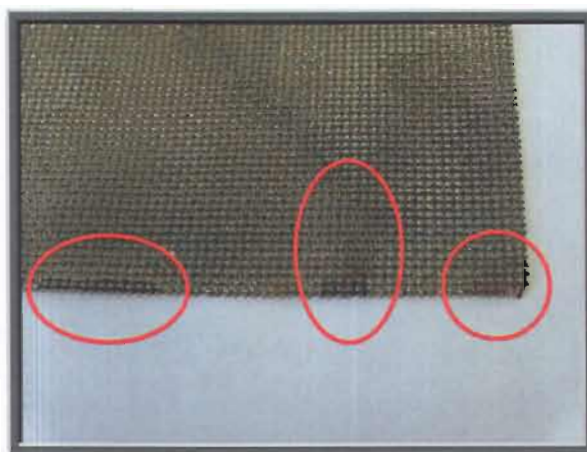
### **5.3 Corrosion of the stack**

The aluminium flow field stack with all of the above mentioned metals inside revealed extensive corrosion. Figure 63 shows the corrosion to the aluminium flow field plates where oxidization of the metal was clearly visible. With further operation of the stack the oxidized metal dissolved in the methanol solution giving it a milky colour.



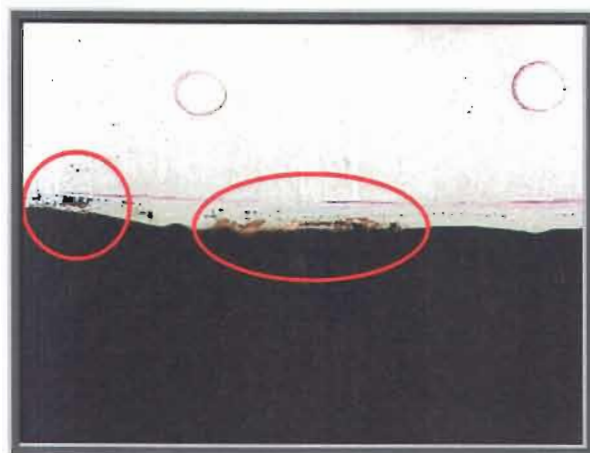
**Figure 63** Corrosion of the flow field plate.

Figure 64 show the corrosion that occurred on the nickel-plated copper grid. It is suspected that this corrosion occurred due to electroplating characteristics that are present in the cell. There is a metal grid on either side of the membrane and at the anode one of these grids is even in soaked in a liquid but what really makes the suspicion of electroplating a reality is the fact that there is a potential difference present across these two grids.



**Figure 64** Corrosion on nickel-plated copper grid.

Figure 65 shows where the copper of the grid leached out onto the membrane probably trying to get to the metal grid at the cathode. The presence of copper can clearly be seen on the membrane.



**Figure 65** Copper on the membrane.

It is also suspected that the nickel and copper collected on the active Pt/Ru catalyst of the anode. It was observed in early experiments done on the aluminium stack that the correct voltage was present over each cell but the current capability of the cell rapidly declined. The initial test done on the stack delivered an output power of about 10 watt but only after a few hours of operation the output power dropped down to only 1 watt.

It was obvious after the corrosion on the aluminium stack that the only metal that must be present in the direct methanol fuel cell must be that of the anode and cathode catalyst. The flow field plates must be manufactured from products such as graphite that doesn't rust nor does it allow oxidation.

#### **5.4 Internal stack currents**

A number of researchers had concerns about  $\text{CO}_2$  that dissolves in the methanol solution. But very little is said about the effects of this occurrence. In a single cell the dissolved carbon dioxide will not play such a major role as in a complete stack. This is probably why so many researchers only mention the disadvantage of dissolved carbon dioxide in the fuel reactant. The problem with  $\text{CO}_2$  generation at the anode is that it makes the methanol solution acidic. If the fuel cell is operated continuously more  $\text{CO}_2$  will be produced. More carbon dioxide will bubble through

the methanol solution in the anode chambers and therefore more  $\text{CO}_2$  will be dissolved in the solution. This was confirmed where newly mixed methanol in distilled water had a pH of about 7 but when the stack was operated for a short time the pH dropped to about 5.5. This is probable due to the formation of carbolic acid. Carbolic acid ( $\text{H}_2\text{CO}_3$ ) is formed in small amounts when its anhydride ( $\text{CO}_2$ ) dissolves water. The problem with this is that the ionic conductivity of the methanol solution increases.

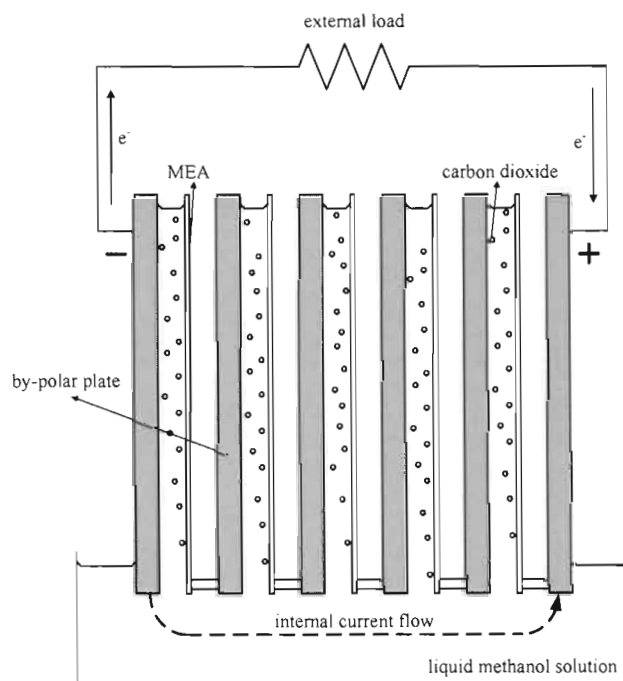


**Figure 66** Internal stack current.

The by-polar plates and MEAs in Figure 66 represent a DMFC stack. Sealing of the liquids and gasses in this stack is ignored. It is clear from the figure that the methanol solution is in contact with all the anodes present in the stack. Therefore, all of the anodes are ionically connected via this liquid. The ionic connectivity is due to the drop in pH of the liquid. The amount of current flow is a function of the pH level of the methanol solution. This phenomenon will bring down the performance of the stack. For this reason the carbon dioxide and carbolic acid must be filtered from the methanol solution.

## **5.5 Contact pressure between flow field plates and the MEA**

It was clear that the contact pressure between the flow field plates and the membrane electrode assembly was very important. This was also mentioned by various other researchers. Another disadvantage that occurred here was the fact that the metal grids that were used to keep even contact pressure over the complete active surface area on either side of the MEA have a woven single metal strand structure. This means that the structure is full of sharp metal bends as the wire zigzagged through the cross wires. These sharp bends pushed through the gas diffusion layer into the MEA where it damaged the electrode catalyst/membrane bond of the MEA. This occurred when the direct methanol fuel cell was bolted together to retain a large contact pressure.

The metal grids also served the function of keeping the membrane in shape and straight. The membrane has the tendency of curling up when it is wetted. The contact area of the metal grid prohibited the membrane from curling up. The supporting grid had to be conductive therefore a metal structure was used.

## **5.6 Redesigning of flow field plates**

In order to get rid of the metal grid that ensured that even pressure was exerted onto the MEA, the ribs in the anode and cathode chamber had to be redesigned. The ribs had to be brought closer to each other and a parallel channel geometry was adopted for the flow field plates. The ribs in this design ensure that the membrane does not curl up when it is wetted by the methanol solution at the anode and the formation of water at the cathode.

In Figures 67 and 68, examples showing clearly the CO<sub>2</sub> bubble generation at the anode side of the DMFC are given. In Figure 67 the DMFC test cell was tilted to the back giving free access for the bubbles to move away from the anode gas diffusion

layer. It can also be seen that these bubbles are very small and can easily move in an anode chamber that is smaller in depth. This could ensure a decrease in total stack volume.



**Figure 67** No carbon dioxide blockage in the DMFC test cell.

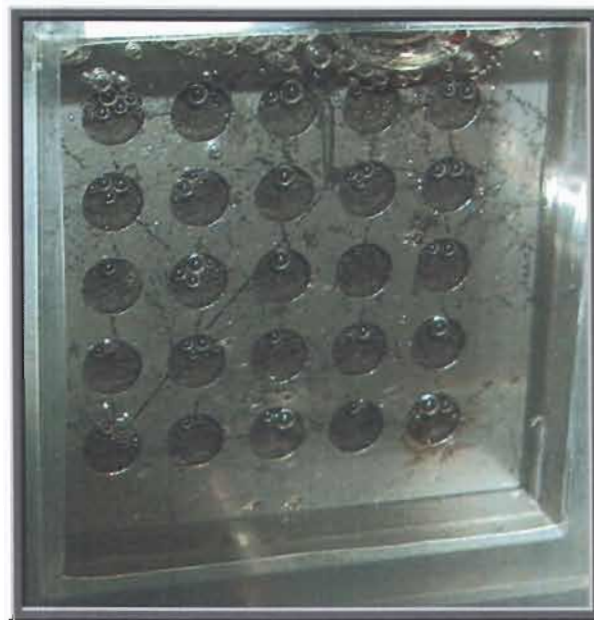


**Figure 68** Carbon dioxide blockage in the DMFC test cell.



But in Figure 68 the DMFC test cell was tilted to the front and the CO<sub>2</sub> bubble escape from the anode GDL was hindered by the supporting grid and the accumulation of the gas bubbles is visible. Therefore, having vertical flow field ribs and getting rid of this supporting grid can definitely improve cell performance.

Figure 69 shows a 3-D generated image of the new graphite flow field plate.

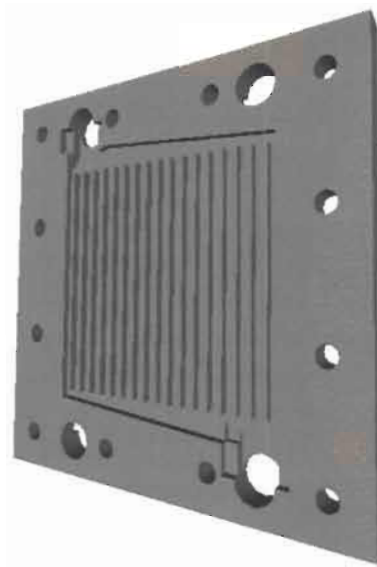


**Figure 69** Graphite flow field plate.

The parallel ribs were placed vertically in both the anode and cathode chambers in order to facilitate in the removal of CO<sub>2</sub>. The methanol solution still flows from the bottom of the anode chamber to the top in all the cells; the same concepts were adopted as in the old aluminium stack design. In the cathode chamber the air is blown from the top to the bottom of the cathode chamber, easily getting rid of any accumulating water.

## **5.7 Results from the aluminium flow field stack**

The aluminium stack was a great idea while it lasted. The metal was easy to obtain and to machine according to the required flow field design. The corrosion on the

metal flow field clearly indicated where the methanol solution flowed and where it had not. As can be seen from Figure 70 the flow left corrosion marks on the surface in the anode chamber. It is also clearly visible that the liquid fuel solution was distributed all over the 100 cm<sup>2</sup> active area designed for the anode chamber. In other words the flow design was confirmed by this effect to be successful.

But the lifetime of the aluminium stack was unacceptably short. No commercial value can be obtained from this stack design and therefore, the aluminium stack will not be considered in further studies or experiments.



**Figure 70** Fuel flow in anode chamber.

## **5.8 Results from the graphite flow field stack**

If one digs a bit deeper in any fuel cell research it is quick to find that the flow fields in fuel cells are mainly produced from graphite, with good reason too. However, graphite is hard to come by in developing countries and if you do find a supplier it is expensive too. But a certain process can decrease the price of graphite flow fields that are used in fuel cells by producing a mould that can be injected with a graphite power mixed resin. A machined graphite plate according to the new design is shown in Figure 71.

Good results have been obtained from the graphite stack and one advantage of this graphite stack is that corrosion of materials, like metals, is almost completely eliminated. The result of this is much more acceptable lifetime for the stack.

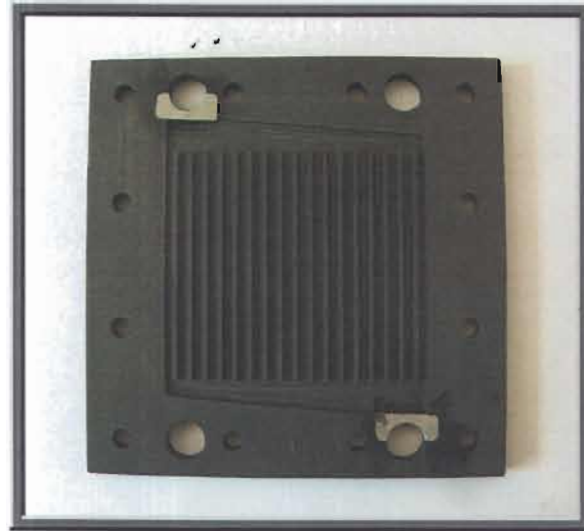


**Figure 71** New graphite flow field plate.

## **5.9 Final word**

The direct methanol fuel cell is definitely a device that can be used to generate electrical power for telecommunications. However some research still needs to be done in order to obtain a highly efficient design that will run without any major maintenance.

Many electronic control circuits that can manage the power delivered by the stack are available. Their functions can be optimized for direct methanol fuel cell systems and hereby controlling an already highly efficient stack.

But as always, any new system needs to be tested and tested and tested..... until failure of such a system is kept to a minimum.

## BIBLIOGRAPHY

- ARICÒ, A.S., ANTONUCCI, P.L., MODICA, E., BAGLIO, V., KIM, H. & ANTONUCCI, V. 2002. Effect of Pt-Ru composition on high-temperature methanol electro-oxidation. *Electrochimica Acta*, 47(3723-3732). [Online]. Available at: <<http://www.sciencedirect.com/>>. Accessed: 11/05/2004.
- ARCHER, M.D. & HILL, R. 2001. *Clean electricity from photovoltaics*. London: Imperial Collage Press.
- BEWER, T., BECKMANN, H., DOHLE, H., MERGEL, J. & STOLTEN, D. 2004. Novel method for investigation of two-phase flow in liquid direct methanol fuel cells using an aqueous H<sub>2</sub>O<sub>2</sub> solution. *Journal of Power Sources*, 125(1-9). [Online]. Available at: <<http://www.sciencedirect.com/>>. Accessed: 21/07/2004.
- CAO, D. & BERGENS, S.H. 2003. A direct 2-propanol polymer electrolyte fuel cell. *Journal of Power Sources*, 124(12-17). [Online]. Available at: <<http://www.sciencedirect.com/>>. Accessed: 21/07/2004.
- CHU, D. & JIANG, R. 2002. Novel electrocatalysts for direct methanol fuel cells. *Solid State Ionics*, 148(591-599). [Online]. Available at: <<http://www.sciencedirect.com/>>. Accessed: 21/07/2004.
- CHU, D., JIANG, R., ERVIN, M.H. & SARNEY, W. 2004. *High performance of direct methanol fuel cells for objective force: from a nano-scale catalyst to a novel fuel cell stack system*. United States Army Research Laboratory, Adelphi. [Online]. Available at: <[http://www.asc2004.com/23rdASC/oral\\_summeries/F/FO-03.pdf](http://www.asc2004.com/23rdASC/oral_summeries/F/FO-03.pdf)>. Accessed: 18/08/2004.

- CHU, Y.H., SHUL, Y.G., CHOI, W.C., WOO, S.I. & HAN, H.S. 2003. Evaluation of the Nafion effect on the activity of Pt-Ru electrocatalysts for the electro-oxidation of methanol. *Journal of Power Sources*, 118(334-341). [Online]. Available at: <<http://www.sciencedirect.com/>>. Accessed: 21/07/2004.
- CREMERS, C. & STIMMING, U. 2004. *Indirect and Direct Methanol Fuel Cells – Current Status and Potential Developments*. Technische Universität München & Department Energy Conversion and Storage. Garching, Germany.
- DIMITROVA, P., FRIEDRICH, K.A., VOGT, B. & STIMMING, U. 2002. Transport properties of ionomer composite membranes for direct methanol fuel cells. *Journal of Electroanalytical Chemistry*, 532(75-83). [Online]. Available at: <<http://www.sciencedirect.com/>>. Accessed: 21/07/2004.
- DOHLE, H., MERGEL, J. & STOLTEN, D. 2002. Heat and power management of a direct-methanol-fuel-cell (DMFC) system. *Journal of Power Sources*, 111(268-282). [Online]. Available at: <<http://www.sciencedirect.com/>>. Accessed: 11/05/2004.
- DOHLE, H., SCHMITZ, H., BEWER, T., MERGEL, J. & STOLTEN, D. 2002. Development of a compact 500 W class direct methanol fuel cell stack. *Journal of Power Sources*, 106(313-322). [Online]. Available at: <<http://www.sciencedirect.com/>>. Accessed: 11/05/2004.
- ENERGY VISIONS INC. 2004. *The Energy Ventures Inc. Direct Methanol Fuel Cell (DMFC)*. Ottawa. [Online]. Available at: <<http://www.energyvi.com/>>. Accessed: 12/08/2004.
- FCTEC. 2004. Fuel cell basics, history. [Online]. Available at: <[http://www.fctec.com/fctec\\_history.asp](http://www.fctec.com/fctec_history.asp)>. Accessed: 12/08/2004.

- FICKETT, A.P. 1984. General characteristics. In Linden, D., ed. *Handbook of batteries and fuel cells*. New York: McGraw-Hill. pp. 41-1 – 41-15.
- FUJIWARA, N., YASUDA, K., IOROI, T., SIROMA, Z. & MIYAZAKI, Y. 2002. Preparation of platinum-ruthenium onto solid polymer electrolyte membrane and the application to a DMFC anode. *Electrochimica Acta*, 47(4079-4084). [Online]. Available at: <<http://www.sciencedirect.com/>>. Accessed: 21/07/2004.
- FY Progress Report. 2003. Hydrogen Fuel Cells, and Infrastructure Technologies. [Online]. Available at: <<http://www.sciencedirect.com/>>. Accessed: 21/07/2004.
- GUO, Z. & CAO, Y. 2004. A passive fuel delivery system for portable direct methanol fuel cells. *Journal of Power Sources*: 1-6, December.
- HAMDAN, M. & KOSEK, J.A. 1999. *Advanced Direct Methanol Fuel Cells*. U.S. Department of Energy. Washington.
- HAMNETT, A. 2003. Direct methanol fuel cells (DMFC). In VIELSTRICH, W, GASTEIGER, H. A, LAMM, A. *Handbook of Fuel Cells – Fundamentals, Technology and Applications*. Volume 1. West Sussex: John Wiley & Sons, Ltd.
- HAN, J. & PARK, E. 2002. Direct methanol fuel-cell combined with a small back-up battery. *Journal of Power Sources*, 112(477-483). [Online]. Available at: <<http://www.sciencedirect.com/>>. Accessed: 21/07/2004.
- HEJZE, T., HOFER, F., SCHMIED, M. & BESENHARD, J.O. 2002. *Methanol crossover suppression in direct methanol fuel cells by sub-micron palladium layers*. Institute of Chemical Technology of Inorganic Materials, Graz University

of Technology, Austria. [Online]. Available at: <<http://147.229.68.79/www.ababrnno.cz/aba2002/abstract/15.pdf>>. Accessed: 11/05/2004.

- HIRSCHENHOFER, J.H. & McCLELLAND, R.H. 1995. The coming age of fuel cells. *Mechanical Engineering*, 117(10): 84-88, Oct.
- HURLEY, P. 2002. *Build Your Own Fuel Cells*. USA: Wheelock Mountain Publications.
- HYDER, A.K., WILEY, R.L., HALPERT, G., FLOOD, D.J. & SABRIPOUR, S. 2000. *Spacecraft power technologies*. London: Imperial College Press.
- JENG, K.T. & CHEN, C.W. 2002. Modeling and simulation of a direct methanol fuel cell anode. *Journal of Power Sources*, 112(367-375). [Online]. Available at: <<http://www.sciencedirect.com/>>. Accessed: 22/09/2004.
- JÖRISSEN, L., GOGEL, V., KERRES, J. & GARCHE, J. 2002. New membranes for direct methanol fuel cells. *Journal of Power Sources*, 105(267-273). [Online]. Available at: <<http://www.sciencedirect.com/>>. Accessed: 22/09/2004.
- KHO, B., OH, I., HONG, S. & HA, H. 2004. The effect of pretreatment methods on the performance of passive DMFCs. *Electrochimica Acta*: 1-5, January.
- KIM, J., KIM, B. & JUNG, B. 2002. Proton conductivities and methanol permeabilities of membranes made from partially sulfonated polystyrene-block-poly(ethylene-ran-butylene)-block-polystyrene copolymers. *Journal of Membrane Science*, 207(129-137). [Online]. Available at: <<http://www.sciencedirect.com/>>. Accessed: 21/07/2004.

- KORDESCH, K. & SIMANDER, G. 2001. *Fuel Cells and their applications*. Weinheim: VCH.
- LAMM, A. & MÜLLER, J. 2003. System design for transport applications. In VIELSTRICH, W, GASTEIGER, H. A, LAMM, A. *Handbook of Fuel Cells – Fundamentals, Technology and Applications*. Volume 4. West Sussex: John Wiley & Sons, Ltd.
- LARMINIE, J. & DICKS, A. 2003. *Fuel Cell Systems Explained*. England: John Wiley & Sons Inc.
- LAUGHTON, M.A. 2002. Fuel cells. *Power engineering journal* 16(1):37-47, Feb.
- LINDEN, D. 1984. *Handbook of batteries and fuel cells*. New York: McGraw-Hill.
- LIU, R. & SMOTKIN, E.S. 2002. Array membrane electrode assembly for high throughput screening of direct methanol fuel cell anode catalysts. *Journal of Electro-analytical Chemistry*, 535(49-55). [Online]. Available at: <<http://www.sciencedirect.com/>>. Accessed: 11/05/2004.
- MA, Z.Q. CHENG, P. & ZHAO, T.S. 2003. A palladium-alloy deposited Nafion membrane for direct methanol fuel cells. *Journal of Membrane Science*, 215(327-336). [Online]. Available at: <<http://www.sciencedirect.com/>>. Accessed: 21/07/2004.
- MENCH, M.M., WANG, Z.H., BHATIA, K. & WANG, C.Y. 2001. *Design of a micro direct methanol fuel cell ( $\mu$ DMCF)*. Pennsylvania State University. [Online]. Available at: <<http://mtrl1.me.psu.edu/Document/imece2001.pdf/>>. Accessed: 21/07/2004.



- MENNOLA, T. 2000. Design and Experimental Characterization of Polymer Electrolyte Membrane fuel cells. Degree of Licentiate of Technology. Thesis. Helsinki University of Technology. [Online]. Available at: <<http://www.hut.fi/Units/AES/studies/theses/mennola.pdf>>. Accessed: 22/10/2004.
- Methanol, Chronic toxicity summary. 2004. Major uses and sources. [Online]. Available at: <[http://oehha.ca.gov/air/chronic\\_rels/pdf/67561.pdf](http://oehha.ca.gov/air/chronic_rels/pdf/67561.pdf)>. Accessed: 28/06/2004.
- MISTUPID.COM, THE ONLINE KNOWLEDGE MAGAZINE. 2004. Composition of air. [Online]. Available at: <<http://www.mistupid.com/chemistry/aircomp.htm>>. Accessed: 07/10/2004.
- MÜLLER, J., FRANK, G., COLBOW, K. & WILKINSON, D. 2003. Transport/kinetic limitations and efficiency losses. In VIELSTRICH, W., GASTEIGER, H.A. & LAMM, A. *Handbook of Fuel Cells – Fundamentals, Technology and Applications*. Volume 4. West Sussex. John Wiley & Sons, Ltd.
- MUNICHANDRAIAH, N., MCGARTH, K., PRAKASH, G.K.S., ANISZFELD, R. & OLAH, G.A. 2003. A potentiometric method of monitoring methanol crossover through polymer electrolyte membranes of direct methanol fuel cells. *Journal of Power Sources*, 117(98-101). [Online]. Available at: <<http://www.sciencedirect.com/>>. Accessed: 21/07/2004.
- NARAYANAN, S.R., VALDEZ, T.I. & ROHATGI, N. 2003. DMFC system design for portable applications. In VIELSTRICH, W., GASTEIGER, H.A. & LAMM, A. *Handbook of Fuel Cells – Fundamentals, Technology and Applications*. Volume 4. West Sussex. John Wiley & Sons, Ltd.

- NASA's JET PROPULSION LABORATORY. 2002. *Direct Methanol Fuel Cells With Aerosol Feed*. Pasadena, California.
- NEERGAT, M., FRIEDRICH, K.A. & STIMMING, U. 2003. New materials for DMFC MEAs. In VIELSTRICH, W., GASTEIGER, H.A. & LAMM, A. *Handbook of Fuel Cells – Fundamentals, Technology and Applications*. Volume 4. West Sussex. John Wiley & Sons, Ltd.
- NUNES, S.P., RUFFMANN, B., RIKOWSKI, E., VETTER, S. & RICHAU, K. 2002. Inorganic modification of proton conductive polymer membranes for direct methanol fuel cells. *Journal of Membrane Science*, 203(215-225). [Online]. Available at: <<http://www.sciencedirect.com/>>. Accessed: 21/07/2004.
- QI, Z. & KAUFMAN, A. 2002. Open circuit voltage and methanol crossover in DMFCs. *Journal of Power Sources*, 110(177-185). [Online]. Available at: <<http://www.sciencedirect.com/>>. Accessed: 21/07/2004.
- REEVE, R.W. 2002. Update on status of direct methanol fuel cell. *DTI Sustainable Energy Programmes*. [Online]. Available at: <<http://www.dti.gov.uk/energy/renewables/publications/pdfs/f0300232.pdf>>. Accessed: 20/07/2004.
- REEVE, R.W., CHRISTENSEN, P.A., DICKINSON, A.J., HAMNETT, A. & SCOTT, K. 2000. Methanol-tolerant oxygen reduction catalysts based on transition metal sulfides and their application to the study of methanol permeation. *Electrochimica Acta*, 45(4237-4250). [Online]. Available at: <<http://www.sciencedirect.com/>>. Accessed: 21/07/2004.
- REEVE, R.W., BURSTEIN, G.T. & WILLIAMS, K.R. 2004. Characteristics of a direct methanol fuel cell based on a novel electrode assembly using microporous

polymer membranes. *Journal of Power Sources*, 128(1-12). [Online]. Available at: <<http://www.sciencedirect.com/>>. Accessed: 21/07/2004.

- SANDHU, S.S., CROWTHER, R.O., KRISHNAN, S.C. & FELLNER, J.P. 2003. Direct methanol polymer electrolyte fuel cell modeling: reversible open-circuit voltage and species flux equations. *Electrochimica Acta*, 48(2295-2303). [Online]. Available at: <<http://www.sciencedirect.com/>>. Accessed: 11/05/2004.
- SCOTT, K., TAAMA W.M., ARGYROPOULOS, P. & SUNDMACHER, K. 1999. The impact of mass transport and methanol crossover on the direct methanol fuel cell. *Journal of Power Sources*, 83(204-216). [Online]. Available at: <<http://www.sciencedirect.com/>>. Accessed: 11/05/2004.
- SCOTT, K., TAAMA W.M., ARGYROPOULOS, P. & SUNDMACHER, K. 2000. Performance of the direct methanol fuel cell with radiation-grafted polymer membranes. *Journal of Membrane Science*, 171(119-130). [Online]. Available at: <<http://www.sciencedirect.com/>>. Accessed: 11/05/2004.
- SCOTT, K., SHUKLA, A.K., JACKSON, C.L. & MEULEMAN, W.R.A. 2004. A mixed-reactants solid-polymer-electrolyte direct methanol fuel cell. *Journal of Power Sources*, 126(67-75). [Online]. Available at: <<http://www.sciencedirect.com/>>. Accessed: 21/07/2004.
- SHAO, Z.G., WANG, X. & HSING, I.M. 2002. Composite Nafion/polyvinyl alcohol membranes for the direct methanol fuel cell. *Journal of Membrane Science*, 210(147-153). [Online]. Available at: <<http://www.sciencedirect.com/>>. Accessed: 21/07/2004.
- SHEN, M., MEUKEMAN, W. & SCOTT, K. 2003. The characteristics of power generation of static state fuel cells. *Journal of Power Sources*, 115(203-209). [Online]. Available at: <<http://www.sciencedirect.com/>>. Accessed: 21/07/2004.

- SHIMIZU, T., MOMMA, T., MOHAMEDI, M., OSAKA, T. & SARANGAPANI, S. 2004. Design and fabrication of pumpless small direct methanol fuel cells for portable applications. *Journal of Power Sources*. [Online]. Available at: <<http://www.sciencedirect.com/>>. Accessed: 21/07/2004.
- SHUKLA, A.K., JACKSON, C.L., SCOTT, K. & MURGIA, G. 2002. A solid-polymer electrolyte direct methanol fuel cell with a mixed reactant and air anode. *Journal of Power Sources*, 111(43-51). [Online]. Available at: <<http://www.sciencedirect.com/>>. Accessed: 21/07/2004.
- SIEBKE, A., MEIER, F., EIGENBERGER, G. & FISCHER, M. 2004. *Modling of liquid Direct Methanol Fuel Cells*. Institut für Technische Thermodynamik, Stuttgart, Germany. [Online]. Available at: <[http://www.icvt.uni-stuttgart.de/meier/siebeetal\\_ecce01.pdf](http://www.icvt.uni-stuttgart.de/meier/siebeetal_ecce01.pdf)>. Accessed: 11/05/2004.
- SUNDMACHER, K., SCHULTZ, T., ZHOU, S., SCOTT, K., GINKEL, M. & GILLES, E.D. 2001. Dynamics of the direct methanol fuel cell (DMFC): experiments and model-based analysis. *Chemical Engineering Science*, 56(333-341). [Online]. Available at: <<http://www.sciencedirect.com/>>. Accessed: 11/05/2004.
- TER-GAZARIAN, A. 1994. *Energy storage for power systems*. Peter Peregrines Ltd. Institute of Electrical Engineers.
- THOMAS, S.C., REN, X., GOTTESFELD, S. & ZELENAY, P. 2002. Direct methanol fuel cells: progress in cell performance and cathode research. *Electrochimica Acta*, 47(3741-3748). [Online]. Available at: <<http://www.sciencedirect.com/>>. Accessed: 21/07/2004.

- VALDEZ, T.I., & NARAYANAN, S.R. 2004. *Recent studies on methanol crossover in liquid-feed direct methanol fuel cells*. Jet Propulsion Laboratory, Pasadena.
- WAGNER, N. & SCHULZE, M. 2003. Change of electrochemical impedance spectra during CO poisoning of the Pt and Pt-Ru anodes in a membrane fuel cell (PEFC). *Electrochimica Acta*, 48(3899-3907). [Online]. Available at: <<http://www.sciencedirect.com/>>. Accessed: 21/07/2004.
- WEI, Z., WANG, S., YI, B., LIU, J., CHEN, L., ZHOU, W., LI, W. & XIN, Q. 2002. Influence of electrode structure on the performance of a direct methanol fuel cell. *Journal of Power Sources*, 106(364-369). [Online]. Available at: <<http://www.sciencedirect.com/>>. Accessed: 11/05/2004.
- WU, H., YUXIN, W. & WANG, S. 2002. A methanol barrier polymer electrolyte membrane in direct methanol fuel cells. *Journal of New Materials for Electrochemical Systems*, 5(251-254). [Online]. Available at: <<http://www.sciencedirect.com/>>. Accessed: 21/07/2004.
- YANG, H., ZHAO, T.S. & YE, Q. 2005. In situ visualization study of CO<sub>2</sub> gas bubble behavior in DMFC anode flow fields. *Journal of Power Sources*, 139(79-90). [Online]. Available at: <<http://www.sciencedirect.com/>>. Accessed: 21/07/2004.
- YU, J., CHENG, P., MA, Z. & YI, B. 2003. Fabrication of miniature silicon wafer fuel cells with improved performance. *Journal of Power Sources*, 124(40-46).[Online]. Available at: <<http://www.sciencedirect.com/>>. Accessed: 11/05/2004.